RL-TR-92-124
Final Technical Report
June 1992

MMIC GaAs BONDING INVESTIGATION

Syracuse University

H. Brumberger, J. Chaiken, P.A. Dowben, J.A. Schwarz,
J.T. Spencer, R.W. Vook

APPROVED FOR PUBLIC RELEASE; DISTRIBUTION UNLIMITED.

Rome Laboratory
Air Force Systems Command
Griffiss Air Force Base, NY 13441-5700

This report has been reviewed by the Rome Laboratory Public Affairs Office (PA) and is releasable to the National Technical Information Service (NTIS). At NTIS it will be releasable to the general public, including foreign nations.

RL-TR-92-124 has been reviewed and is approved for publication.

APPROVED:

THOMAS A. MCEWEN
Project Engineer

FOR THE COMMANDER

DONALD W. HANSON, Director
Surveillance & Photonics Directorate

If your address has changed or if you wish to be removed from the Rome Laboratory mailing list, or if the addressee is no longer employed by your organization, please notify RL(OCTP) Griffiss AFB NY 13441-5700. This will assist us in maintaining a current mailing list.

Do not return copies of this report unless contractual obligations or notices on a specific document require that it be returned.

REPORT DOCUMENTATION PAGE

Form Approved
OMB No. 0704-0188

1. AGENCY USE ONLY (Leave Blank)	2. REPORT DATE	3. REPORT TYPE AND DATES COVERED
	June 1992	Final Aug 90 - Dec 91

4. TITLE AND SUBTITLE

MMIC GaAs BONDING INVESTIGATION

5. FUNDING NUMBERS

C - F30602-89-C-0113
PE - 62702F
PR - 4506
TA - 12
WU - 1N

6. AUTHOR(S)

H. Brumberger, J. Chaiken, P. A. Dowben, J. A. Schwarz, J. T. Spencer, R. W. Vook

7. PERFORMING ORGANIZATION NAME(S) AND ADDRESS(ES)

Syracuse University
Office of Sponsored Programs
Skytop Office Building
Syracuse NY 13244-5300

8. PERFORMING ORGANIZATION REPORT NUMBER

N/A

9. SPONSORING/MONITORING AGENCY NAME(S) AND ADDRESS(ES)

Rome Laboratory (OCTP)
Griffiss AFB NY 13441-5700

10. SPONSORING/MONITORING AGENCY REPORT NUMBER

RL-TR-92-124

11. SUPPLEMENTARY NOTES

Rome Laboratory Project Engineer: Thomas A. McEwen/OCTP/(315) 330-4381

12a. DISTRIBUTION/AVAILABILITY STATEMENT

Approved for public release; distribution unlimited.

12b. DISTRIBUTION CODE

13. ABSTRACT (Maximum 200 words)

Results of an investigation into methods of applying thin film technology to improve Gallium Arsenide (GaAs) Monolithic Microwave Integrated Circuit (MMIC) fabrication and packaging technologies are discussed. Progress in parallel research efforts to better understand the bonding of III-V compounds to substrates, to develop novel thin film deposition methods, and to design and synthesize new source compounds for III-V materials are reported. Techniques investigated include graphoepitaxy, "upside-down" structures, Ti bonding layers between metal and ceramic, and metal-organic chemical vapor deposition. The resulting interfaces of thin films and bulk materials were characterized in situ, where possible, by spectroscopic and diffraction analysis. A number of significant Rama spectra are provided.

14. SUBJECT TERMS

MMIC Fabrication, Raman Spectroscopy, MOCVD, Graphoepitaxy

15. NUMBER OF PAGES

84

16. PRICE CODE

17. SECURITY CLASSIFICATION OF REPORT	18. SECURITY CLASSIFICATION OF THIS PAGE	19. SECURITY CLASSIFICATION OF ABSTRACT	20. LIMITATION OF ABSTRACT
UNCLASSIFIED	UNCLASSIFIED	UNCLASSIFIED	UL

NSN 7540-01-280-5500

Standard Form 298 (Rev. 2-89)
Prescribed by ANSI Std. Z39-18
298-102

Table of Contents

I. INTRODUCTION

This report summarizes the progress made on the "MMIC GaAs Bonding Investigation" project during its final 18 months, briefly describes some spin-offs resulting from the work, and outlines directions for future and continuing research.

The major goal of this project was to study the formation of GaAs layers on various substrates, metallic or ceramic, in order to improve fabrication and packaging technology. A number of parallel research efforts were directed towards a better understanding of bonding of III-V compounds to substrates, towards the development of novel deposition methods, and towards the design and synthesis of new source compounds for III-V materials. Graphoepitaxy, "upside-down" structures, and Ti bonding layers between metal and ceramic were to be investigated, with various deposition methods (such as MOCVD). The interfaces, thin films and bulk materials produced were to be characterized, where possible in situ, by spectroscopic and diffraction methods, especially Raman spectroscopy.

Substantial progress, and a number of specific milestones, can be reported in nearly all areas of investigation. Details are described in subsequent sections of this report, which were compiled by the investigating groups. The technique of projection lithography was developed considerably, and good feature resolution was demonstrated. A laser rastering system was obtained (after considerable delay), and its control software is currently being written. While the latter system was being developed, a great many experiments on GaAs deposition on various substrates were being done by more conventional techniques and have reached a point of great interest and potential with the work on CaF_2 substrates with Pd ground planes and GaAs deposited on CaF_2 buffer layers formed on the Pd. Much has been achieved along the synthetic route. Copious theoretical calculations have pointed the way in the search for optimum GaAs precursors for MOCVD deposition. A cyclic Ga_2As_2 dimer was synthesized but was found to be very difficult to prepare in any quantity, and thus technologically impractical. An extensive synthetic search for simpler new precursors is still in progress, and has yielded a new AlGaAs precursor and a variety of III-V analogs. A high-yield synthetic pathway for phosphorus incorporation was discovered. "Upside-down" structures have begun to be looked at with the MOCVD deposition of pure

polycrystalline Al_2O_3 on GaAs(100). This has been a very fruitful and productive part of our project, and particularly rich in spin-offs of technical potential which are extensively described in the Interim Technical Report and, for present developments, in this report.

An extremely important aspect of all our endeavors was to develop and test Raman spectroscopy as a characterization technique for GaAs deposited on various substrates by different methods. This has been successfully accomplished. The sensitivity of this non-invasive technique to orientation and crystallinity, even in a production environment, has been demonstrated. Indeed, some preliminary graphoepitaxy and annealing experiments have been conducted on GaAs, manually laser-rastered, and the results are promising.

The study of bonding between metal and ceramic has yielded some interesting results on adhesion of various metals (Cu, Ni, Co, W) - possible prototypes - to ceramic systems, largely Al_2O_3. We cannot at this stage predict whether the results will be directly useful. This portion of the project must still be considered very preliminary.

We are working on the rastering system. We can prepare patterned substrates with acceptable resolution and sharpness by projection lithography. We are making excellent progress towards new GaAs and AlGaAs MOCVD precursors. We have found a promising system for epitaxial GaAs films, CaF_2/Pd/CaF_2/GaAs. We have a proven characterization method in place with Raman spectroscopy. It is not overoptimistic to say that we are close to achieving several of the major objectives originally envisioned in our proposal.

II. ACCOMPLISHMENTS

A. MBE Experiments with GaAs on a Ground Plane. R.W. Vook group

The initial work on this portion of the project involved designing and constructing an ultra- high vacuum MBE system with a load lock facility, a quartz window for laser- rastering the GaAs films, an XYZ specimen manipulator, a substrate heater, a quartz crystal thickness monitor and two effusion cells for the Ga and As sources. The basic conception of the UHV system and its accessories involved contributions by Vook, Dowben and their students. Details of the completed system were shown in the Interim Technical Report. The graphite effusion cells that were constructed proved unsatisfactory, and the ones used eventually consisted of boron nitride baskets heated by means of tungsten wire coils. The actual engineering design of the current system and testing were primarily carried by two of Dr. Vook's students, B. Oral and B.H. Jo.

This system is pumped with a liquid nitrogen-trapped diffusion pump and achieves a base pressure of 1.2×10^{-8} torr. This pressure could be improved by the addition of an ion pump for use after initial pumping and bakeout, while experiments are actually in progress. Unfortunately there were not enough funds in the budget for obtaining the needed ion pump and gate valve.

The proposed graphoepitaxy experiments required a carefully patterned substrate consisting of an amorphous or polycrystalline insulator. A laser rastering system and control computer were purchased for the actual rastering of the sample. While the rastering system and the patterning of the substrate were being developed, it was necessary to attempt to grow epitaxial GaAs on a metallic ground plane in some other way. This experimental work was carried out by Dr. Vook's research group and is described in the next several paragraphs.

The basic insulating substrate was ultimately selected to be the (111) cleavage plane of CaF_2, a good UHV material. [Thin films of CaF_2 were studied extensively by one of Dr. Vook's students approximately 20 years ago.] The development of the epitaxial conditions was carried out. In the first experiments GaAs was grown epitaxially in the (111) orientation on this substrate. Then a Pd film, which would serve as the ground plane for the MMIC multilayer device, was grown epitaxially on CaF_2. The next step was to grow GaAs on top of the Pd film. Various

experiments showed that GaAs and Pd interacted to form numerous polycrystalline alloy phases. It was then decided to attempt to grow an epitaxial CaF_2 film on the Pd(111) film grown on the bulk CaF_2(111) substrate. This vapor-deposited CaF_2 film would serve as a buffer layer between the Pd ground plane and the superimposed GaAs film. A number of experiments were carried out to determine a suitable CaF_2 film thickness, because it was found that thin CaF_2 layers did not prevent Pd-GaAs interaction. Table I gives the data for the various films formed.

The current status of the work is as follows: A thin -film multilayer consisting of a bulk CaF_2(111) substrate, an epitaxial Pd(111) film, an epitaxial CaF_2(111) film and lastly a polycrystalline GaAs film with a strong <111> preferred orientation has been formed (Fig. 1). Figures 2 and 3 give some X-ray and RHEED data on the film shown in Fig. 1. The X-ray pattern in Fig. 2 shows that only (111) planes of GaAs, CaF_2 and Pd are parallel to the bulk CaF_2(111) film. Figure 3 shows two superimposed RHEED patterns. One is a single crystal spot pattern from the CaF_2(111) film in the <110> azimuth. The ring pattern comes from GaAs and indicates that the surface layers have become randomly oriented polycrystals, no doubt as a result of air exposure. This randomization is not evident in the X-ray trace in Fig. 2 because the X-rays are much more sensitive to the microstructure of the bulk GaAs film than to the thin surface layers.

What is needed now is more work to determine the conditions (substrate temperature, deposition rate, perhaps a better vacuum) which will give an epitaxial GaAs film. Dr. Vook has no doubt that such a result can be achieved. Such an epitaxial multilayer is what is needed in MMIC devices.

B. Synthetic Developments, Projection Lithography, GaAs Precursors, MOCVD, "Upside-Down" Structures. P.A Dowben and J.T.Spencer

1. Introduction

In the last several years, there has been an enormous interest in the deposition of technologically important main group thin film materials, such as GaAs and $Al_xGa_{1-x}As$ and related materials, using metal-organic source compounds. Few existing epitaxial growth technologies can meet the demanding requirements needed for electronic applications. The older epi-growth techniques, such as liquid phase epitaxy (LPE) and vapor phase epitaxy (VPE), operate

T A B L E I : Films Formed on This Project

Film(Thickness A^0)	Substrate	Deposition Temp.(0^0C)	XRD	RHEED
GaAs(500)	glass	25	amorphous	-
GaAs(500)	glass	555	111 preferred	-
GaAs(500)	W(110)/Si	524	110 preferred	-
GaAs(500)	CaF_2(111)	515	single crystal	single crystal
GaAs(500)/Pd(1500)	CaF_2(111)	GaAs(550) Pd(250)	alloying	-
GaAs(500)/Pd(1500)	CaF_2(111)	GaAs(550) Pd(250)	polycrys. +alloying	-
GaAs(500)/As(1500)/ Pd(2000)	CaF_2(111)	GaAs(550) As(25) Pd(250)	alloying	-
GaAs(500)/CaF_2(1000)/ Pd(1500)	CaF_2(111)	GaAs(540) CaF_2(370) Pd(280)	alloying	-
GaAs(500)/CaF_2(1500)/ Pd(1500)	CaF_2(111)	GaAs(524) CaF_2(530) Pd(280)	alloying	-
GaAs(500)/CaF_2(2000)/ Pd(1500)	CaF_2(111)	GaAs(524) CaF_2(530) Pd(280)	alloying	-
GaAs(500)/CaF_2(4000)/ Pd(1800)	CaF_2(111)	GaAs(526) CaF_2(530) Pd(280)	GaAs:111 preferred CaF_2:111 preferred Pd: 111 preferred	
GaAs(500)/CaF_2(3000)/ Pd(1800)	CaF_2(111)	GaAs(550) CaF_2(600) Pd(390)	GaAs:111F.A.	random surface
			CaF_2, Pd: single crystal	single crystal

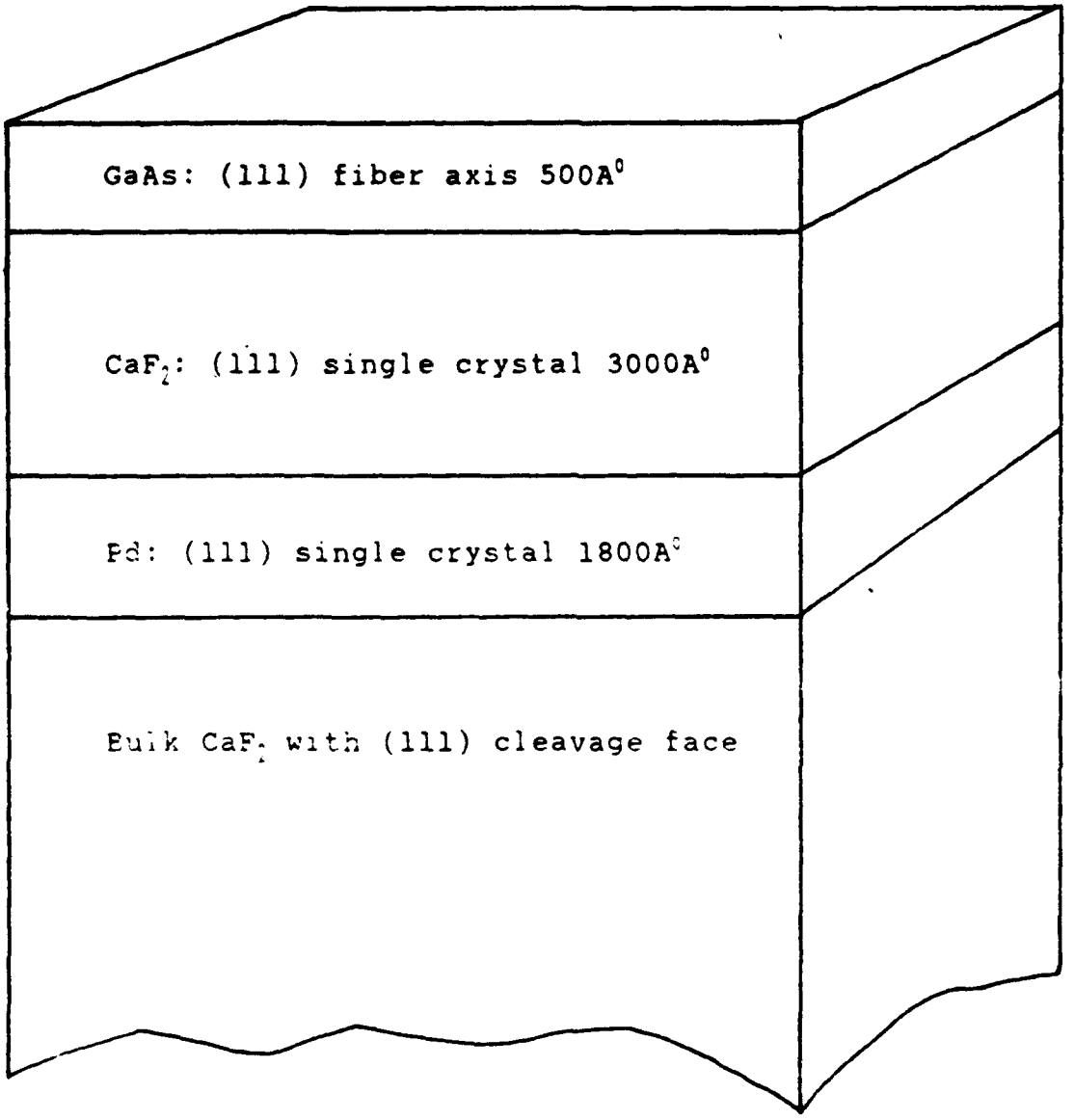

(Fig.1) Most recent multilayer film

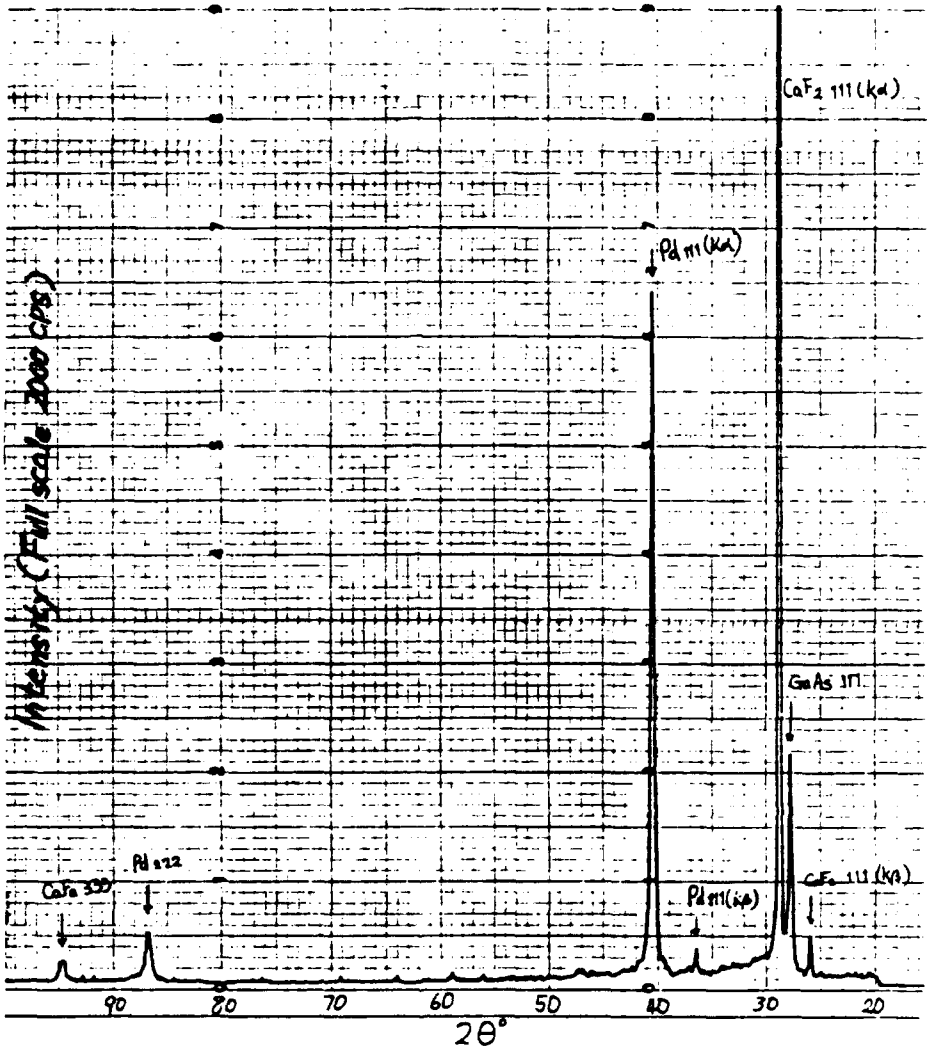

(Fig.2) A XRD pattern from GaAs/CaF$_2$/Pd/CaF$_2$ bulk

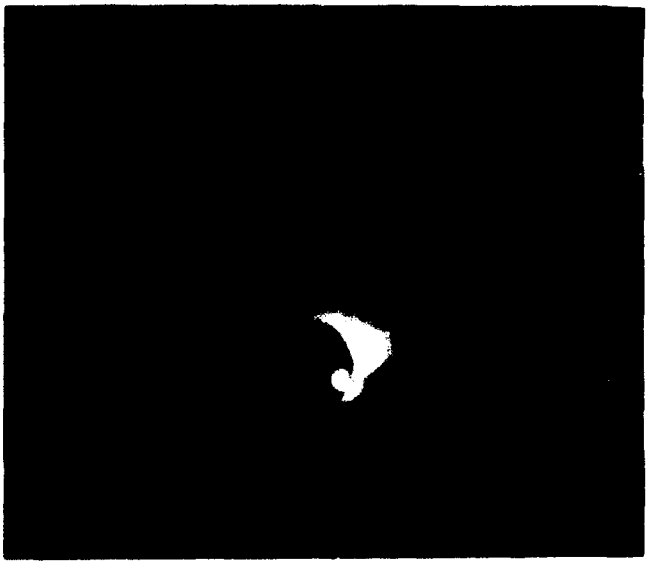

(Fig.3) A RHEED pattern from GaAs/CaF$_2$/Pd/CaF$_2$ thin film multilayer surface

relatively close to thermodynamic equilibrium. Consequently, growth rate and composition are highly temperature-sensitive. Metal-organic chemical vapor deposition (MOCVD) technology, which is kinetically controlled, shows great promise for solving many of the problems associated with the older technologies. In addition, chemical vapor deposition (CVD) technology provides significant advantages over traditional depositional methods including; (1) kinetic deposition control, (2) selective area and pattern deposition capabilities, (3) lower deposition temperatures, (4) superior step coverage and via filling, (5) monolayer interfacial control and (6) the formation of high purity materials.

2. Theoretical Calculations

Research in CVD has dealt primarily with the development of new epitaxial techniques and the purification of existent main group precursors. While these compounds have proven adequate in many instances, further developments in epitaxial processes must now rely upon new precursors designed systematically to exhibit enhanced chemical properties for depositional processes. Thus, a more detailed understanding of the deposition chemistry of CVD precursor compounds and the identification of potential new families of main group precursors for application to CVD technology is critical to the continued development of new thin film technology.

In the development of new chemical vapor deposition precursor compounds for the formation of III-V materials, we have investigated the theoretical modelling of a variety of potential precursors. *Semi-empirical* and *ab initio* calculations were employed in the study of these compounds in order to gain a more complete understanding of the potential bonding and chemical stabilities of these new chemical systems. Two general classes of compounds have been investigated. The first class of precursors contains only a single depositionally important elemental source within the precursor. The second class of precursors are multi-elemental source materials, containing both the group III and group V elements within a single precursor source material. Examples of the systems examined are shown below in Scheme I.

We have completed the theoretical modeling of approximately ninety group III-group V containing compounds.[1] These calculations have provided a more complete understanding of the structural, thermodynamic, decomposition and electronic properties of these compounds. While these model compounds primarily utilize lighter congeners of the group III [boron] and V

Scheme I. CVD Source Systems

Class I (Mono Elemental Source)

Group III: $E(BH_4)_3$, $ER_2(B_3H_8)$, $E_2(B_5H_4)_3$
EH_3-B, ER_3 (where E = Gp III Element, particularly Ga or Al)

Group V: $R_2P(B_5H_8)$, $R_2C{=}P(B_5H_8)$
$H_2P(C_6H_7)$, $H_2P(C_2H_3)$

Class II (Multi-Elemental Source)

GaAs: $As(SiMe_3){=}Ga(OSiMe_3)$
$As(SiMe_3)$-$GaMe_3$

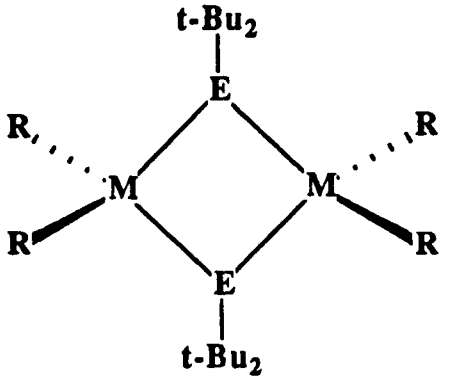

R = Me; M = Ga; E = As, M = Al, Ga, In; E = P, As

[phosphorus] elements (because of the calculational limitations encountered with basis sets and parameterization available for the calculations), conclusions and trends based on these calculations are fully expected to extend to the heavier members of the groups. We have also modelled the energy barriers to internal geometric modifications of the small precursor compounds. These studies relate directly to potential gas-phase (CVD) decomposition and fragmentation pathways. We have also undertaken the calculation of a 3D potential energy map for internal group III - group V bond rotation and dihedral angle deformations. In our research, the MNDO (Modified Neglect

of Differential Overlap) semiempirical method of Dewar has been extensively used. MNDO has been shown to provide superior structural and thermodynamic data for boron hydride and heteroborane systems. Besides our calculations, only a single phosphaborane MNDO calculation has thus far been reported, 1,2-$PCB_{10}H_{11}$.[2]

In our work, we have explored the use of the MNDO-SCF *semi-empirical* calculational method in the systematic study of a wide variety of phosphaborane cluster systems, both those which are structurally known and those whose structures are still unknown. We have also investigated the relationship between bridged and inserted phosphaborane systems in polyhedral borane cluster systems.[1,3] The theoretical study of heteroborane cluster species by *semi-empirical* molecular orbital calculational methods provides a valuable tool for the exploration of the fundamental nature of these species.[1]

In order to establish the validity and accuracy of the MNDO calculational method for phosphaborane cluster systems, the geometry- optimized calculations of all the known, structurally characterized phosphaborane systems were undertaken first.[4-12] These systems provide convenient benchmarks with which to evaluate the validity of the application of the calculational method to related structurally unknown and chemically interesting systems. In each case, our calculated structural data were compared with the data from the crystallographically determined structure, and exceptionally good agreement between the calculated and the experimentally determined parameters was found, with an average difference between the experimental and calculated bond lengths of Δ = 0.04Å (about 2.2% difference; Δ = calculated value - experimental value). The strikingly good agreement between the calculated and the experimentally determined structures provides clear evidence of the utility of the MNDO method for investigating unknown phosphaborane systems. Finally, our PES and NEXAFS studies of a variety of cluster systems have shown remarkable correlations between the calculated energies and symmetries of the MO's and those found experimentally.[13-15]

3. Synthetic Studies

We have successfully synthesized a small quantity of the Ga_2As_2 cyclic dimer described previously.[16] The final step in this synthesis is summarized in Scheme II.[16] The synthesis of starting materials [$GaCl_3$ and $LiAs^tBu_2$] was fairly straightforward. The final dimerization step,

however, was very difficult. Nonseparable complex mixtures of products were obtained from these reactions from which only a small amount of product could be isolated. The products were also very air -and moisture-sensitive and rapidly decomposed to colorless polymeric materials. The complexity of the reaction is thought to arise from a lack of control in the dimerization step, which typically leads to numerous oligomeric and polymeric products. Because the synthesis of the Ga_2As_2 cyclic dimer

Scheme II. Synthesis of Ga_2As_2 cyclic dimer .[16]

$$GaCl_3 + 3\,LiAs^tBu_2 + 4\,MeLi \text{ --------> } (GaMe_2As^tBu_2)_2$$

compound proved to be significantly more difficult than originally anticipated, we found it necessary to investigate the synthesis of simpler III-V analogs in order to overcome this synthetic barrier and to develop new synthetic pathways for the synthesis of complex III-V source materials. These new, and simpler, compounds incorporate a group V element directly within a group III framework, such as phosphorus or arsenic within a group III (borane) cluster framework. Pathways developed with these simpler systems are expected to lead the way to the systematic preparation of new GaAs/AlGaAs precursor systems. In this synthetic exploration, we have discovered a new high-yield synthetic pathway for the direct incorporation of phosphorus (group III) within a boron framework (group III).

Borane complexes are potentially useful, not only as models for other III-V systems, but also as precursors for the CVD of main group thin film materials (especially refractory and compound semiconductor materials such as BC, BN and BP films). One important goal has been to discover high- yield, facile methods for the synthesis of new heteroborane and metallaborane species having deposition chemistries that can be explored in depth. Polyhedral heteroborane cluster species, $B_nH_mE_y$ (where E = carbon, phosphorus or nitrogen), are fully expected to be particularly useful as CVD source materials for boron carbide and phosphide thin films. Boron phosphide is a particularly attractive material for refractory compound semiconductor applications.

In the chemistry of small boranes, the reaction of substituted alkynes with polyhedral borane clusters has been shown to insert the sp carbons of the alkyne directly into the cage framework in good yields. We believed that it should be possible to directly synthesize a wide variety of heteroborane species by using similar reactions between inorganic alkyne analogues and

polyhedral boranes. Phosphaalkynes, RC≡P, have been known since the report of the formation of HCP in 1961. Recently, several phosphaalkynes have been reported which are rather stable, primarily due to the presence of relatively bulky substituents on the carbon atom. For example, the compounds ^{t}BuC≡P, AdC≡P, and (Mes)C≡P are all stable both in the air and at elevated temperatures under an inert atmosphere. Phosphaalkynes have been found to react similarly to alkynes in a variety of reactions.

We have synthesized and reacted several phosphaalkyne compounds, RC≡P, with decaborane(14) to form the *nido*, 16-cage-electron, phosphorus-inserted compound, $R(H)C{=}PB_{10}H_{13}$, **1**, shown in Scheme III.[17a] This compound has been characterized by ^{11}B, ^{13}C, ^1H NMR, IR and mass spectroscopic data. A 2D homonuclear ^{11}B COSY NMR experiment of this new species confirms our assignment, and allows full assignment of the ^{11}B NMR. A reaction for the phosphaalkynes directly analogous to that for alkynes would have inserted both the phosphorus and the carbon, forming a *closo* cage system. The observed insertion of the phosphorus atom without the insertion of the carbon atom of the phosphaalkyne unit is apparently due to a combination of steric interactions and the polarity of the phosphaalkyne bond. MNDO calculations provide further support for the idea that electronic as well as steric factors influence whether or not the carbon or phosphorus inserts into the cage. We have proposed that the mechanism for this insertion is similar to that proposed for the reaction of phosphaalkenes with

Scheme III. Synthesis of Phosphaboranes by Phosphaalkyne Insertion.[17a]

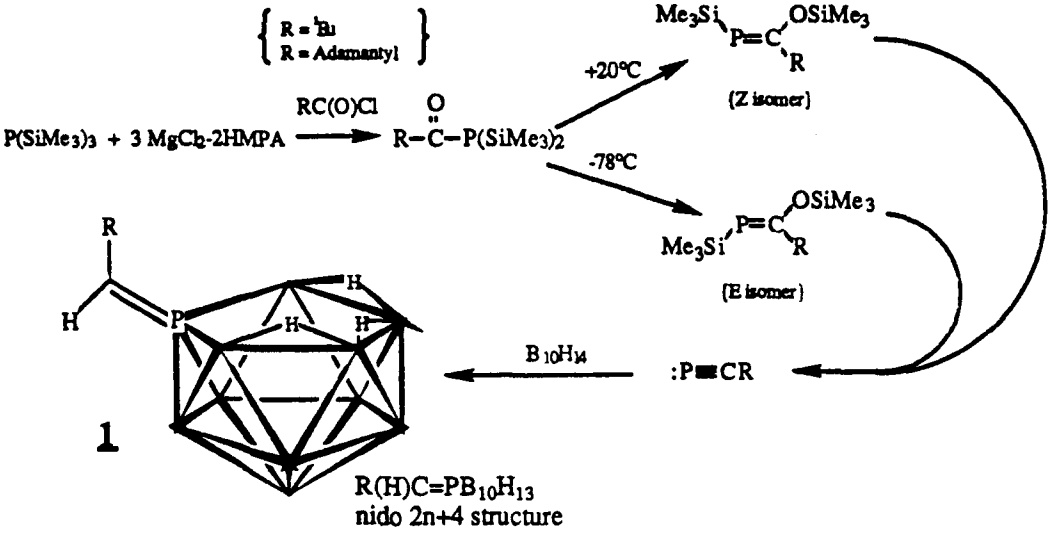

pentaborane(9) as discussed below.[17b-19] The preparation of **1** demonstrates an excellent route to relatively large quantities of phosphaboranes. In addition, compounds such as **1** provide a P=C group which would be available for further chemical reactivity studies, relative to other P=C systems.

The reaction of other low-valent phosphorus compounds with borane species also provides a convenient synthetic entry into small phosphaborane chemistry. We have found that the reaction of phosphaalkenes with an equivalent of neutral pentaborane(9) under mild conditions produces synthetically versatile, small bridging phosphinoboranes, [μ-(RR'HCPR"B_5H_8], in excellent yields as shown in Scheme IV.[17b-19] The preparation of **2** by this synthetic pathway represents the first reported reaction of a neutral borane cluster and a low-valent phosphorus system. These systems exhibit a wide diversity of substitution and elimination reactions, including the elimination of hydrogen to form an unprecedented P=C bridged system, **6**.[18] These phosphino-bridged clusters are also conveniently prepared by the reaction of $[B_5H_8]^-$ with $ClPR_2$ compounds.[19] These bridging phosphinoboranes were found to be quantitatively bridge-deprotonated by the action of NaH to produce the corresponding anion, [μ-(RR'CH-PR"B_5H_7]$^-$. The silyl-substituted phosphinoboranes also readily undergo electrophilic substitution reactions as demonstrated by their quantitative conversion to [μ-(RR'CHP(X))B_5H_8] species, (where X = H, **3** and X = D, **4**), by water, D_2O or alcohols. Compound **3**, when deprotonated to form the corresponding anion and reacted with metal halides, forms metallaphosphinoborane complexes. Characterization of the new cluster compounds was done by multinuclear NMR, FT-IR, mass spectra, elemental analyses and X-ray diffraction of derivatives.

In the calculational work described above,[1] an interesting linear relationship was observed between the charge on phosphorus and both the phosphorus-apical boron and the B(2)-B(3) bond distances. As the phosphorus charge increases, the structure shifts toward an inserted structure. This suggested a possible route to the preparation of phosphaborane species from the reaction of low coordinate phosphorus electrophiles, phosphenium ions, $+P(NR_2)_2$, with borane cage anions. Indeed, the cage polyhedral expansion reaction by BH_4^- has been proposed in the literature to

Scheme IV. The synthesis and reactivity of small bridging phosphaborane systems.[17b-19]

[⌒ indicates B-H-B bridge]

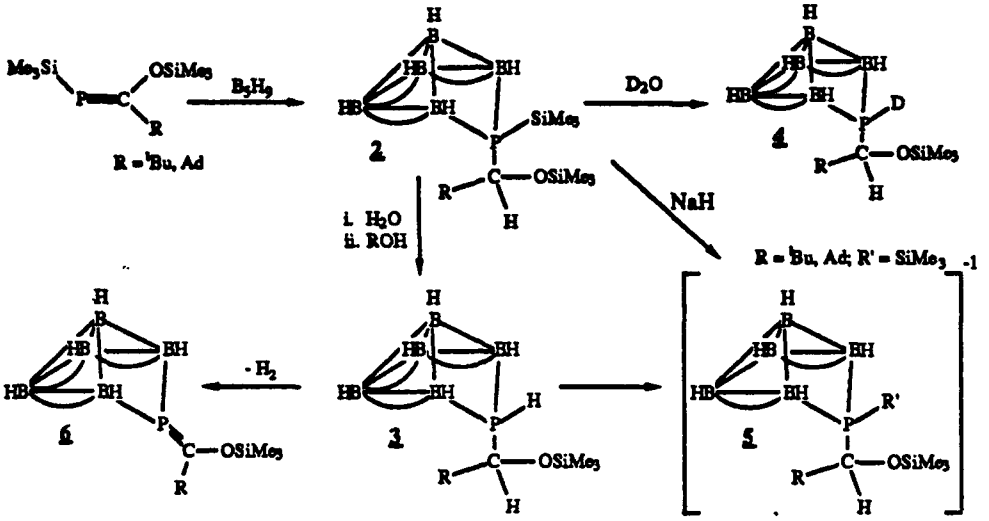

proceed via a multi-step, electrophilic insertion reaction in which the cage is first deprotonated by BH_4^- and then the residual BH_3 undergoes electrophilic insertion into the cage. We have explored the reaction of both neutral chlorophosphines and phosphenium ions with polyhedral borane anions, an example of which is shown in Scheme V. As anticipated, the chlorophosphine forms a phosphorus- bridged species, **2**. The phosphenium ion, with a large charge localized on the phosphorus, is believed to insert into the borane anion to form a capped structure, **8**. Similar bridged and inserted metallatriborane structures have been previously reported by Gaines for the photochemically interconvertible $Mn(CO)_3B_3H_8$, **10**, and $Mn(CO)_4B_3H_8$, **11**, clusters.

These synthetic studies with group III-V containing compounds have laid a substantial groundwork for further synthetic studies with the heavier group III-V congeners with direct applications to III-V CVD precursor synthesis.

4. Aluminum-Containing Thin Films by CVD. "Upside-Down" Structures

The development of deposition techniques for forming metal films on GaAs was originally proposed to be an essential part of our research program. Also, as mentioned previously, there has been enormous interest in the deposition of main group thin film materials, including $Al_xGa_{1-x}As$, pure aluminum and related materials, using MOCVD source compounds. The use of these

Scheme V. Electrophilic Substitution and Insertion Chemistry of Small Boranes.

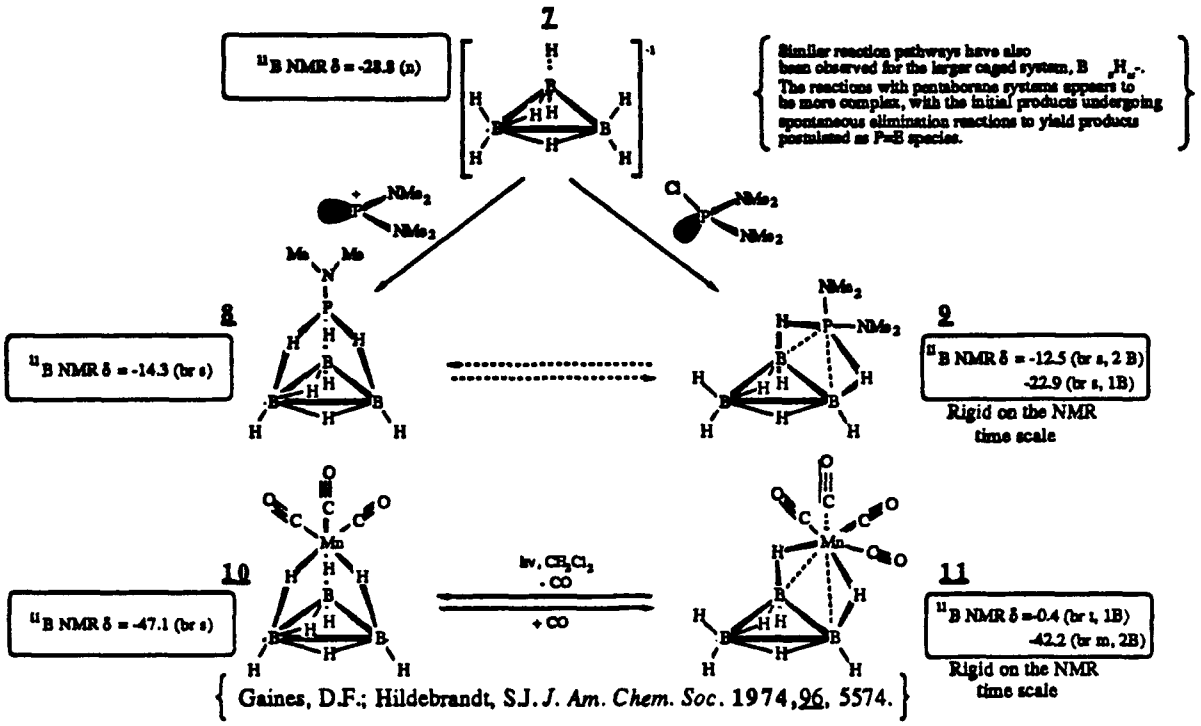

new materials in high- performance applications, such as high electron mobility transistors (HEMT), ultra-high speed systems, and optoelectronic devices, presents very challenging materials requirements. In part of our work, we have explored the CVD deposition of pure aluminum-containing thin film materials.

The formation of pure aluminum and aluminum alloy, such as aluminum oxide, thin films has typically been among the most synthetically troublesome. Many of the currently employed precursor compounds are particularly prone to significant carbon contamination and reactivity problems. With the emergence of structures, such as $Al_xGa_{1-x}As$ and aluminum oxide (especially for the "upside-down" heterostructures originally proposed) as vital electronic materials, and the recent demand for pure aluminum and related materials (such as alumina and aluminum boride), the development and practical application of new CVD source compounds for the deposition of aluminum is therefore an area of major concern.

"Upside-down" GaAs heterostructures use a variety of materials as buffer layers between

GaAs and ceramic layers. Necessary properties of the buffer layer are that it should have good adhesion properties, sufficient thermal conductivity, and a reasonable thermal expansion match. Aluminum oxide is a good material for such buffer layers. In this structural approach, the metallic buffer layer is deposited in correct stoichiometric ratio upon crystalline GaAs. Then with low temperature heating (less than 300° C), the GaAs can be bonded to the ceramic substrate which has a similar metal coating. Alternatively, a ceramic base layer could be grown upon the metal buffer layer. Since the heterostructure is grown up from the crystalline GaAs block, rather than from the ceramic block, this process can be designated as the formation of an "upside-down "structure.

While coatings upon ceramic substrates can be processed at fairly high temperatures, processing that includes a crystalline GaAs block with "via" holes and other patterned features cannot include high temperature processing because of the incongruent evaporation of GaAs. We have investigated the low- temperature deposition of aluminum-containing films (pure aluminum, aluminum oxide and aluminum boride) to explore the use of organometallic chemical vapor deposition as a means of depositing suitable buffer layers in well-defined stoichiometries as a means for making ceramic-metal-GaAs heterostructures using conventional technologies. The novelty of this approach lay in using organometallic complexes specifically designed for application to chemical vapor deposition techniques.

Several organoaluminum precursors have been intensely investigated as CVD source materials including trimethylaluminum, $Al(CH_3)_3$ (TMA), and triisobutylaluminum, $Al(i\text{-}C_4H_9)_3$ (TiBA). Problems encountered with the use of these materials include high carbon contamination of the film, rough surface morphologies and reactor memory effects. Most recently, the volatile donor-acceptor complexes of alane, $AlH_3{\cdot}(NR_3)_2$, have been explored.

The use of specifically designed boron cluster compounds which contain depositionally important elements, was expected to circumvent many of the problems encountered with the known source materials. These boron-based materials have the advantage of not containing any group IV elements strongly bonded to the metal ,thus eliminating the possibility of any group IV element incorporation into the deposited thin films. The boron-containing source materials are frequently relatively thermally stable, volatile liquids, that provide nearly ideal precursor properties for CVD depositions. In addition, the deposition chemistry of this family of boron-containing precursor compounds can be extended to other main group depositions, such as gallium and

indium. This is, in general, not possible for other classes of sources due to the difficulties encountered with the syntheses and instabilities of these compounds. Thus, one of the primary goals of our work was to develop new sources based upon boron-containing clusters for the formation of Group III-containing thin films. In this research, we have prepared polycrystalline thin films of pure aluminum, aluminum boride and aluminum oxide from the chemical vapor deposition (CVD) of volatile boron-containing precursor compounds.

CVD depositions on a variety of amorphous and monolithic substrates, including thermally sensitive substrates, have been explored in our work for the source compounds $Al(BH_4)_3$, **12**, $AlH_2(BH_4) \cdot N(CH_3)_3$, **13**, and $Al(CH_3)_2(B_3H_8)$, **14**.[20-23]

Although the initial synthesis of aluminum borohydride, $Al(BH_4)_3$, **12**, was reported over fifty years ago by Schlesinger, the use of this borane compound for the CVD deposition of aluminum-containing thin films had not been explored. This compound was chosen as our first system to investigate since it is readily synthesized from the reaction of aluminum trichloride with either lithium or sodium borohydride and has a vapor pressure of 119.5 Torr at 0° C. In a typical deposition, the aluminum borohydride is cooled to lower its vapor pressure and then passed over a heated substrate in a dynamic vacuum flow system. Films were grown on a variety of substrates using many depositional parameters. Thicknesses ranging between 100 Å and 2 μ have been prepared by modifying the precursor flow rate and the deposition time. The resultant thin films were characterized by scanning electron microscopy (SEM), Auger electron spectroscopy (AES) and X-ray electron spectroscopy (XES).

The deposition of high purity aluminum oxide (Al_2O_3) thin films on GaAs was successfully achieved by admitting a small partial (10^{-3} Torr) pressure of oxygen into the deposition chamber during the deposition with compound **12**. This aluminum oxide deposition on GaAs, in essence, thus created inverse heterostructural layers. The aluminum oxide films were found to adhere very well to the substrate surface. The AES depth profile for a typical alumina film is shown in Figure 4. The spectrum shows the uniform composition of the film corresponding to the Al_2O_3 stoichiometry. The surface has a small amount of carbon contamination which, however, very rapidly decreased to the detection threshold. The surface also shows some boron contamination, presumably due to residual $Al(BH_4)_3$ in the deposition chamber after the completion of the deposition; this also very rapidly decreased to the AES detection

threshold.

X-ray diffraction data (XRD) for the alumina films show the formation of polycrystalline materials. The XRD spectrum showed the expected peaks and intensities for polycrystalline alumina relative to the standard. The observed 2θ angles (in degrees), relative peak intensities and peak assignments for polycrystalline alumina thin films in the CVD samples relative to the standard literature values were; 31.81° ($2\theta_{lit}$ = 31.45°, Al_2O_3(12-2 or 215)), and 66.35° ($2\theta_{lit}$ = 67.19°, Al_2O_3(004)).

Depositions with pure compound **12** without an oxygen partial pressure resulted in the formation of high-boron content aluminum-containing films. An X-ray electron spectrum for a film deposited on GaAs (100) is shown in Figure 5. The spectrum shows peaks corresponding to aluminum and the GaAs substrate. Since the boron content of the films could not be determined directly using XES, the AES depth-profile of a typical film is shown in Figure 6. The plot shows that the film is compositionally uniform with a relatively high boron content.

The films clearly showed boron contents which were unacceptably high for use in electronics applications; however, aluminum boride films are of significant technological interest in their own right. By substituting precursor **12** with the aluminaborohydride precursor complex **13**, however, we have now been able to reduce to the detection limits the boron content of the bulk film. The formation of pure polycrystalline aluminum thin films from **13** was accomplished at 100° C without substrate pre-treatment, and at 25° C with the substrate briefly pre-treated with $TiCl_4$. Room temperature depositions of mirror-like pure polycrystalline aluminum films were demonstrated on thermally sensitive substrates. The result of an Auger electron depth profile of a typical film grown on a Si (100) substrate following a $TiCl_4$ pre-treatment is shown in Figure 7. Depositions in a partial pressure of oxygen yielded pure polycrystalline alumina (Al_2O_3) films. All films were characterized by XES, AES, SEM, XRD, and resistivity measurements. Each film was shown by AES to be compositionally uniform in the bulk sample with only very shallow surface contaminations of oxygen and carbon from atmospheric exposure. Film thicknesses ranging from 500 Å to 2 μm were readily prepared by controlling the precursor flow rate into the cell, the substrate temperature, the precursor exposure times to the substrate, and the nature of the substrate pre-treatment .

Figure 4. Auger electron depth profile of a aluminum oxide thin film prepared from the pyrolytic CVD of aluminum borohydride, $Al(BH_4)_3$, **12**, on copper. The depth profile was constructed from Auger electron spectra as the film was sputtered using Ar+ ion milling. Aluminum oxide (Al_2O_3) film deposited from $Al(BH_4)_3$, **1**, on GaAs (100). The substrate temperature during the deposition was 332° C and the precursor reservoir was maintained at -78° C during deposition.

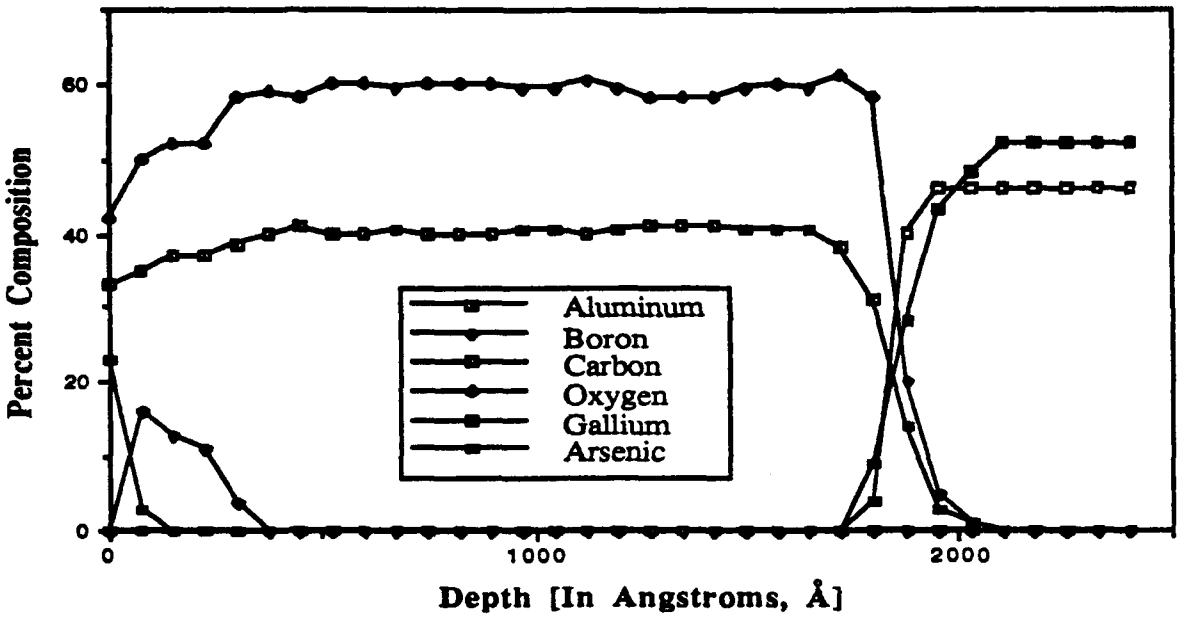

Figure 5. Electron microprobe analysis of an aluminum-containing thin film. The film was deposited at 367 °C on GaAs by the pyrolysis of aluminum borohydride, $Al(BH_4)_3$, **12**.

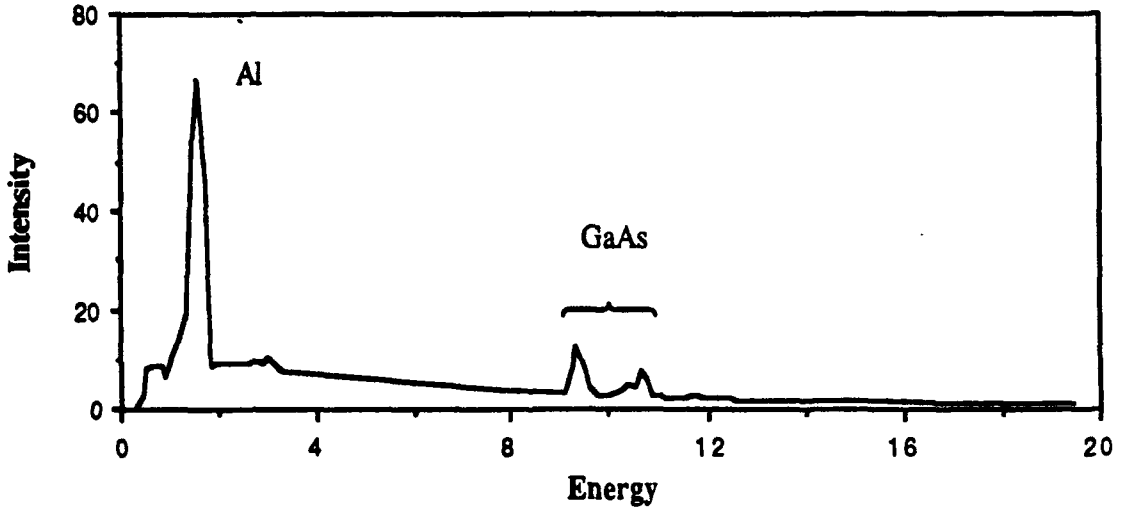

Figure 6. Auger electron depth profile of a boron-containing aluminum thin film prepared from the pyrolytic CVD of aluminum borohydride, $Al(BH_4)_3$, **12**, on copper. The depth profile was constructed from Auger electron spectra as the film was sputtered using Ar+ ion milling. The substrate temperature during the deposition was 307° C and the precursor reservoir was maintained at -78° C during deposition.

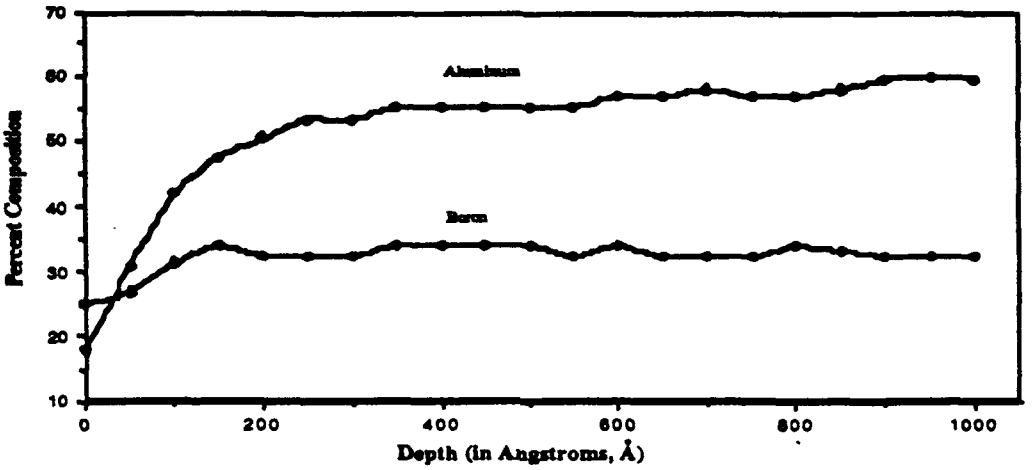

Figure 7. Auger electron spectrum (AES) of a thin film deposited from compound **13** on Si(100) at room temperature.

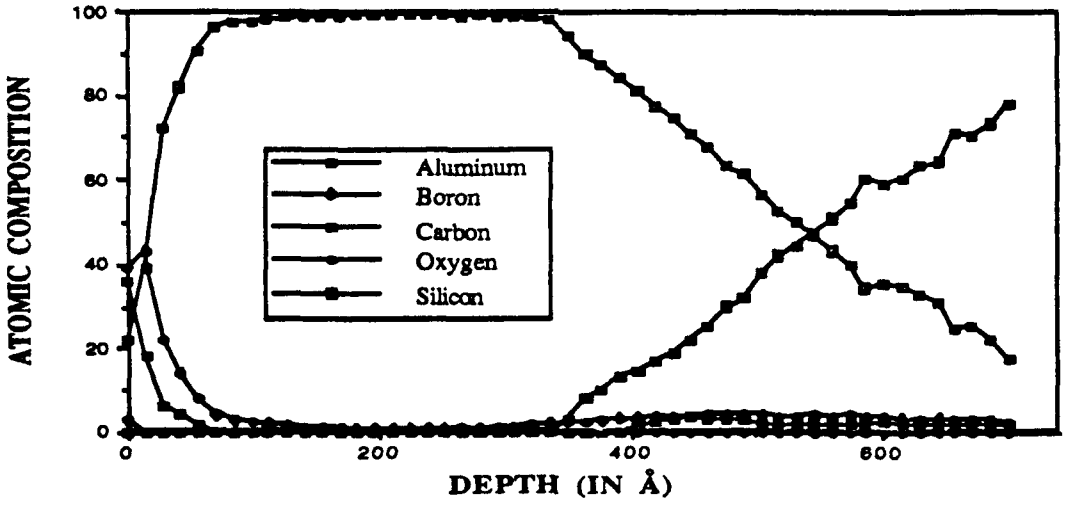

The three source compounds, **12** - **14**, were, in general, relatively thermally stable, volatile, air-sensitive liquids, thus providing nearly ideal precursor properties for chemical vapor deposition experiments.

5. Metal Borides

As an extension of our work, we have explored the use of our new metallaborane complexes in the formation of technologically very important metal boride thin films. The fundamental interest in the preparation, theoretical modelling and solid state characteristics of metal borides arises both from their unique physical properties among solid state materials and their structural diversity. Metal borides are typically extremely refractory materials with melting points frequently far in excess of the pure metal or other metal binary systems. These metal borides are also exceptionally hard materials which are not significantly affected even by the most rigorous of chemical environments. The metal borides are typically rather good electrical conductors, with some displaying superconducting properties at low temperatures. Thus, metal borides have found increased use not only in traditional applications, such as hard coatings for cutting tools, but also in thermally and chemically taxed aerospace components, high-energy optical systems and in new magnetic materials.

In an effort to extend the use of boron-based source materials in the preparation of metal borides by MOCVD, we initially investigated the formation of nickel boride films.[24-27] In our work, we demonstrated that high purity conformal nickel boride thin films can be readily prepared with stoichiometric control from the pyrolytic reaction of $NiCl_2$ with boron clusters using a "hot wall" reactor system shown in Figure 8. The deposition of both metal-rich and boron-rich thin film phases of nickel boride from boron-containing precursor compounds by a cluster deposition process was demonstrated. The films were formed either adhered to various substrates, such as copper, SiO_2, GaAs or pyrex, or as a substrate-free material. It was possible to control the nickel:boron ratio of the film by controlling reactor temperature, borane flow rate and base vacuum conditions. Films with nickel contents as high as 99.9 % and as low as 56.6 % have been prepared using this technique. The thin films were characterized by XES, AES, SEM, XRD, FT-IR, TEM and electron diffraction experiments. The films were shown by AES to be compositionally uniform in bulk sample (Figure 9). A relationship was found to exist between the

temperature during deposition and the film composition, with a maximum nickel content reached at approximately 530°C. The effects of annealing were studied for the nickel-rich and the boron-rich

Figure 8. The experimental setup for the formation of nickel boride thin film materials from boron-containing source compounds using a "hot wall" reactor system.

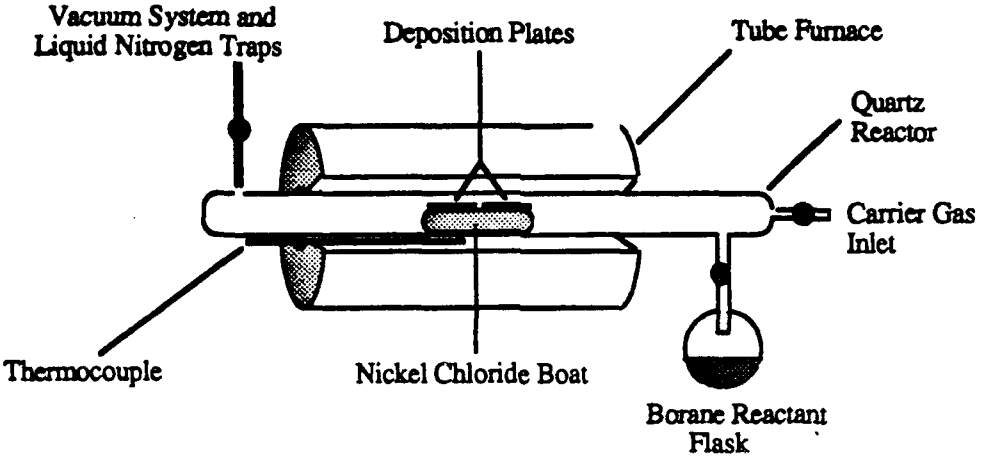

Figure 9. Representative Auger electron spectrum of a nickel boride thin film deposited using a *nido*-pentaborane(9), B_5H_9, borane source kept at -78° C during the deposition. The depth profile was constructed from Auger electron spectra as the film was sputtered using Ar+ ion milling. Sputter times are given in minutes and the atomic compositions are given in percent.

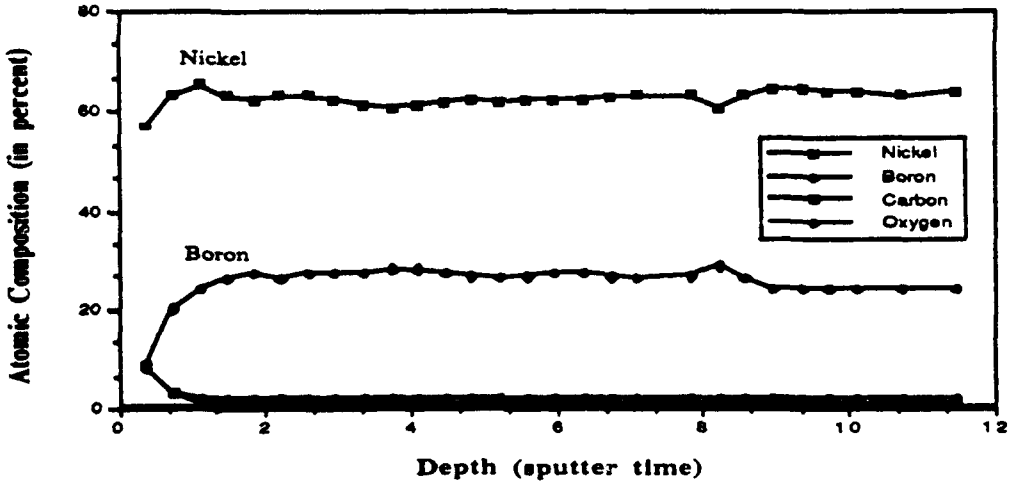

films by SEM, XRD and electron diffraction experiments. SEM data for the annealed boron-rich films showed the formation of perfect hexagonal crystals in a channeled columnar matrix. Electron diffraction data showed that this crystalline phase is orthorhombic Ni_3B_7 isolated in a Ni_3B matrix. The as-deposited nickel-rich films were found by XRD studies to be primarily pure nickel, containing relatively small amounts of Ni_3B. Vacuum annealing of these nickel-rich films resulted in an observed decrease in the Ni_3B phase relative to the pure nickel phase in the XRD. The magnetic properties of the nickel boride thin films were determined using a torque magnetometer. The magnetic moment of a typical NiB film was calculated to be 81.2 Gauss. The NiB alloy films were found to be very soft magnets, thus making them good candidates for such applications as magnetic recording media. In comparison, CrO_2, a common recording medium, has a magnetic saturation of either 470 to 480 G or 326 to 355 G for particles of 0.6 μm. Defects may play an important role in determining the magnetic properties of the NiB films. Mutlu and Aydinuraz have reported that the room temperature susceptibility for large particles of NiB is 1.4×10^{-6} emu/g, but that the susceptibility increases significantly for small particles ($d \leq 0.23$ mm). These differences have been attributed primarily to film defects. We have continued our investigation of this deposition and CVD chemistry, including the applicability of the process to other metal systems. Recent results have shown that films of titanium, iron and lanthanide boride are formed in analogous deposition chemistry. The mechanism of the deposition and the magnetic properties of the thin films are also under investigation. In addition, pure copper films were prepared from the CVD of Cu_2Cl_2 and B_5H_9 in a similar process.

6. Metal reactions with GaAs

A large portion of our research program was directed toward growing GaAs on metals. The GaAs/metal interface was deemed to be of considerable importance, in particular chemical reactions at the interface were suspected to be a potential problem.

Surface segregation, interdiffusion and reactivity at the GaAs interface were estimated, based upon simple thermochemical reasoning.[28] The results from these simple models were found to be in good agreement with experimental data.

Metals are known to form Schottky barrier diodes with GaAs, with the quality of the

Schottky barrier dependent upon the quality of the GaAs surface and orientation.[29,30] We concluded from these results that the growth of GaAs on metals should be undertaken at the lowest temperatures possible to suppress the interdiffusion and reactivity problems encountered at the GaAs/metal interface.

A videotape we recently furnished RADC demonstrated our capability of depositing Pd on GaAs, forming good Schottky barrier diodes, with submicron aspect ratios and good (micron) spatial resolution. No photoemission was observed unless the system was illuminated, indicating that these junctions are of high quality. These photolithography experiments were conducted at the Wisconsin synchrotron facility.

7. Projection Lithography

One methodology for depositing metals at very low temperatures is to use an organometallic source compound. A metal film can be grown from these complexes at significantly reduced temperatures (near room temperature, as demonstrated for the Al work described above).[31] Incident radiation- induced depositions can be spatially very selective[31,32] and non-pyrolytic[31] when electrons or photons are used to overcome the activation barriers to molecular dissociation.[33-36]

Selective area deposition is important for several reasons; (1) if metal features can be deposited on GaAs by projection, damage to preexisting features on the GaAs surface is likely to be reduced,[35,36] (2) the many steps of conventional lithography can be reduced to one or two steps, (3) "snow-plowing" and other interfacial problems can be minimized, and (4) lithographic features can be fabricated on potential substrates (a metal ground plane in the case of this project) and device quality features (field effect transistor and p-n junctions on GaAs in this work) can be deposited on the semiconductor film.

We undertook to develop projection lithography of metals on a wide variety of substrates[31,34,37] to demonstrate that metallic features for ohmic contact on GaAs ground planes could be fabricated with the correct topography and feature resolution (<1 μm). The success of this part of the project varied with the organometallic source compound and was not universal, though good feature resolution was demonstrated (Figs. 10-12). Fabricating the desired corrugated topography in the metal substrate was nonetheless demonstrated to be clearly feasible.[31,34,37]

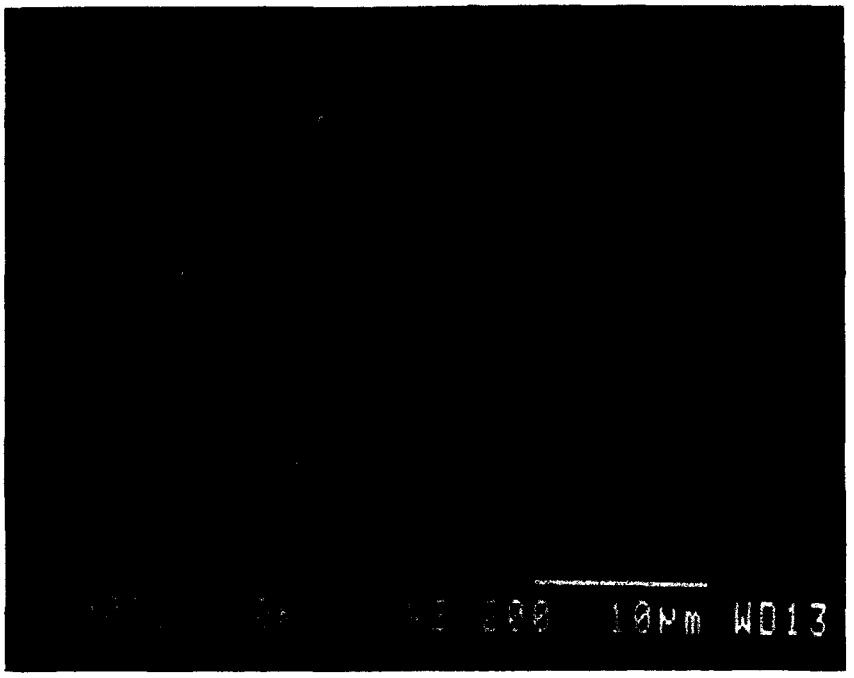

Figure 10.

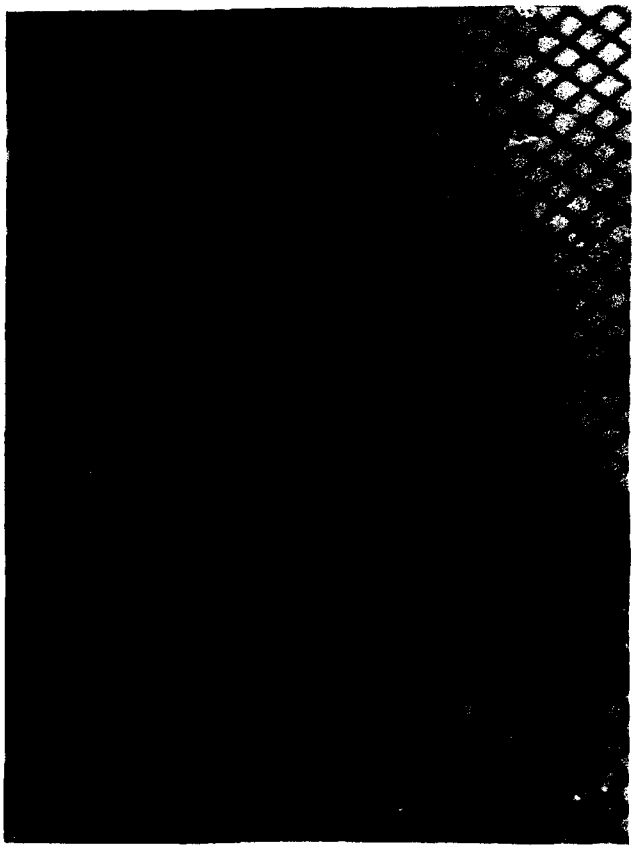

Figure 11.

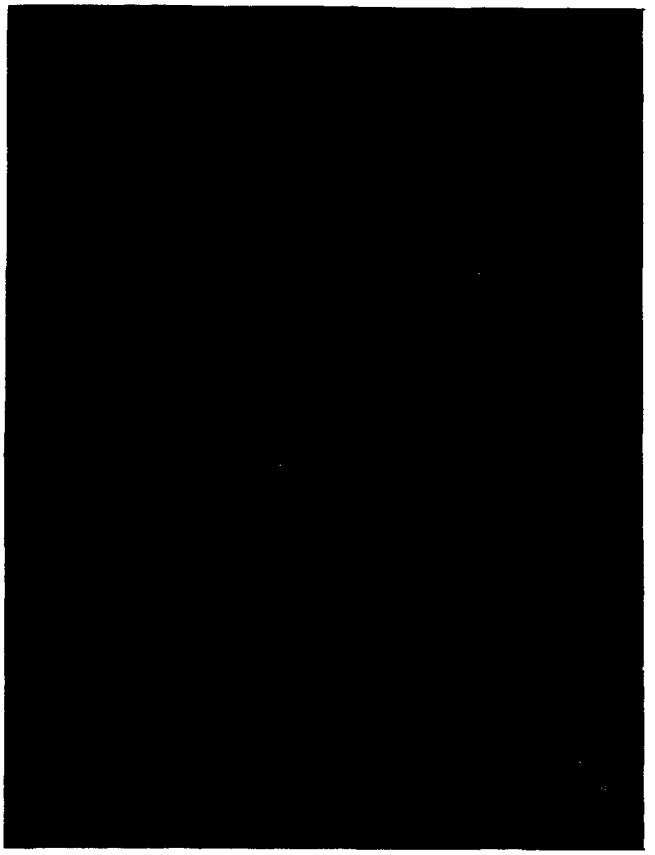

Figure 12.

8. Metal-Organic Chemical Vapor Deposition

Considerable effort was given to attempting the deposition of compound semiconductors at ambient (room) temperature. This work concentrated upon the deposition of quality thin films from single rather than multiple source compounds.[28,31] Because of the synthetic restrictions above, the deposition of "electronic" grade boron[32,33] and boron-carbide thin films was explored.[38]

We found that devices such as p-n junctions and delta doping layers could be fabricated from large borane cluster compounds.[32,33] Feature resolution much less than 1 μm could readily be achieved. These compounds were demonstrated to be compatible with synchrotron radiation (X-ray) projection lithography.[32,33] This proved to be the first practical demonstration of this technology - and while devices were not directly characterized, optical properties, compositions and structures of the deposited films were determined.

Compositionally modulating the compound semiconductor for boron carbides was also shown to be feasible and the band gap and electron mobilities could be modified in this manner.[38,39] Boron carbide films are also seen to be extremely hard protective coatings and sputter resistant.[39]

9. Graphoepitaxy

Little now stands in the way of developing graphoepitaxial technology for compound semiconductors. To this end, a laser annealing (CO_2) system with less than 1 μm movement control has been designed and the computer software is currently being developed.

References to Section B.

1. Glass, J. A., Jr.; Whelan, T. A.; Spencer, J. T. *Organometallics* **1991**, 10, 1148.
2. Brint, P.; Sangchakr, B.; McGrath, M.; Spalding, T.; Suffolk, R.J. *Inorg. Chem.* **1990**, 29, 47.
3. Glass, J. A., Jr.; Whelan, T. A.; Spencer, J. T. unpublished results.
4. Haubold, W.; Keller, W.; Sawitzki, G. *Angew. Chem. Int. Ed. Engl.* **1988**, 27, 925.
5. Friedman, L.B.; Perry, S.L. *Inorg. Chem.* **1973**, 12, 288.

6. Todd, L.J.; Paul, I.C.; Little, J.L.; Welcker, P.S.; Peterson, C.R. *J.Am. Chem. Soc.* **1968**, 90, 4489.
7. Mastryukov, V.S.; Atavin, E.G.; Vilkov, L.V.; Golubinskii, A.V.; Kalinin, V.N.; Zhigareva, G.G.; Zakharkin, L. I. *J. Mol. Struct.* **1979**, 56, 139.
8. Wong, H.S.; Lipscomb, W.N. *Inorg. Chem.* **1975**, 14, 1350.
9. Getman, T.D.; Deng, H.-B.; Hsu, L.-Y.; Shore, S.G. *Inorg. Chem.* **1989**, 28, 3612.
10. Little, J.L.; Kester, J.G.; Huffman, J.C.; Todd, L.J. *Inorg. Chem.* **1989**, 28, 1087.
11. Thornton-Pett, M.; Beckett, M.A.; Kennedy, J.D. *J. Chem. Soc., Dalton Trans.* **1986**, 303.
12. Wood, G.L.; Duesler, E.N.; Narula, C.K.; Paine, R.T.; Noth, H. *J. Chem. Soc., Chem. Commun.* **1987**, 496.
13. Lee, S. -W.; Li, D.; Dowben, P. A.; Perkins, F. K.; Onellion, M.; Spencer, J. T. *J. Am. Chem. Soc.* **1991**, 113, 8444.
14. Lee, S. -W.; Dowben, P. A.; Wen, A. T.; Hitchcock, A. P.; Glass, J. A., Jr.; Spencer, J. T. *J. Vac. Sci. Technol.* **1992.**
15. Hitchcock, A. P.; Wen, A. T.; Lee, S. ; Glass, J. A., Jr.; Spencer, J. T.; Dowben, P. A. in preparation for submission to *J. Am. Chem. Soc.*
16. (a) Arif, A. M.; Benac, B. L.; Cowley, A. H.; Geerts, R.; Jones, R. A.; Kidd, K. B.; Power, J. M.; Schwab, S. T. *J. Chem. Soc., Chem. Commun.* **1986**, 1543. (b) Tzschach, A.; Deylig, W. *Z. Anorg. Allg. Chem.* **1965**, 336, 36.
17. (a) Miller, R. W.; Spencer, J. T. manuscript completed and pending submission. (b) Miller, R. W.; Donaghy, K. J.; Spencer, J. T. *Phosphorus, Sulfur and Silicon* **1991**, 57, 287-292.
18. Miller, R. W.; Donaghy, K. J.; Spencer, J. T. *Organometallics* **1991**, 10, 1161.
19. Goodreau, B. H.; Ostrander, R. L.; Spencer, J. T. *Inorg. Chem.* **1991**, 30, 2066.
20. Glass, J. A., Jr.; Kher, S.; Hersee, S. D.; Ramseyer, G. O.; Spencer, J.T. *Mat. Res. Soc. Symp. Proc.* **1991**, 204, 397.
21. Glass, J. A., Jr.; Kher, S.; Spencer, J. T. *Thin Solid Films* **1992**, 207, 15.
22. Glass, J. A., Jr.; Kher, S.; Spencer, J. T. *Chem. Mater.* **1992.**
23. Datta, S.; Glass, J. A., Jr.; Kher, S.; Kim, Y. -G.; Dowben, P. A.; Spencer, J. T.

accepted for publication in *Electrochem. Soc. Symp. Proc.* **1992.**

24. Glass, J. A., Jr.; Kher, S.; Kim, Y. -G; Dowben, P. A.; Spencer, J. T. *Mat. Res. Soc. Symp. Proc.* **1991**, 204, 439.
25. Kher, S.; Spencer, J. T. *Chem. Mater.* **1992.**
26. Kher, S.; Spencer, J. T. "Chemical Vapor Deposition of Pure Nickel and Nickel Boride Refractory Thin Films From Borane Cluster Compounds" *Mat. Res. Soc. Symp. Proc.* **1992** in press.
27. Kher, S.; Spencer, J. T. in preparation for submission to *Chem. Mater.*
28. Dowben, P.A.; Miller, Eds., *Surface Segregation*: CRC Press: Boca Raton, 1990 [ISBN-0-8493-6893].
29. Chang, S.; Brillson, L.J.; Kime, Y.J.; Rioux, D.S.; Kirchner, P.D.; Pettit, G.D.; Woodall, J.M. *Phys. Rev. Lett.* **1990**, 64, 2551.
30. Chang, S.; Brillson, L.J.; Rioux, D.S.; Kime, Y.J.; Kirchner, P.D.; Pettit, G.D.; Woodall, J.M. *J. Vac. Sci. Technol. B* **1990**, 8, 1008.
31. Dowben, P.A.; Spencer, J.T.; Stauf, G.T. *Mat. Sci. Eng.* **1989**, B2, 297.
32. Rosenberg, R.A.; Perkins, F.K.; Mancini, D.C.; Harp, G.R.; Tonner, B.P.; Lee, S.; Dowben, P.A. *Appl. Phys. Lett.* **1991**, 58, 607.
33. Perkins, F.K.; Rosenberg, R.A.; Lee, S.; Dowben P.A. *J. Appl. Phys.* **1991**, 69, 4103.
34. Kim, Y.-G.; Bialy, S.; Stauf, G.T.; Miller, R.W.; Spencer, J.T.; Dowben, P.A.; Datta, A. *J. Micromech. Microeng.* **1991**, 1, 42.
35. Kim, Y.-G. Ph.D. Thesis, Solid State Science and Technology, in preparation.
36. Lee, S. Ph.D. Thesis, Solid State Science and Technology, in preparation.
37. Mancini, D.C.; Varma, S.; Simons, J.K.; Rosenberg, R.A.; Dowben, P.A. *J. Vac. Sci. Technol.* **1990**, A8, 1804.
38. Mazurowski, J.; Baral-Tosh, S.; Ramseyer, G.O.; Spencer, J.T.; Kim, Y.-G.; Dowben, P.A. *Mat. Res. Soc. Proc.* **1991**, 190, 101.
39. Mazurowski, J., M.S. Thesis, Physics Department, Syracuse University, in preparation.

C. Raman Characterization of Graphoepitaxial GaAs, J. Chaiken

Our purpose was to characterize thin film GaAs on a variety of substrates using Raman spectroscopy. The degree of crystallinity[1], the presence of surface damage[2] and/or strain[3], the stoichiometry[4], the orientation[5], and qualities related to interfaces involving GaAs films[6], are potentially accessible using Raman spectroscopy. Because the process of graphoepitaxy[7] would affect precisely those properties of the films, Raman is a characterization method of choice. We present Raman characterization of four GaAs films/samples. These spectra are consistent with established selection rules[5], related spectra in the literature and those taken of authentic samples as a part of the effort. Our results suggest that, even in a production type environment, it is possible to discern orientation and the degree of crystallinity of a given sample of GaAs using Raman spectroscopy. We show that Raman is adequately sensitive to monitor the progress of graphoepitaxy. With regard to the ability to use graphoepitaxy to produce improved MMIC device performance, the prognosis is still uncertain but optimistic.

1. Introduction

Vibrational spectroscopy was applied to GaAs at least as far back as 1962. By 1964, the Raman polarizability tensor had been tabulated[5], allowing exploitation of polarization and wavevector selection rules for GaAs characterization. Using inelastic neutron scattering[8] and IR absorption[9] to assign the phonon spectrum, Raman has since been routinely used on bulk GaAs and thin films. Whether we are characterizing discrete films, or one layer of a superlattice[10], there is substantial literature for comparison with our results.

Indeed, to evaluate the unique films used in this MMIC study, it was essential to have spectra for comparison. The skin depth of GaAs[3] at 4880Å is ≈950Å so the Raman spectra reflect the condition of the GaAs within that distance of the surface. Because we were interested in evaluating the process of graphoepitaxy, we were careful to use as low a laser power level and the shortest exposure times possible. Because of the work which has been done to characterize the perturbed Raman spectrum observed when doped GaAs is used, we felt confident that we would be able to perform the Raman characterization without inducing loss of arsenic. We were able to

extend the scope of our study to include "graphoepitaxy-like" changes induced by the Raman excitation laser.

Graphoepitaxy has not been investigated using Raman spectroscopy before. The goal of the graphoepitaxy was to allow fabrication of ceramic-under-metal-under GaAs heterostructures that could then be used as a substrate for deposition of a device- quality epilayer. This epilayer would be the substrate for an MMIC device. The graphoepitaxy process is not well understood but involves repeated transient annealing of GaAs which has had physical boundaries imposed on its microscopic morphology that apparently aid in the elimination of defects, and enforcement of a given orientation in the material produced after the final laser annealing stage.

During the transient annealing, the material has a tendency to lose arsenic due to evaporation, so it is usually necessary to utilize a backing pressure of arsenic[11] to maintain the stoichiometry of the material throughout the process. There are disorder-induced modes and selection rule breaking, which should be observable if the excitation laser heats the surface enough to induce loss of arsenic.

It should be recognized that graphoepitaxy is a composite process which has a series of stages, and all must proceed successfully to achieve the desired effects. The correct surface relief pattern (physical boundary) must be fabricated, a middle metal(backplane) layer must be placed and serve as the substrate for the deposition of GaAs. The GaAs must be deposited and characterized. Given successful fabrication of a suitable sample, the graphoepitaxy procedure must be executed, i.e. the laser must be rastered across the surface of the trilayer and the material successively recharacterized.

The order in which the sample fabrication steps are performed, and the materials used, are only two of the myriad questions which arise in attempting graphoepitaxy. Conflicting criteria applying to what is needed to successfully complete each of the different steps make the enterprise a balancing act. We have identified criteria, potential candidates for materials, and methods of characterization. This is an important initial accomplishment towards the overall goal of bringing graphoepitaxy to an MMIC production/manufacturing environment.

2. Experimental Details

All Raman spectra were taken with the apparatus[12] depicted in Figure 13 and schematically elsewhere. A line- tuned argon ion laser (Lexel)fitted with a polarization selection element is capable of delivering ≈60 mW @ 5145Å, and nearly twice that at 4880Å, of laser power to the sample. After exiting the polarization selector, the laser light traverses 4 mirrors, a laser plasma line filter, a focussing lens(500 cm focal length), and a 0.635cm- thick glass observation port. All spectra are taken in a 100% backscattering geometry. The scattered light is collected using a mirror with a hole which allows the incident light to contact the sample, and the specularly backreflected light beam to exit the collection zone. The scattered light is directed by the mirror with a hole towards a glass lens (10cm focal length), through a holographic edge filter(POC 4880Å and 5145 Å), and into the Spex Triple Mate spectrograph.

At the exit slit of the "Triple Mate's" filter stage a piece of plastic polarizer was inserted. Using a reflective metal sample, it was possible to rotate the polarizer in the Spex to completely block the Rayleigh line. The plastic polarizer could then be easily rotated by 90°. This arrangement, together with the polarization selector of the laser, allowed the systematic observation of polarization effects. The spectra are presented in the format<-I> which we describe as follows: The first line indicates the polarization of the laser with respect to an arbitrary direction in the lab frame; - means perpendicular to the lab axis and I means parallel. The second refers to the polarization selected in the detection system with respect to the incident polarization.

Because of the 100% backscattering orientation used, the light was always incident along the crystal "z" axis. Here, and always, we use the coordinate system conventions of Louden and Nye[13]. The orientation of the laboratory-fixed axes with respect to the x and y axes of the (100)GaAs crystal faces was chosen as follows. We observed that the material had a severe directional preference when we attempted to cleave it. Clean breaks could always be obtained when the material was cleaved in one direction, but severe fracturing always occured when we attempted to cleave the material in the orthogonal direction. Even while scribing, a decided directionality was evident. This procedure allowed us to place this particular material in the Raman chamber and choose the orientation of the laser polarization selector, such that the light was either polarized parallel(I) or perpendicular(-) to the "direction of easy cleavage". Given fully oriented film

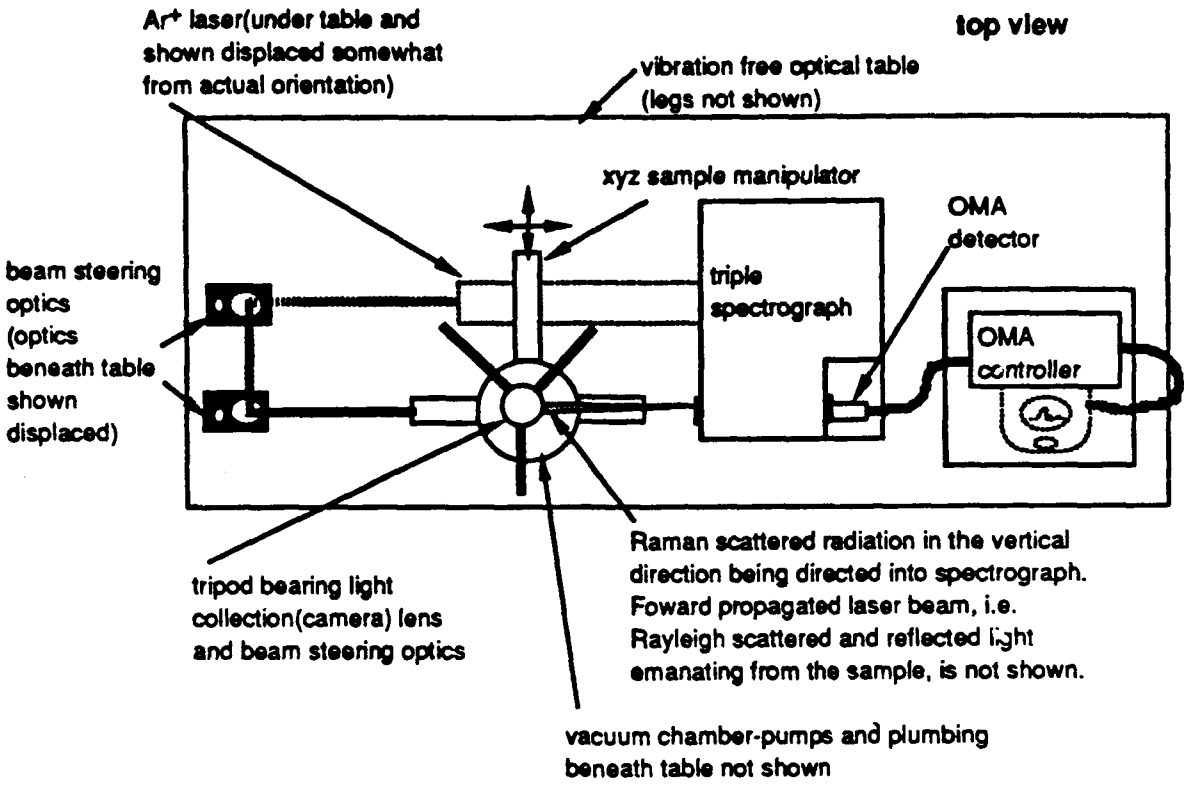
Ar+ laser(under table and
shown displaced somewhat
from actual orientation)
top view
vibration free optical table
(legs not shown)
xyz sample manipulator
OMA
detector
beam steering
optics
(optics
beneath table
shown
displaced)
triple
spectrograph
OMA
controller
Raman scattered radiation in the vertical
direction being directed into spectrograph.
Foward propagated laser beam, i.e.
Rayleigh scattered and reflected light
emanating from the sample, is not shown.
tripod bearing light
collection(camera) lens
and beam steering optics
vacuum chamber-pumps and plumbing
beneath table not shown

Figure 13.

samples, it would be possible to use the first designation together with crystal symmetry and selection rules, to obtain even more information concerning the GaAs. For our present purposes, we had adequate information

The spectra represented by the following two designations, <I-> and <-->, have the same orientation for the detection polarizer *but the polarizer on the laser has been rotated by 90°*. In the case of the film samples, we had no independent observable upon which to guide our attempt to orient the cystal x and y axes with respect to the laser polarization vector. Because GaAs is a tetrahedral compound, unless the sample is oriented so that its planes are at exactly 45° to our initial choice of laser polarization, which incidentally can be chosen arbitrarily, a rotation of the light polarization angle by 90° guarantees a different projection of the incident laser polarization vector onto the GaAs samples' x and y axes. In the case of the (100)GaAs bulk material, the "direction of easy cleavage" was used to insure maximal polarization effects. For the film samples, our current goal is well served because we can use the data taken to deduce which Raman features are polarized and which are depolarized.

The light was detected using an EG&G OMA III system. All spectra were taken with the photocathode and detector array at -40°C with a dark current of ≈16 counts per second. The optical detection system was arranged to minimize the effect of light scattering involving the obervation port. Besides subtraction of the detector dark current, another correction was made for rejection of observation port related stray light. A piece of thick black paper was placed over the observation port, which just allowed the Raman excitation beam to enter and exit the port. In this configuration, light detected by the OMA contains a very small component of Raman- scattered signal and so can be subtracted from a GaAs spectrum to remove residual stray light not eliminated in the earlier optimizations of the collection system. Spectra taken with and without the black paper show unequivocally that the Raman signal is coming from inside the chamber. This is particularly important when observing Raman at very small wavenumber shifts, ≤100 cm^{-1}.

All film spectra were taken at room temperature in a vacuum ranging from ≈10^{-7} to ≈10^{-9} torr. Spectra of the bulk (100)GaAs were obtained under a variety of conditions including atmospheric conditions. The tendency of GaAs not to form a native oxide is well supported by our observations.

3. Results

Sample preparation and characterization was performed by Vook's group and will not be discussed here. The (100)GaAs sample was obtained from GE. A Raman spectrum of bulk (100)GaAs, obtained using 4880Å excitation, is shown in Figure 14. All the others shown were obtained using 5145Å, and are very similar. The spectra clearly show broad features which begin very close to the Rayleigh line and extend out to as far as 400 cm^{-1} to the Stokes side. Antistokes spectra are consistent with the Stokes spectra. The most important point is that the spectra are essentially independent of excitation wavelength, so we may safely assume that the features we are observing are Raman scattering and not photoluminescence.

Before surveying the spectra which are presented in Figures 15-39, a discussion of the applicable selection rules is particularly important. Raman spectra of (100) and (110)GaAs, taken in a 100% backscattering geometry, have forbidden A and E fundamentals. However, there are modes of F symmetry which are allowed. Because the (111) material in our apparatus forces a projection of the laser polarization vector onto all of the crystal axes, there are allowed A and E modes for (111)GaAs in addition to allowed F type modes. Because of the uncertainty in aligning the GaAs x and y axes with the laser polarization vector, the depolarized spectra(either(-I) or (I-)) were not expected to be identical. In addition, it was observed that the reflectivity of the surface was a strong function of the laser polarization direction. Although this observation is consistent with the fact that the conductivity of GaAs is direction- dependent, we did not use the observation to find the GaAs x and y axes. We do note that it might be possible in the future.

We begin our survey of Raman spectra by noting that the undoped GaAs with the (100) orientation, which might be arsenic- deficient at the surface due to its exposure to the air, displays broad features, in Figures 15-18, just like those obtained using the films. The depolarized spectra of this material show a decided peak, near 238 cm^{-1}, which appears in only one orientation. The sum of the spectra of Figures 15-18 resembles Figure 14. Note that the power level used to excite the Raman spectrum in Figure 14 was at least a factor of two larger than that used in all the 5145Å spectra. Selection rules dictate that only one *depolarized* mode, of F(x) character, is allowed for this arrangement of laser and sample. Furthermore, the fact that this mode is x- polarized means that, as can be seen in the figures, its activity is not isotropic with respect to the polarization of the

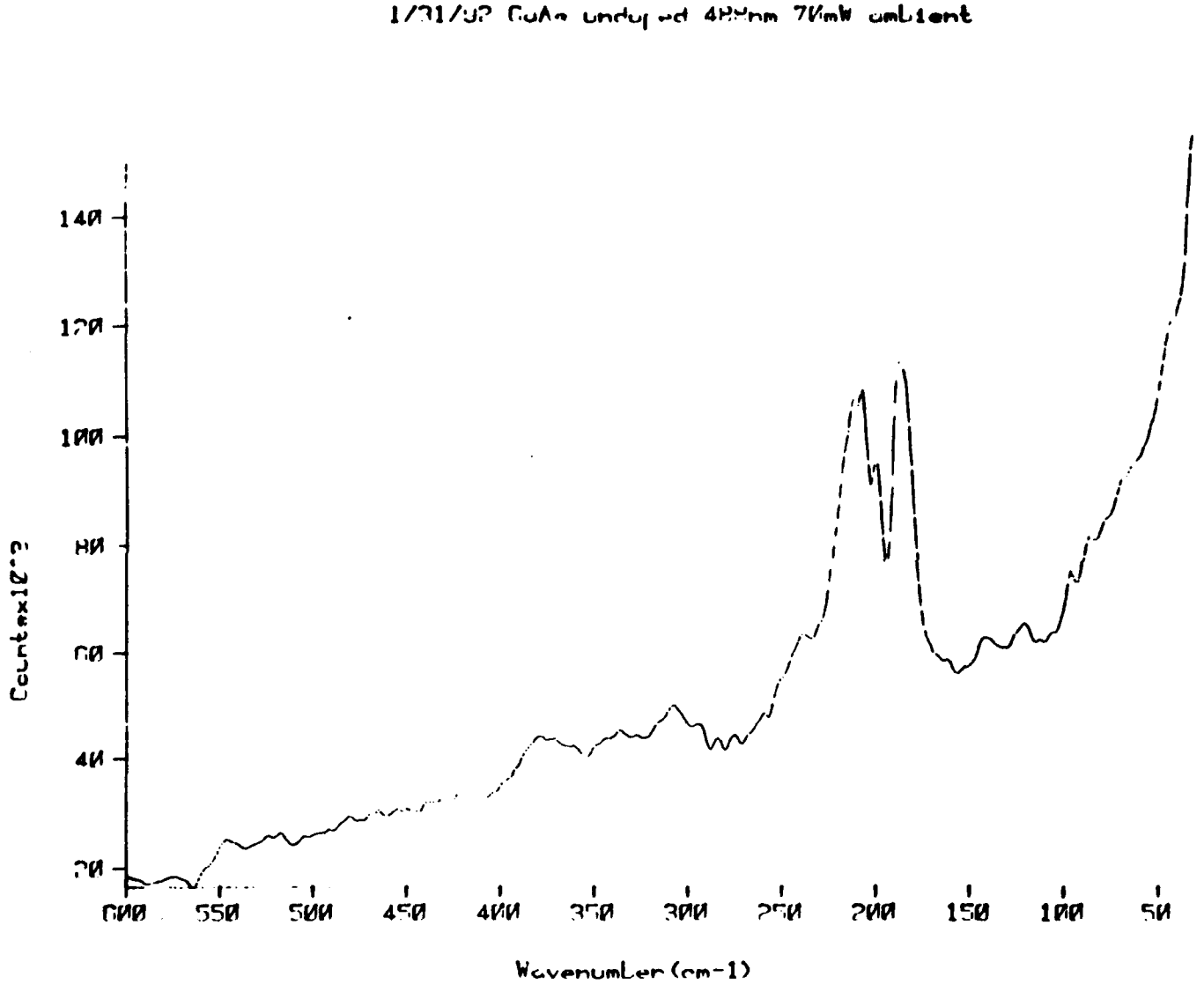
1/31/92 GaAs undoped 488nm 70mW ambient
140
120
100
80
60
40
20
Counts x10^2
600
550
500
450
400
350
300
250
200
150
100
50
Wavenumber (cm-1)

Figure 14.

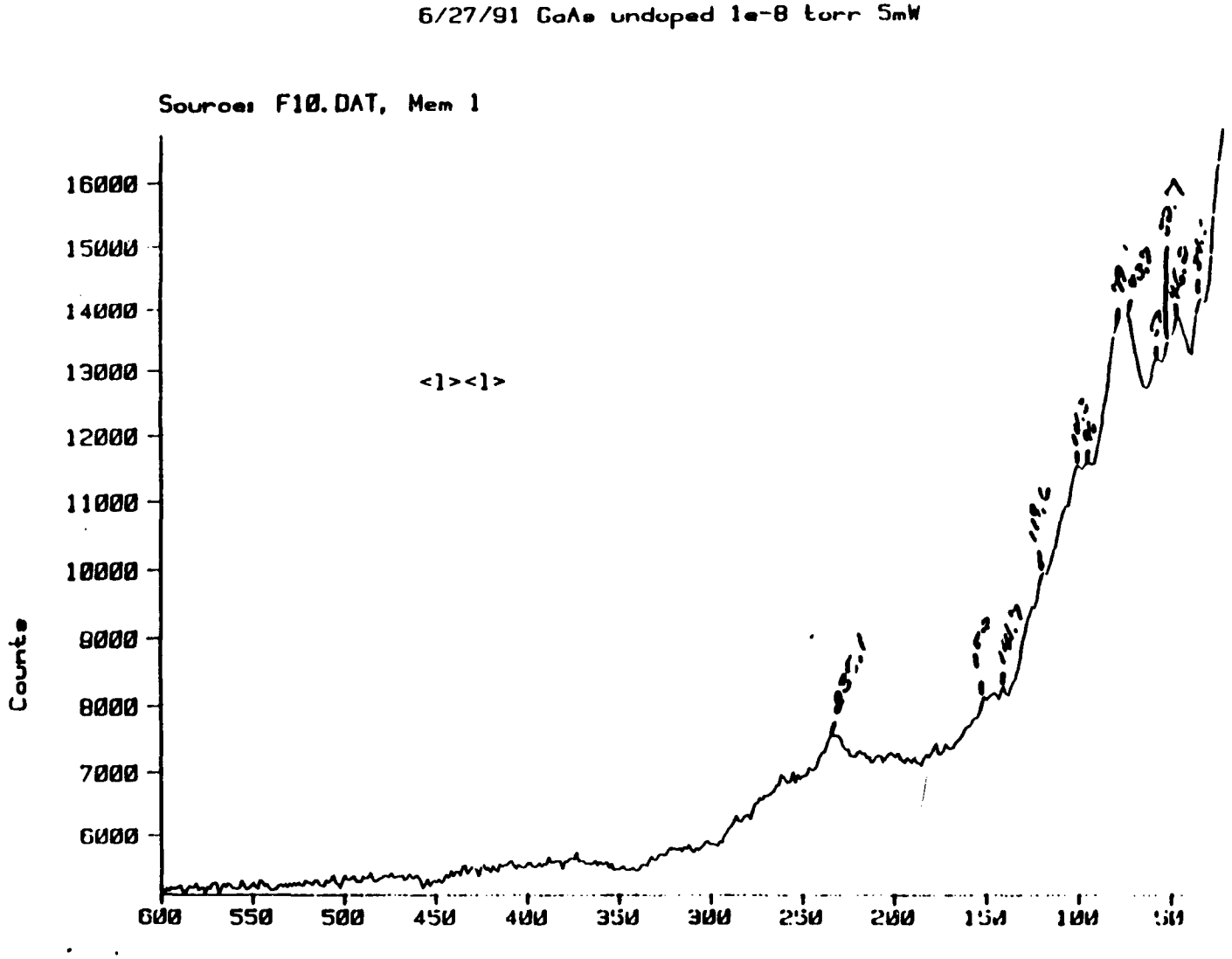
6/27/91 GaAs undoped 1e-8 torr 5mW
Source: F10.DAT, Mem 1
<1><1>
Counts
16000
15000
14000
13000
12000
11000
10000
9000
8000
7000
6000
600
550
500
450
400
350
300
250
200
150
100
50

Figure 15.

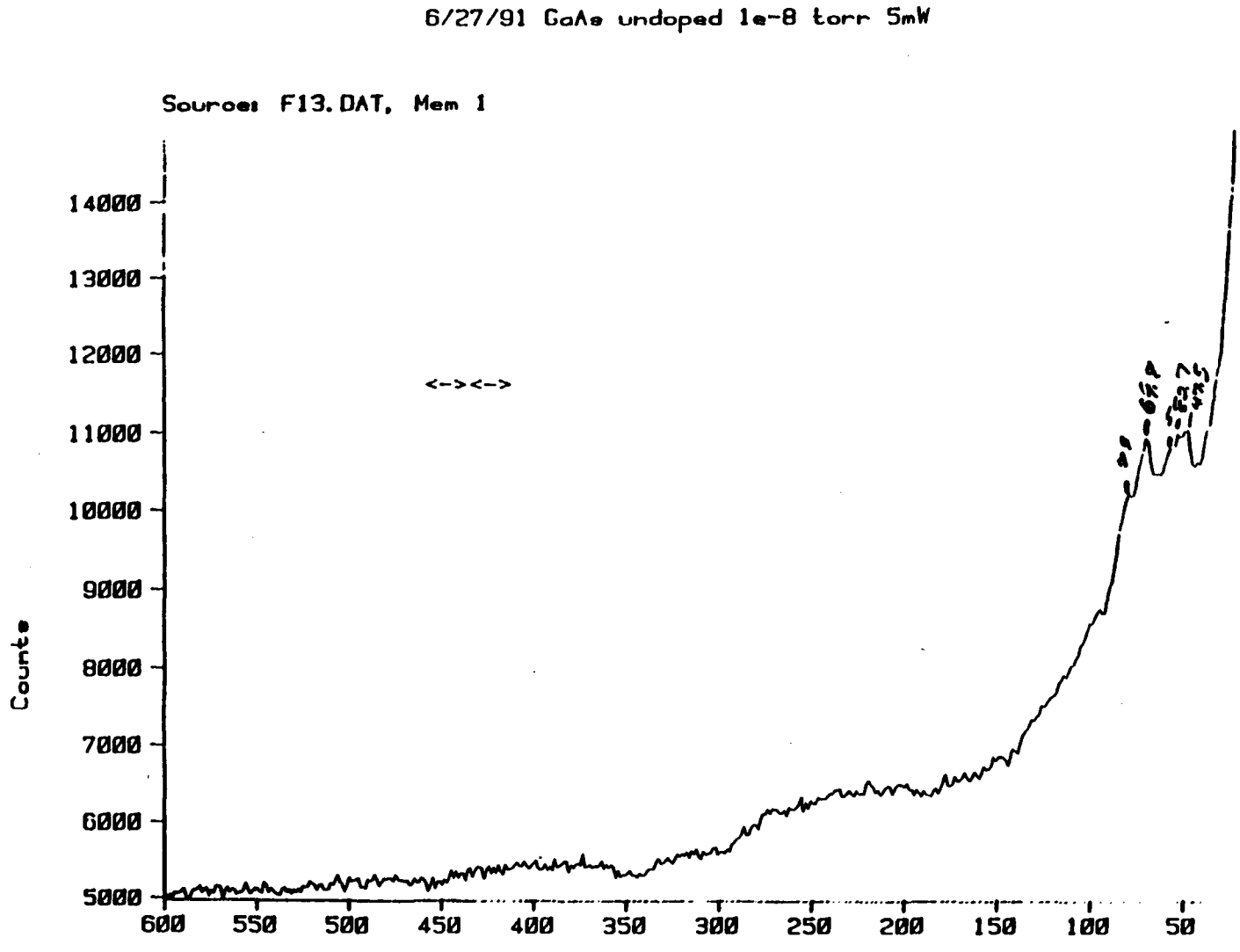
6/27/91 GaAs undoped 1e-8 torr 5mW
Source: F13.DAT, Mem 1
Counts
14000
13000
12000
11000
10000
9000
8000
7000
6000
5000
600
550
500
450
400
350
300
250
200
150
100
50

Figure 16.

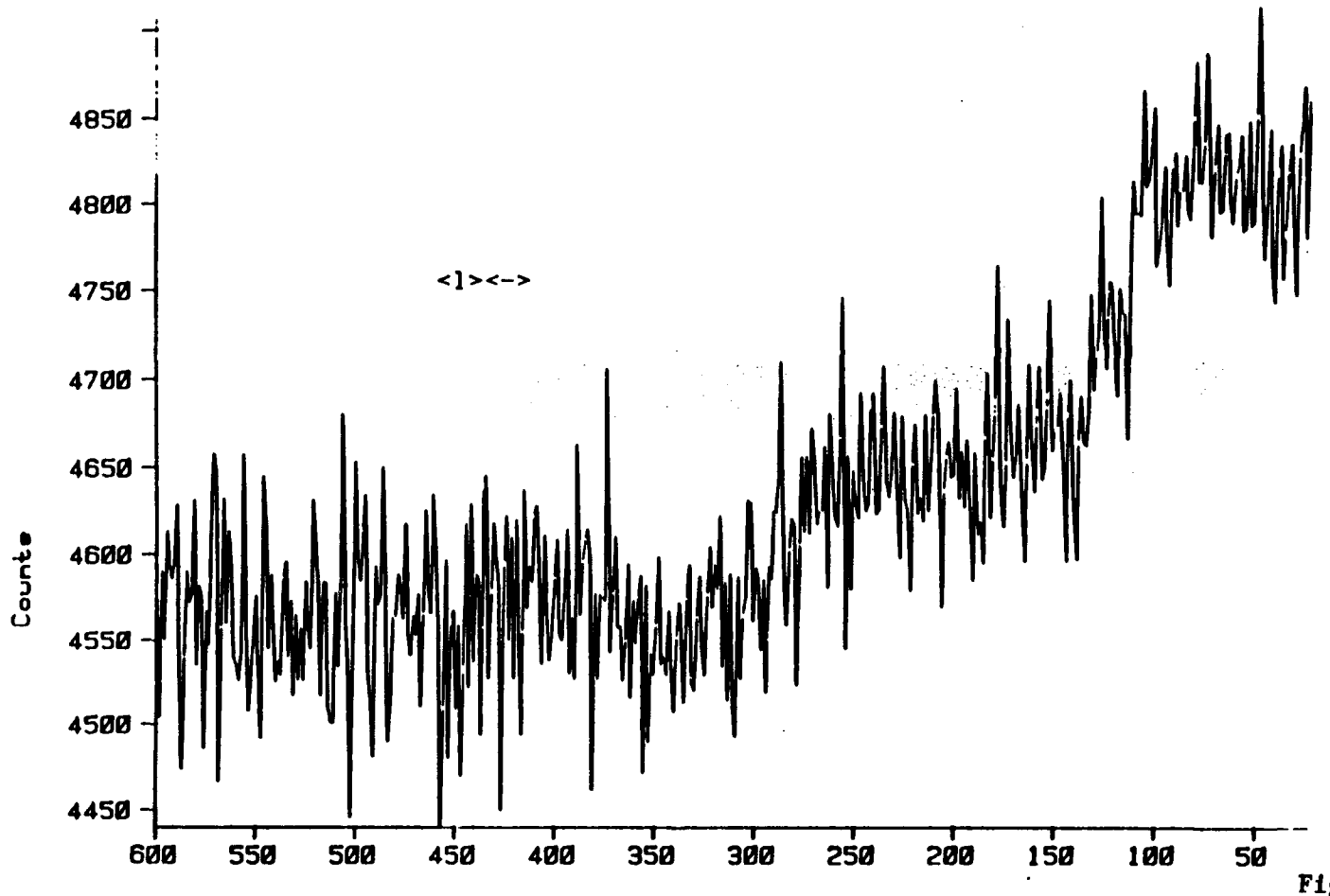
6/27/91 GaAs undoped 1e-8 torr 5mW
Source: F11.DAT, Mem 1
<1><->
Counts
4850
4800
4750
4700
4650
4600
4550
4500
4450
600
550
500
450
400
350
300
250
200
150
100
50

Figure 17.

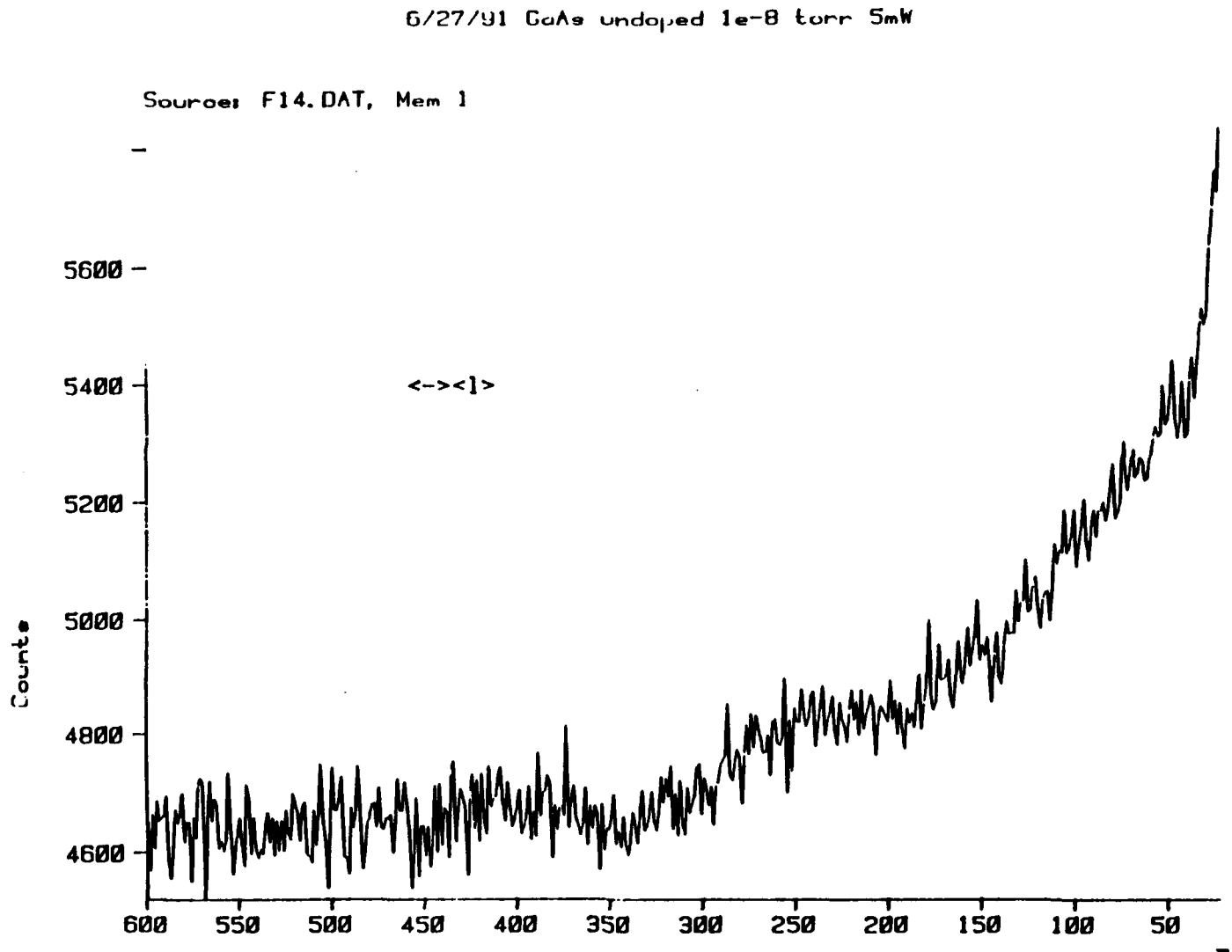
6/27/91 GaAs undoped 1e-8 torr 5mW
Source: F14.DAT, Mem 1
<-><1>
Counts
5600
5400
5200
5000
4800
4600
600
550
500
450
400
350
300
250
200
150
100
50

Figure 18.

exciting laser. Thus, our Raman spectra are consistent with applicable selection rules.

In comparison with the literature, our spectra show weak and broad Raman activity. We usually observe a diffuse feature centered at ≈400 cm^{-1}, another at ≈250 cm^{-1} and stronger activity at lower shifts. The combination of neutron diffraction and infrared absorbance has identified the frequencies of all the GaAs modes and it would be easy to assign the frequencies we observe to labels from the literature. Instead, because we are interested in issues relating to morphology and orientation, we choose to relate less of actual frequencies and more of the sensitivity of the spectra to polarization and directional tests. It must be remembered that our spectra were typically taken with less than one tenth the incident excitation power and in very short accumulation times, compared to nearly all the literature spectra. Furthermore, the literature spectra usually employ much tighter focussing and photomultiplier detection. Thus our spectra should exhibit the weaker signals we observe. Following a computer- aided search of literally hundreds of references, only one literature spectrum that we know of shows stronger Raman activity using lower incident power, but in this case the excitation wavelength is 6328Å and, being nearer to the band gap, would be expected to exhibit somewhat enhanced Raman activity.

The GaAs-on-glass samples (25°C deposition temperature; see Table I) are shown in Figures 19-22. These samples are opaque, and are likely to be much thicker than the other films. The spectra are very smooth with shoulders at several wavenumbers below 200 cm^{-1}. In terms of the broad smooth envelope which contains the spectra, all orientations are essentially identical. Thus, unlike the oriented material described above, there is very little anisotropy in the GaAs deposited directly on glass. This is not surprising. Studies of amorphous GaAs demonstrate both the existence and observability of disorder-activated modes and the relaxation of selection rules even for materials which are not extremely disordered. This particular GaAs-on-glass sample is highly amorphous .

On the other hand, another sample of GaAs grown on glass at 555°C, provided by the Vook group, displayed a (111)fiber axis orientation when studied in situ by electron diffraction. Raman spectra of this film, as shown in Figures 23-26, had a notable dependence on orientation of the material as well as on the relative orientation of the polarization of the incident and scattered light. To deduce the direction of the fiber axis with respect to the scattering plane would require the ability to rotate the sample continuously, while holding the laser polarization direction constant. At the maximum of scattering intensity, identification of a totally symmetric mode, combined with a

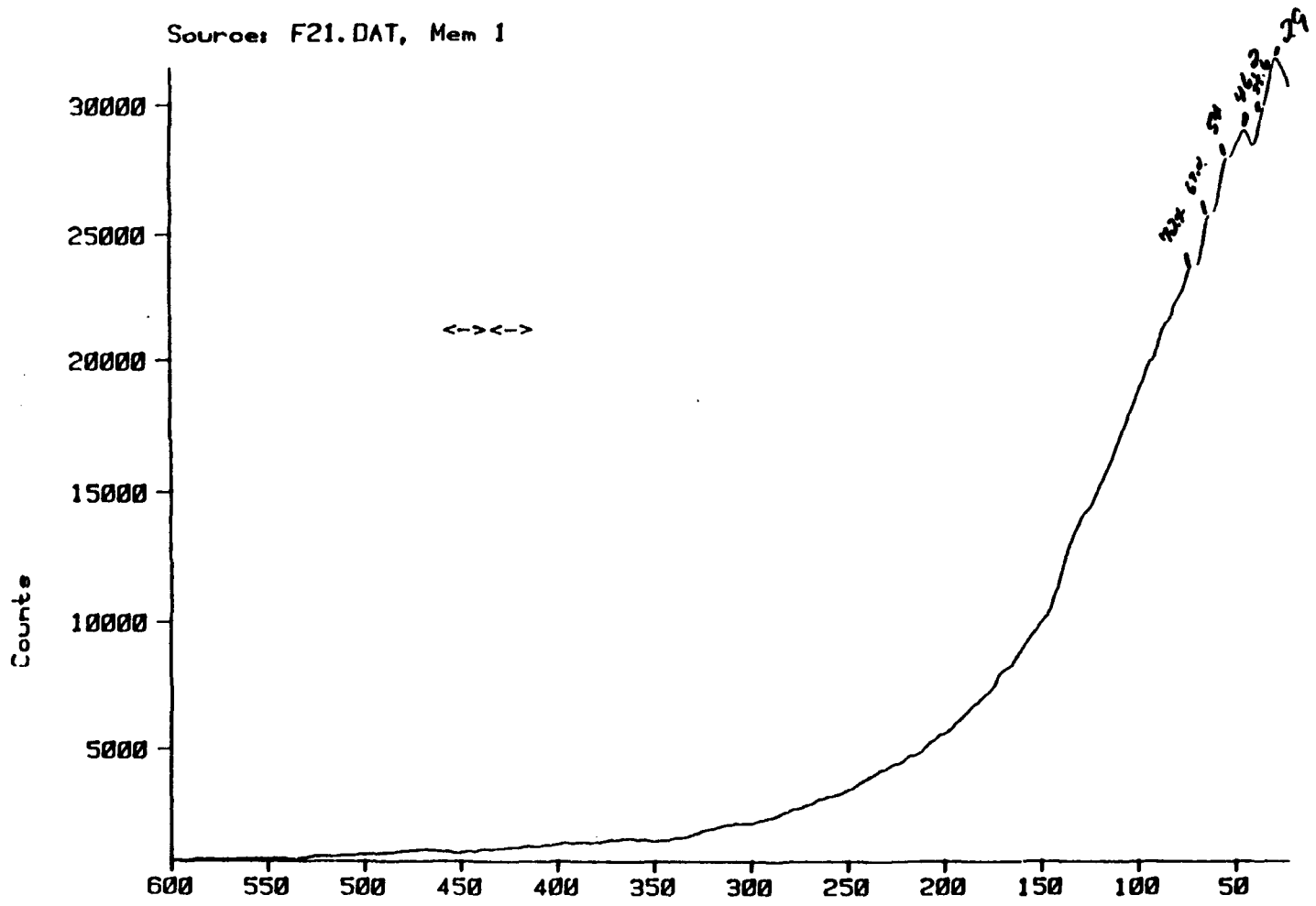
7/1/91 GaAs/glass 1e-8 torr 5mW
Source: F21.DAT, Mem 1
30000
25000
20000
15000
10000
5000
Counts
600
550
500
450
400
350
300
250
200
150
100
50

Figure 19.

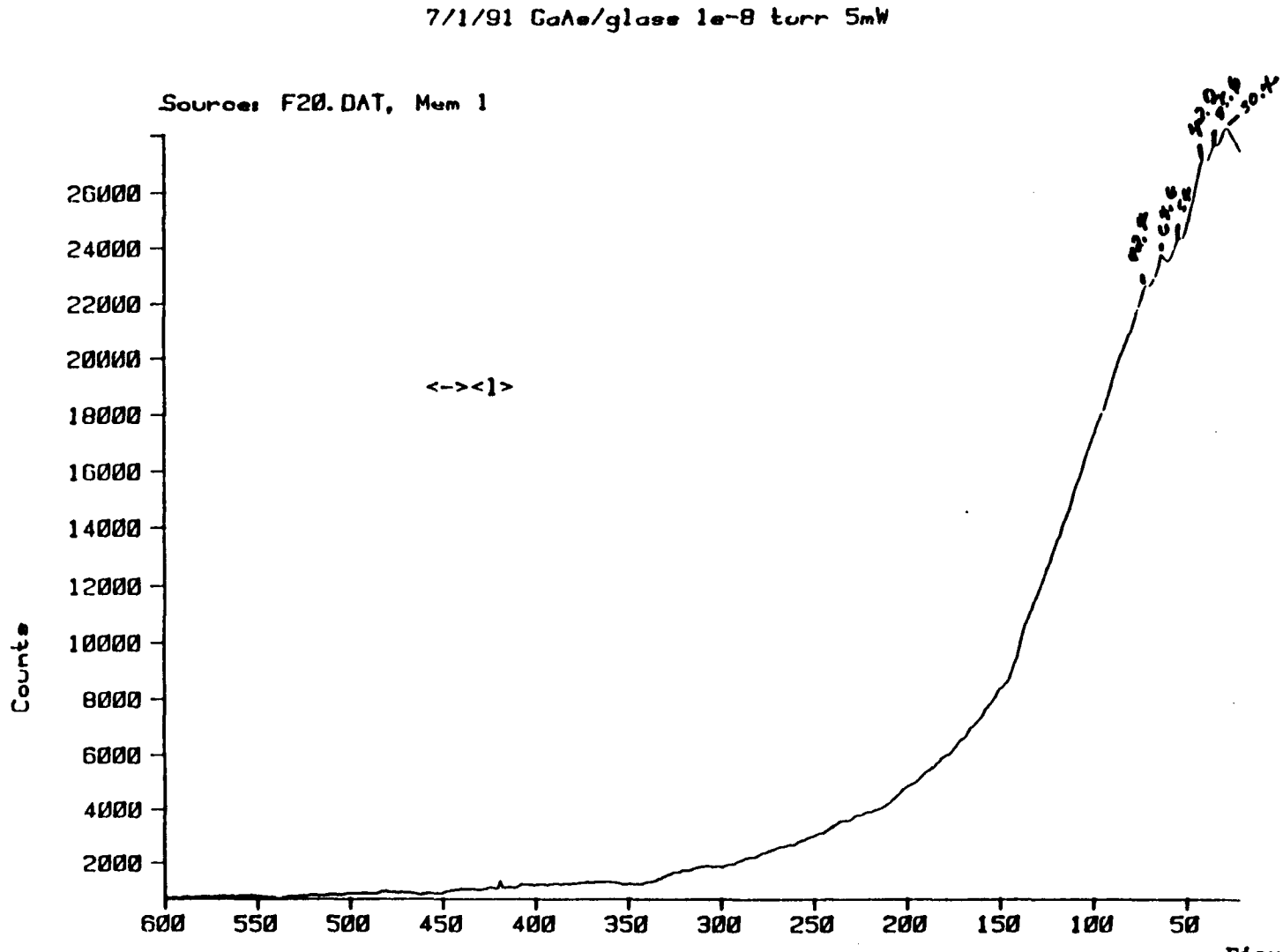
7/1/91 GaAs/glass 1e-8 torr 5mW
Source: F20.DAT, Mem 1
Counts
26000
24000
22000
20000
18000
16000
14000
12000
10000
8000
6000
4000
2000
600
550
500
450
400
350
300
250
200
150
100
50
<-><1>

Figure 20.

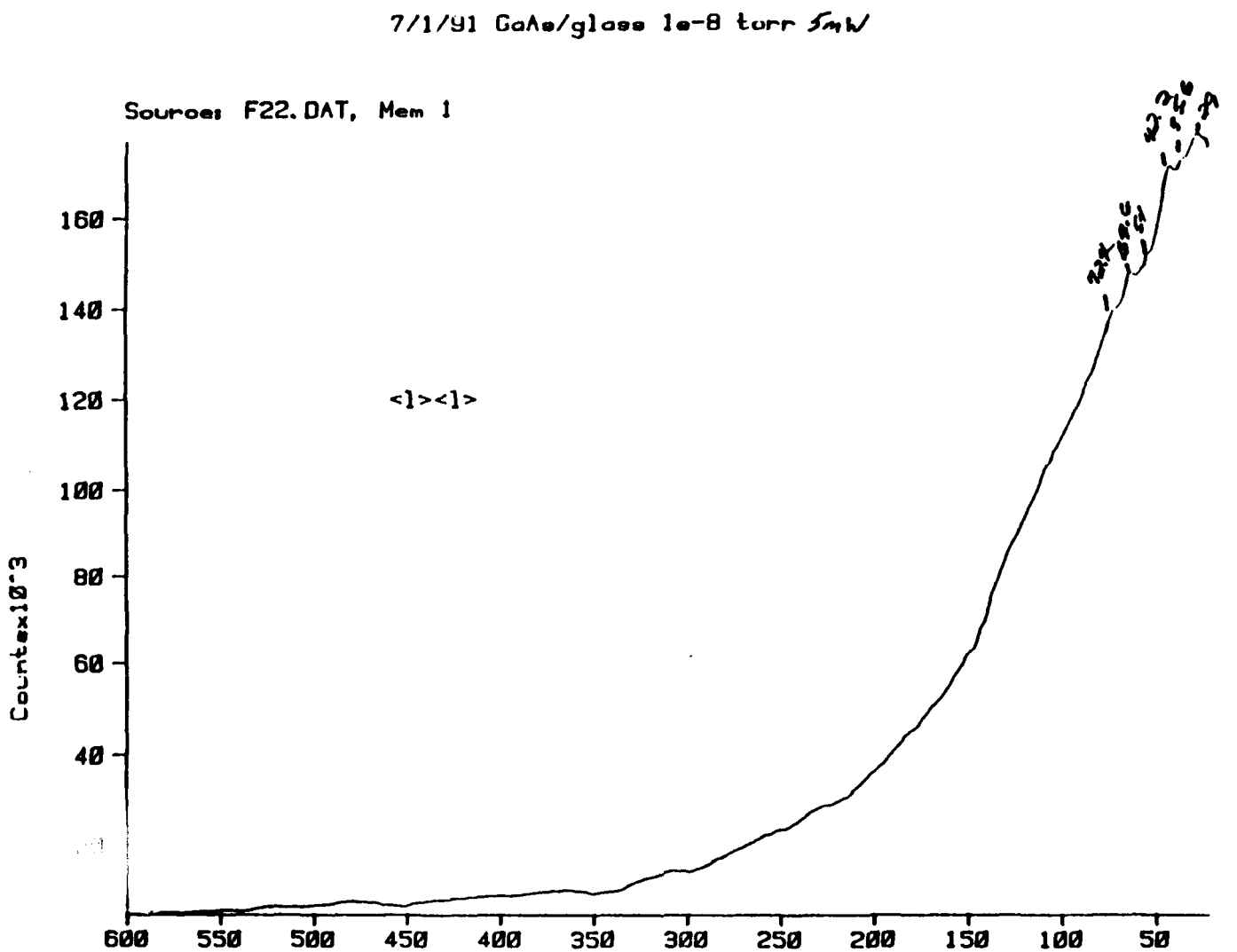
7/1/91 GaAs/glass 1e-8 torr 5mW
Source: F22.DAT, Mem 1
<1><1>
Counts x10^3
160
140
120
100
80
60
40
600
550
500
450
400
350
300
250
200
150
100
50

Figure 21.

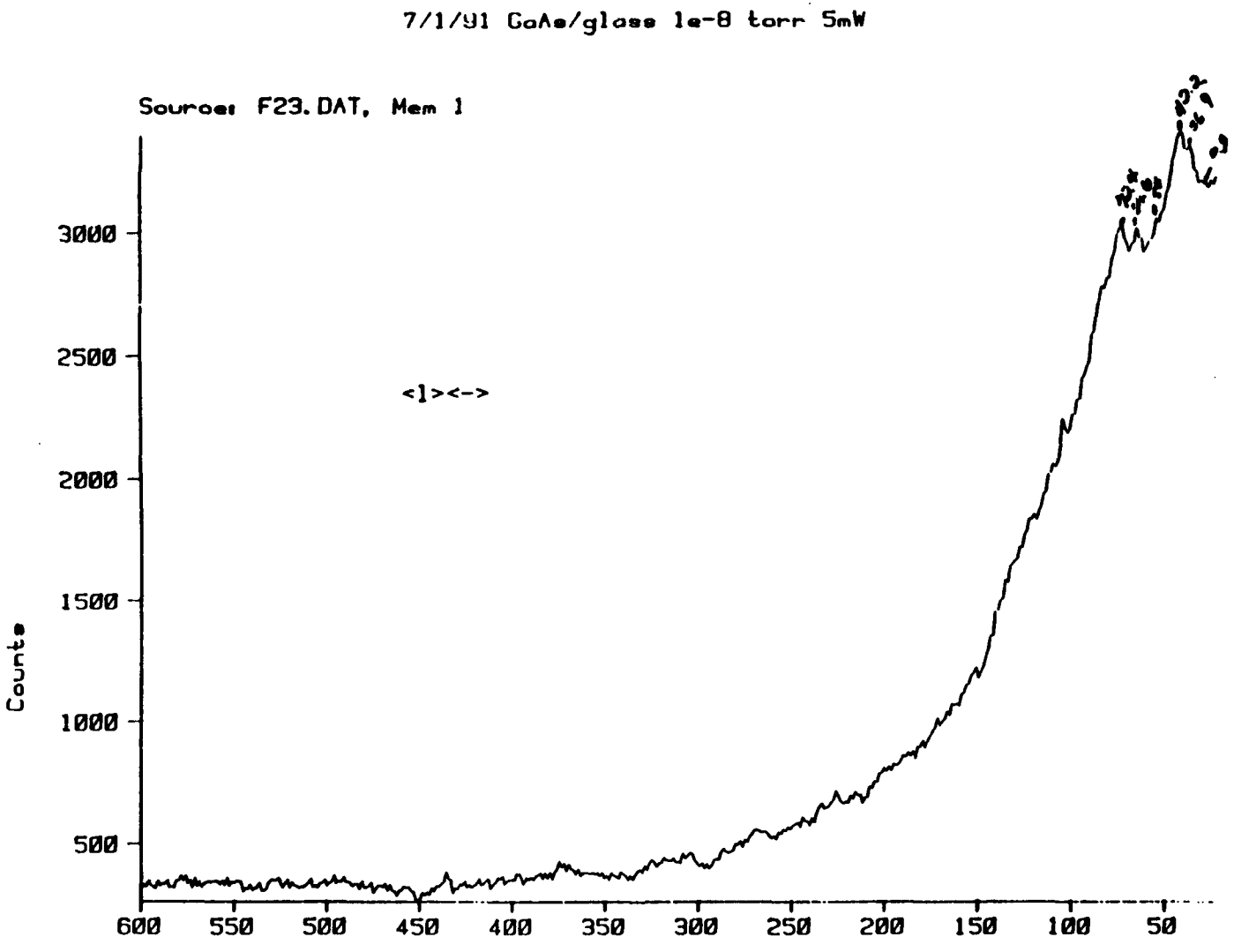
7/1/91 GaAs/glass 1e-8 torr 5mW
Source: F23.DAT, Mem 1
<1><->
Counts
3000
2500
2000
1500
1000
500
600
550
500
450
400
350
300
250
200
150
100
50

Figure 22.

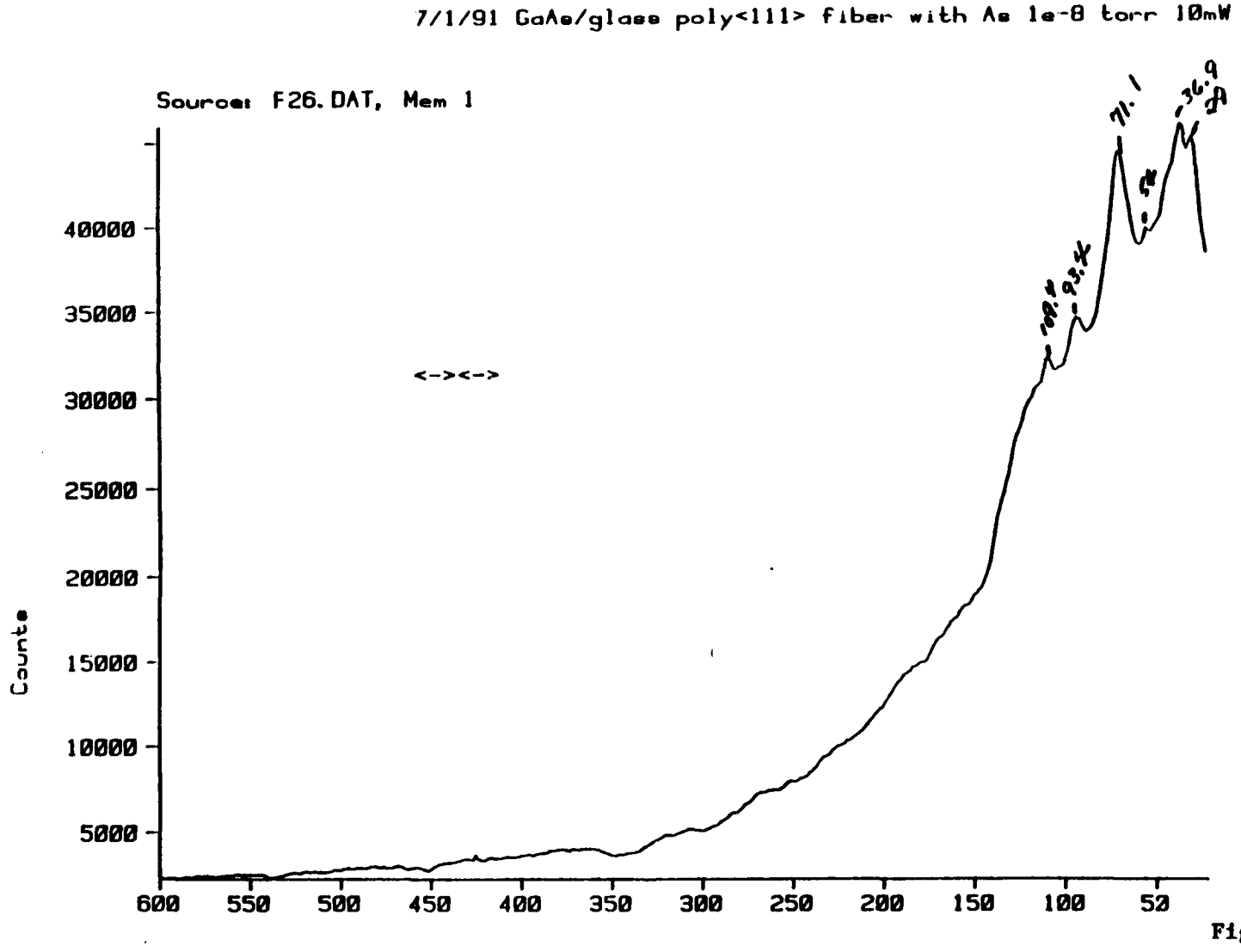
7/1/91 GaAs/glass poly<111> fiber with As 1e-8 torr 10mW
Source: F26.DAT, Mem 1
Counts
40000
35000
30000
25000
20000
15000
10000
5000
600
550
500
450
400
350
300
250
200
150
100
50
71.1
36.9
93.4

Figure 23.

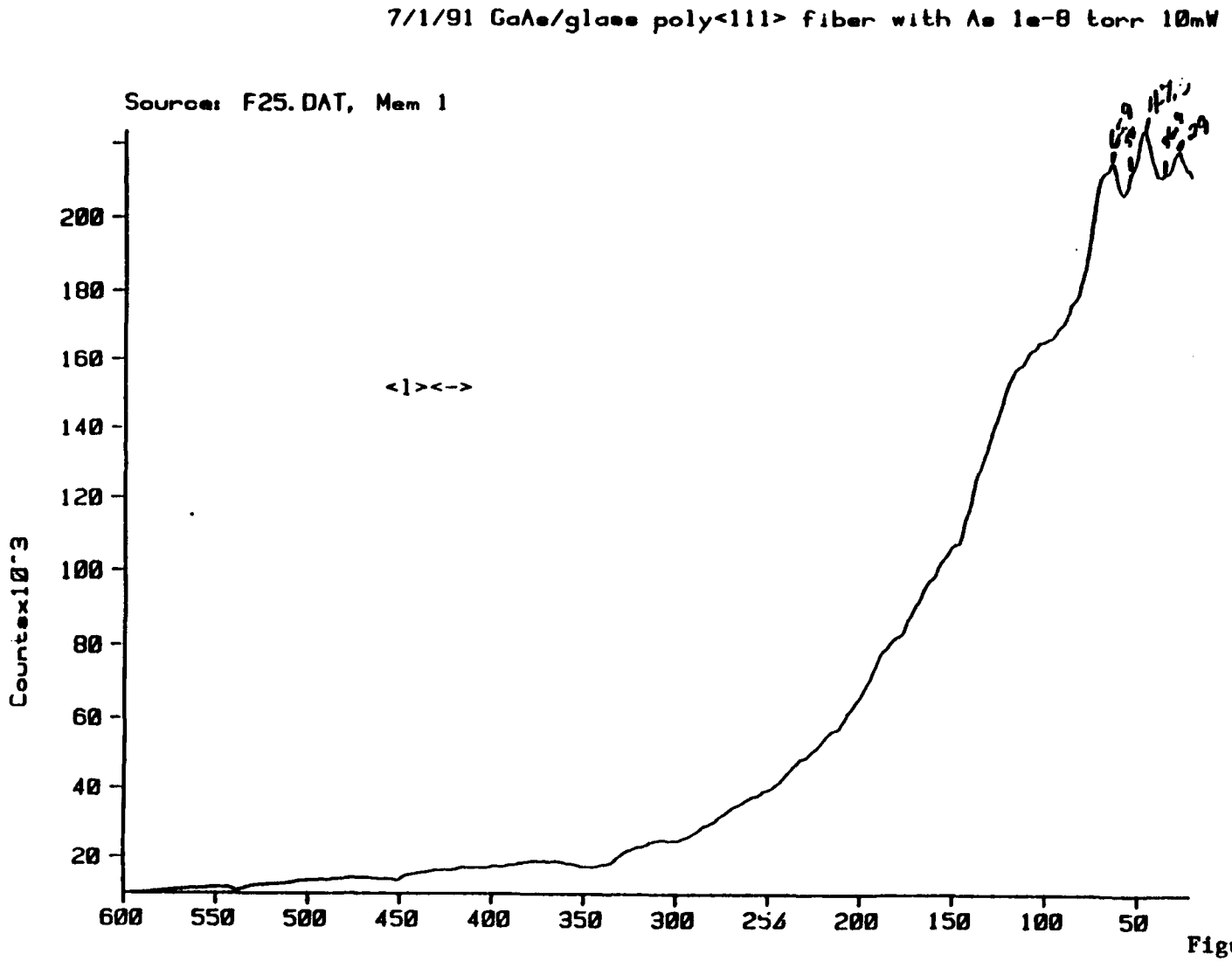
7/1/91 GaAs/glass poly<111> fiber with As 1e-8 torr 10mW
Source: F25.DAT, Mem 1
<1><->
Counts x10^3
200
180
160
140
120
100
80
60
40
20
600
550
500
450
400
350
300
250
200
150
100
50

Figure 24.

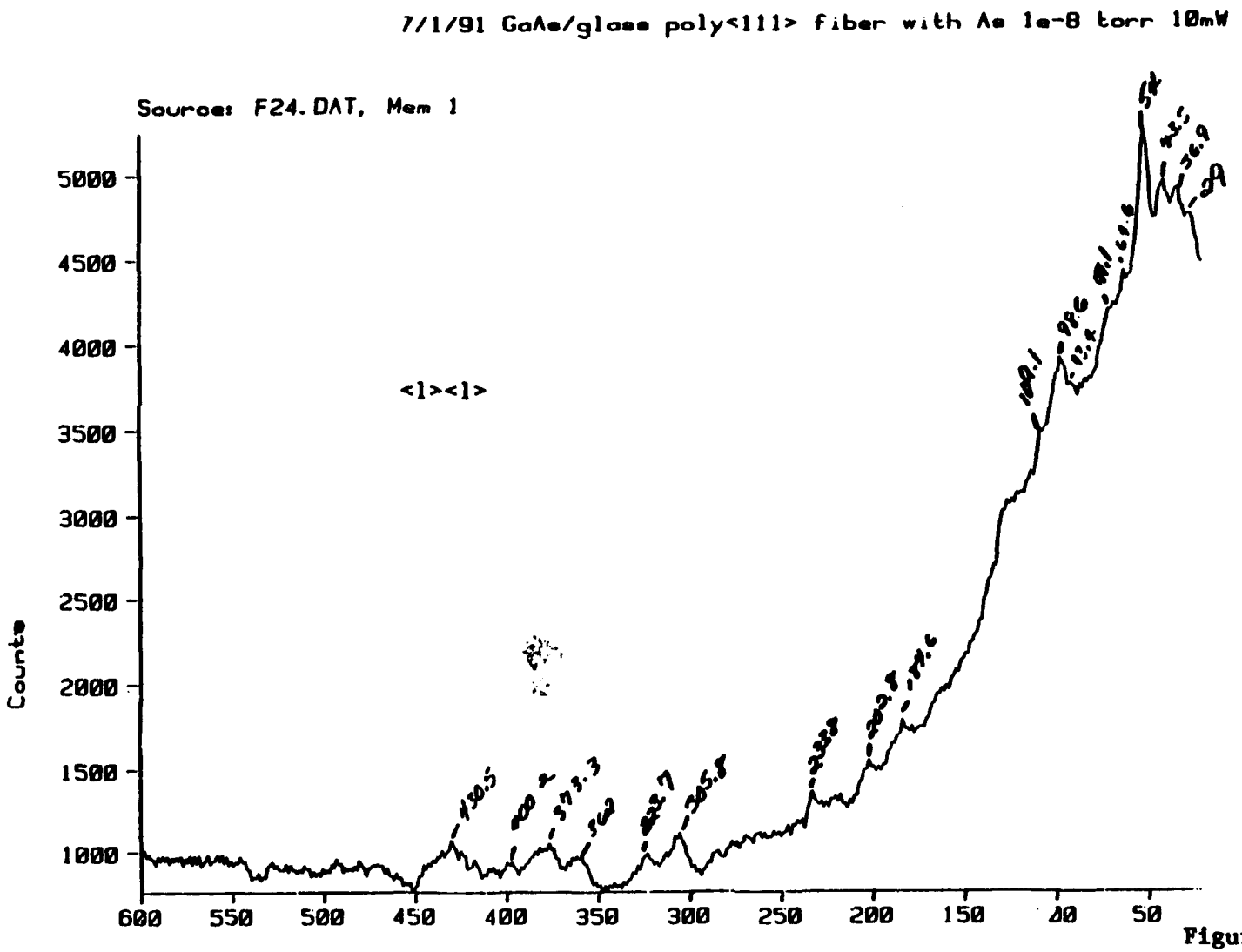
7/1/91 GaAs/glass poly<111> fiber with As 1e-8 torr 10mW
Source: F24.DAT, Mem 1
<1><1>
Counts
5000
4500
4000
3500
3000
2500
2000
1500
1000
600
550
500
450
400
350
300
250
200
150
100
50

Figure 25.

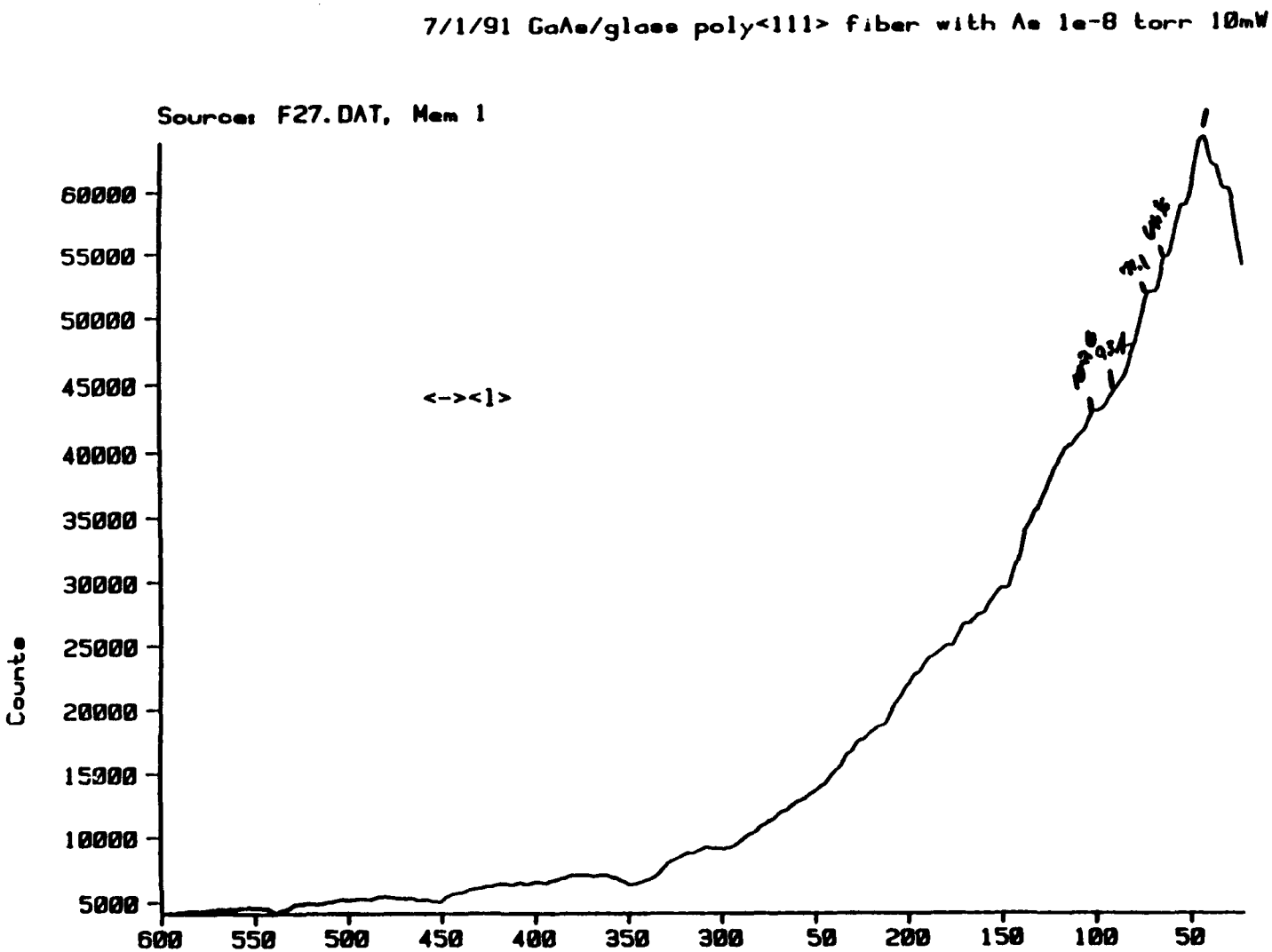
7/1/91 GaAs/glass poly<111> fiber with As 1e-8 torr 10mW
Source: F27.DAT, Mem 1
<-><1>
Counts
60000
55000
50000
45000
40000
35000
30000
25000
20000
15000
10000
5000
600
550
500
450
400
350
300
50
200
150
100
50

Figure 26.

study of the signal intensity as a function of scattering angle, would allow unequivocal deduction of the fiber axis direction.

Another sample, grown on a freshly cleaved (111)surface of CaF_2, shows more directionality, in Figures 27-30, and even some modes not seen for the other samples. It is quite reasonable to postulate that the extra modes seen are due to the (111) orientation selection rules discussed above and possibly a higher degree of crystallinity. The appearance of substantial Raman activity in the 150-200 cm^{-1} region for this sample, but not for the (111) fiber axis sample described above argues either 1) that the light is not incident along the (001) direction in the fiber axis sample or 2) that the film on CaF_2 possesses some anisotropy in the xy-plane not present in the sample grown on glass.

Since Vook's characterization showed the fibers to be oriented perpendicular to the substrate, the first option is eliminated. If this is true, then the three-dimensional order present at the freshly cleaved CaF_2 surface oriented the fiber texture. The directionality of the Raman signals displayed by the sample grown on cleaved CaF_2 shows that, as expected, GaAs grown on a highly crystalline substrate has good quality, and a strong tendency to grow in the orientation displayed by the substrate. Figures 31-32 show two spectra taken under identical conditions, except that the entrance slit to the spectrograph was changed. The relative variation in the peaks with the improvement in spectral resolution shows that the peak at ≈210 cm^{-1} has a broad base even in this sample.

The final sample characterized was a trilayer consisting of GaAs deposited on a tungsten relief pattern, which in turn was deposited on single- crystal silicon. The spectra, shown in Figures 33-36, display virtually no directionality. Figures 37-38 show distinct broad features at ≈ 760 cm^{-1} and another near 3000 cm^{-1}, which over the course of this study have become more and more evident. This feature can be unequivocally assigned[14] to WO_3 formed by oxidation and hydration of the tungsten relief pattern. This clearly suggests that the GaAs was either not contiguous or very thin, i.e. <950Å. The spectra varied somewhat from place to place on the film, and we are inclined to believe the film is not contiguous. All the other samples show very minor effects, if any, due to exposure to air, and so we suspect that if a GaAs film is contiguous, there would be very little formation of oxide underlayers.

This film was used for a series of annealing and graphoepitaxy experiments. In one case,

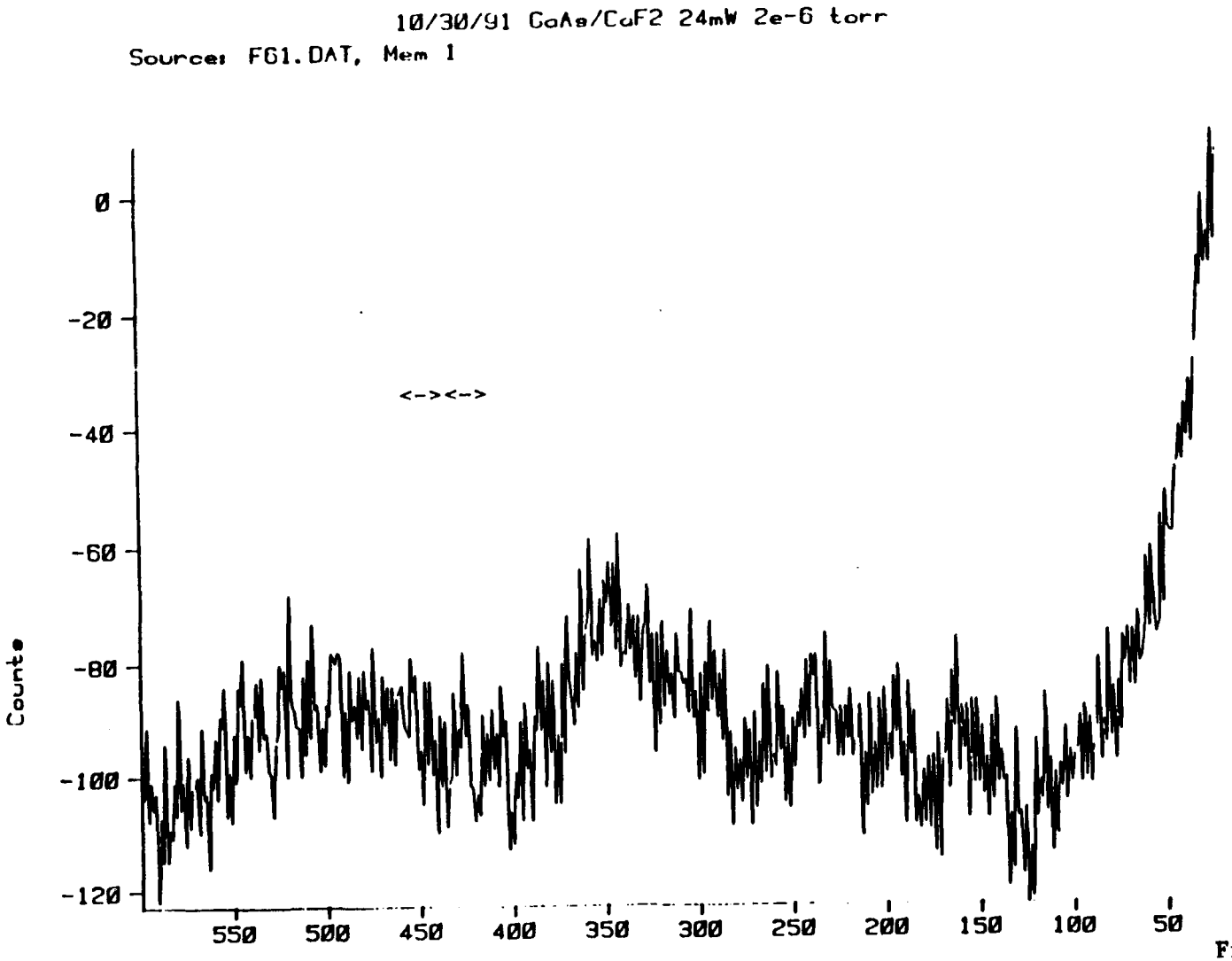
10/30/91 GaAs/CaF2 24mW 2e-6 torr
Source: FG1.DAT, Mem 1
0
-20
-40
-60
-80
-100
-120
Counts
<-><->
550
500
450
400
350
300
250
200
150
100
50

Figure 27.

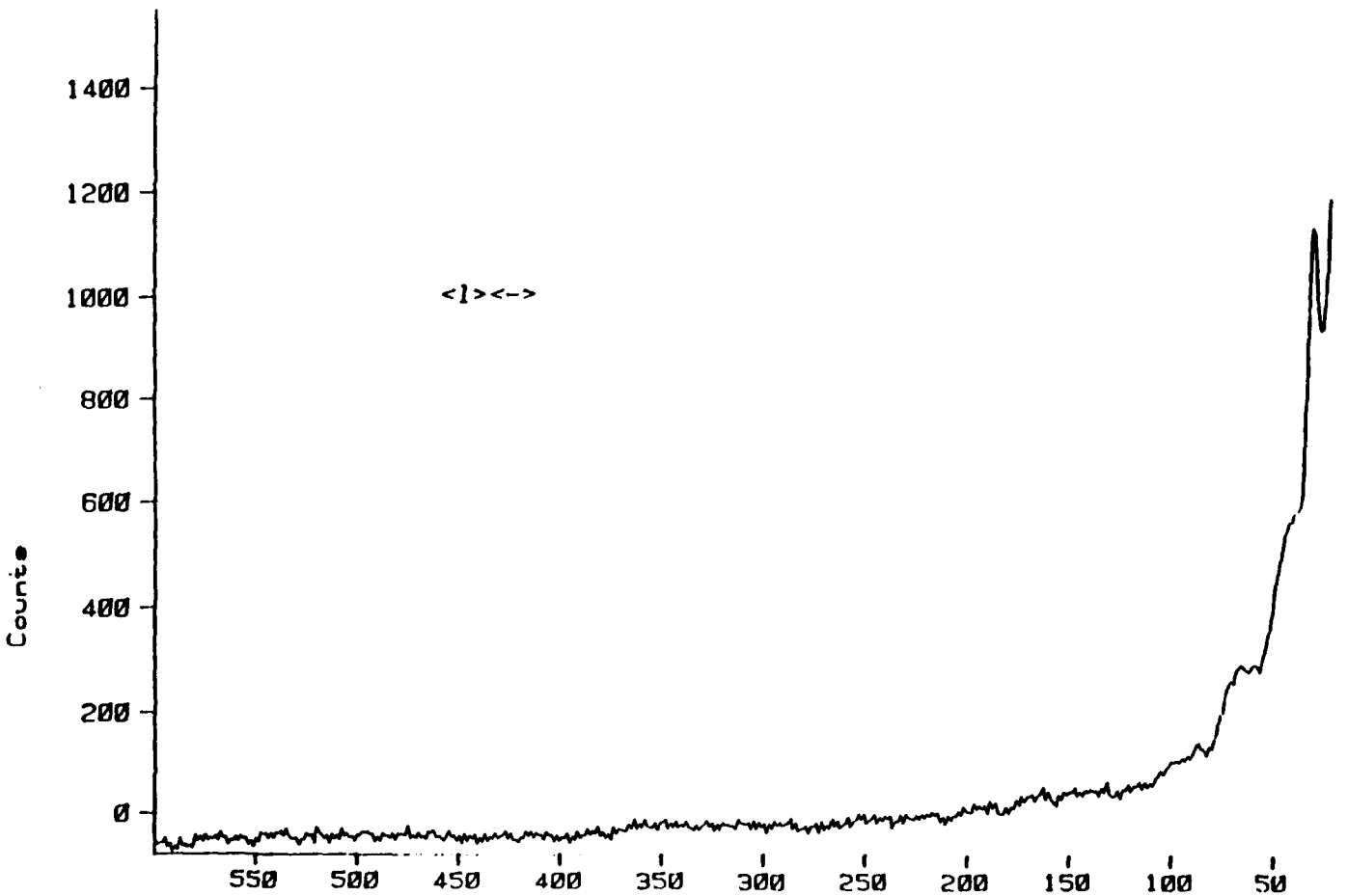
10/30/91 GaAs/CaF2 24mW 2e-6 torr
1400
1200
1000
800
600
400
200
0
Counts
<1><->
550
500
450
400
350
300
250
200
150
100
50

Figure 28.

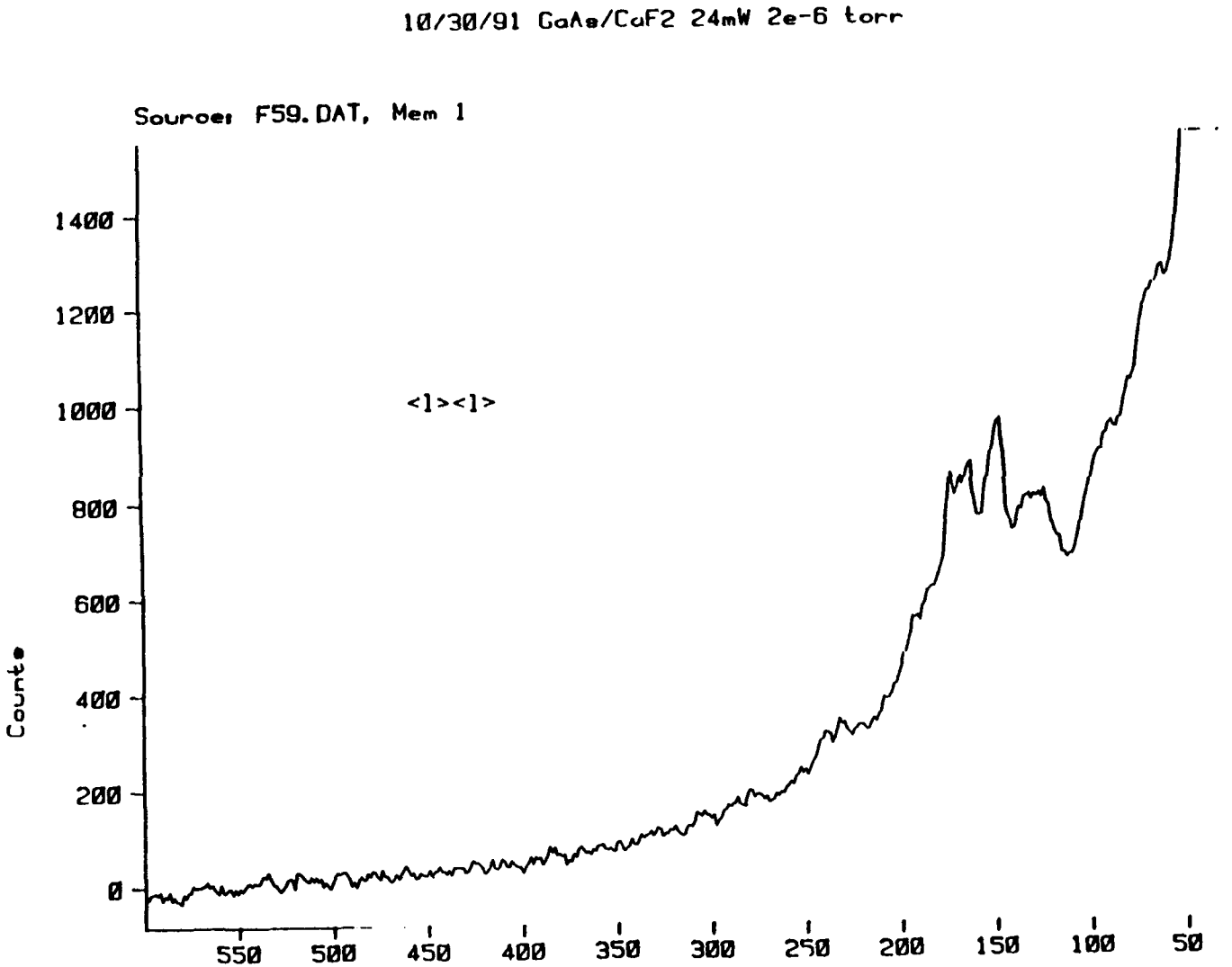
10/30/91 GaAs/CaF2 24mW 2e-6 torr
Source: F59.DAT, Mem 1
<1><1>
Counts
1400
1200
1000
800
600
400
200
0
550
500
450
400
350
300
250
200
150
100
50

Figure 29.

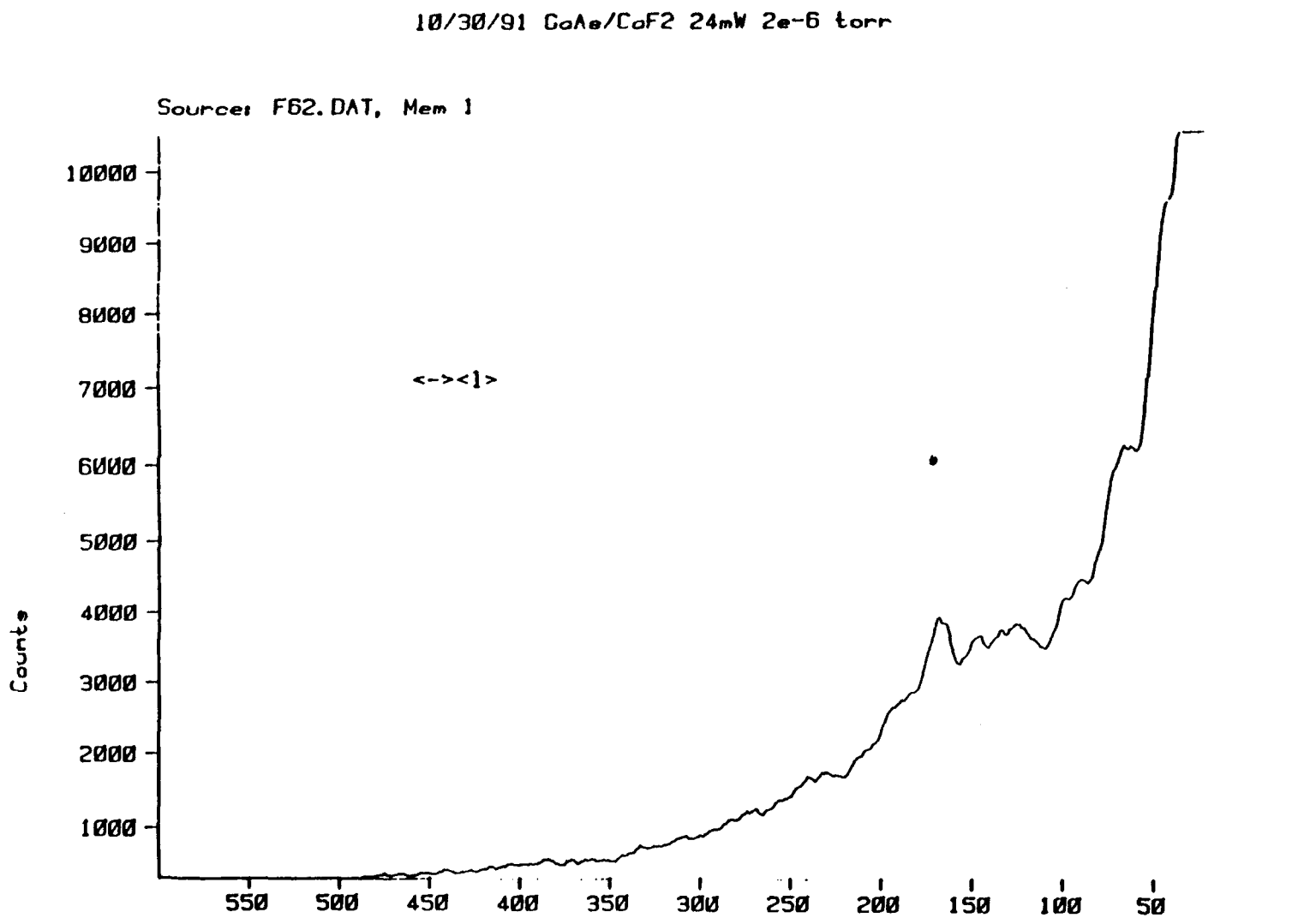
10/30/91 GaAs/CaF2 24mW 2e-6 torr
Source: F62.DAT, Mem 1
<-><1>
Counts
10000
9000
8000
7000
6000
5000
4000
3000
2000
1000
550
500
450
400
350
300
250
200
150
100
50

Figure 30.

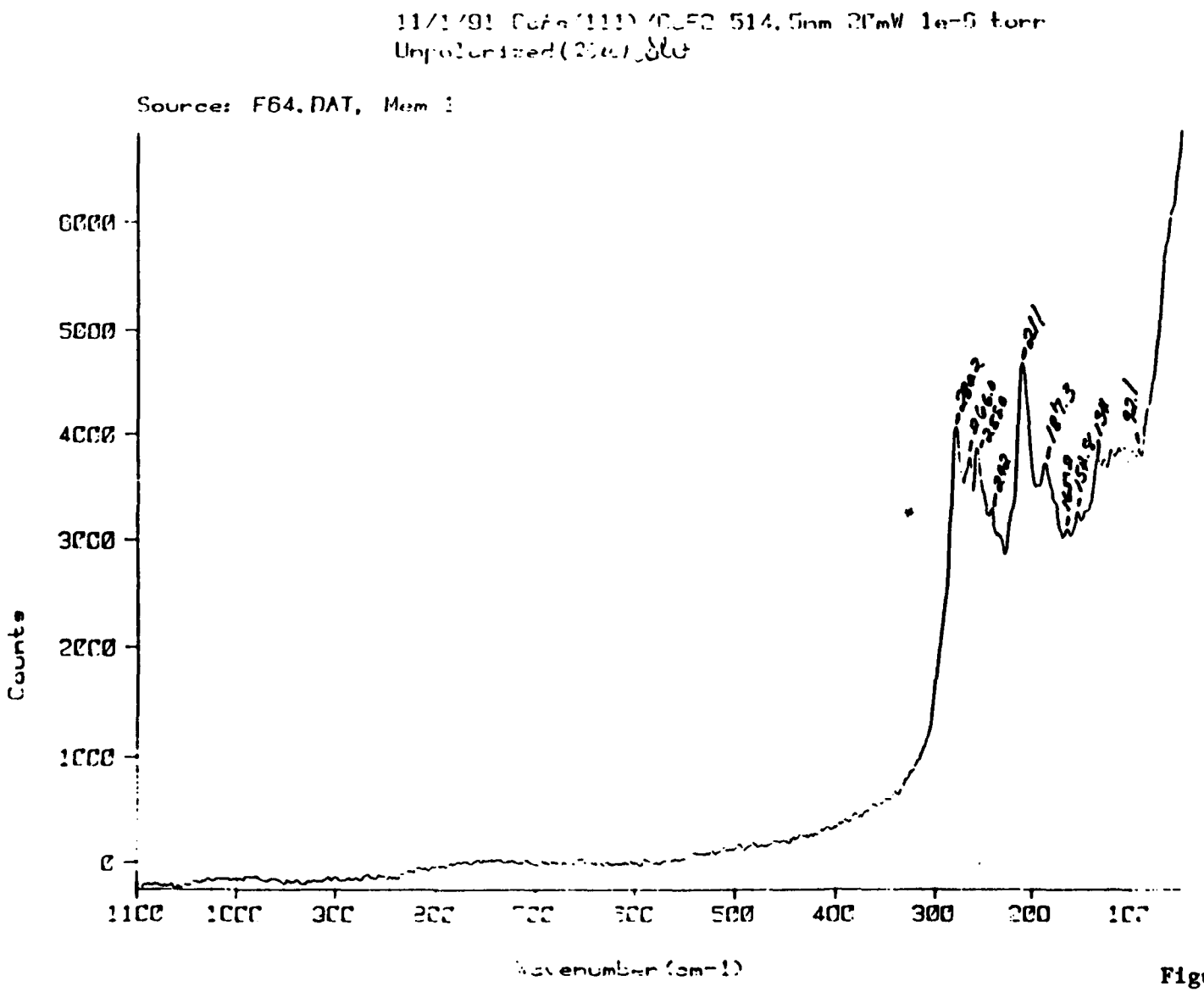
11/1/91 Data (111) (C-52) 514.5nm 20mW 1e-6 torr
Unpolarized (2cm-1 slit)
Source: F64.DAT, Mem 1
6000
5000
4000
3000
2000
1000
0
Counts
1100
1000
900
800
700
600
500
400
300
200
100
Wavenumber (cm-1)

Figure 31.

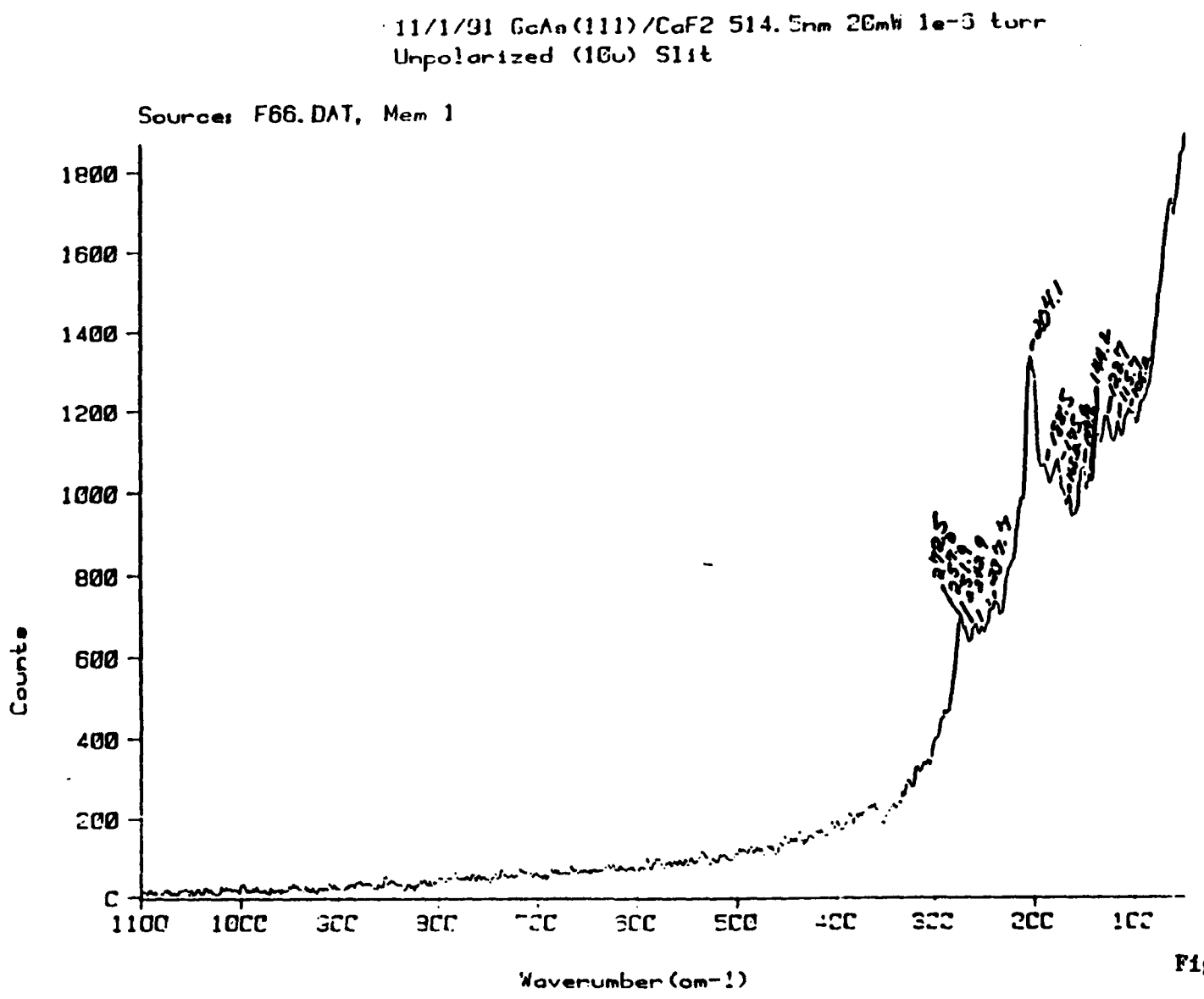
11/1/91 GaAs(111)/CaF2 514.5nm 20mW 1e-3 torr
Unpolarized (10u) Slit
Source: F66.DAT, Mem 1
Counts
1800
1600
1400
1200
1000
800
600
400
200
0
1100
1000
900
800
700
600
500
400
300
200
100
Wavenumber (cm-1)

Figure 32.

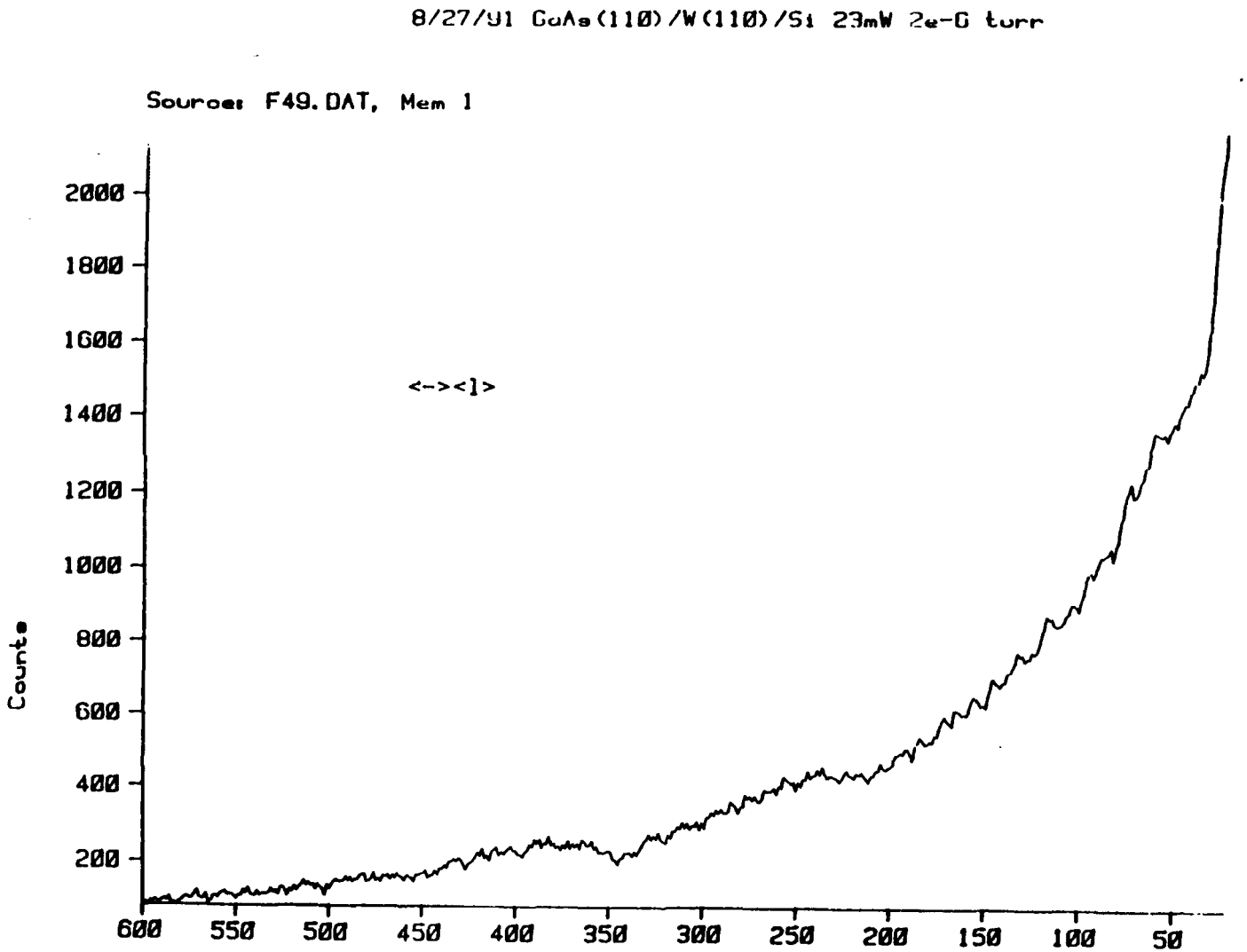
8/27/91 GaAs(110)/W(110)/Si 23mW 2e-6 torr
Source: F49.DAT, Mem 1
<-><1>
Counts
2000
1800
1600
1400
1200
1000
800
600
400
200
600
550
500
450
400
350
300
250
200
150
100
50

Figure 33.

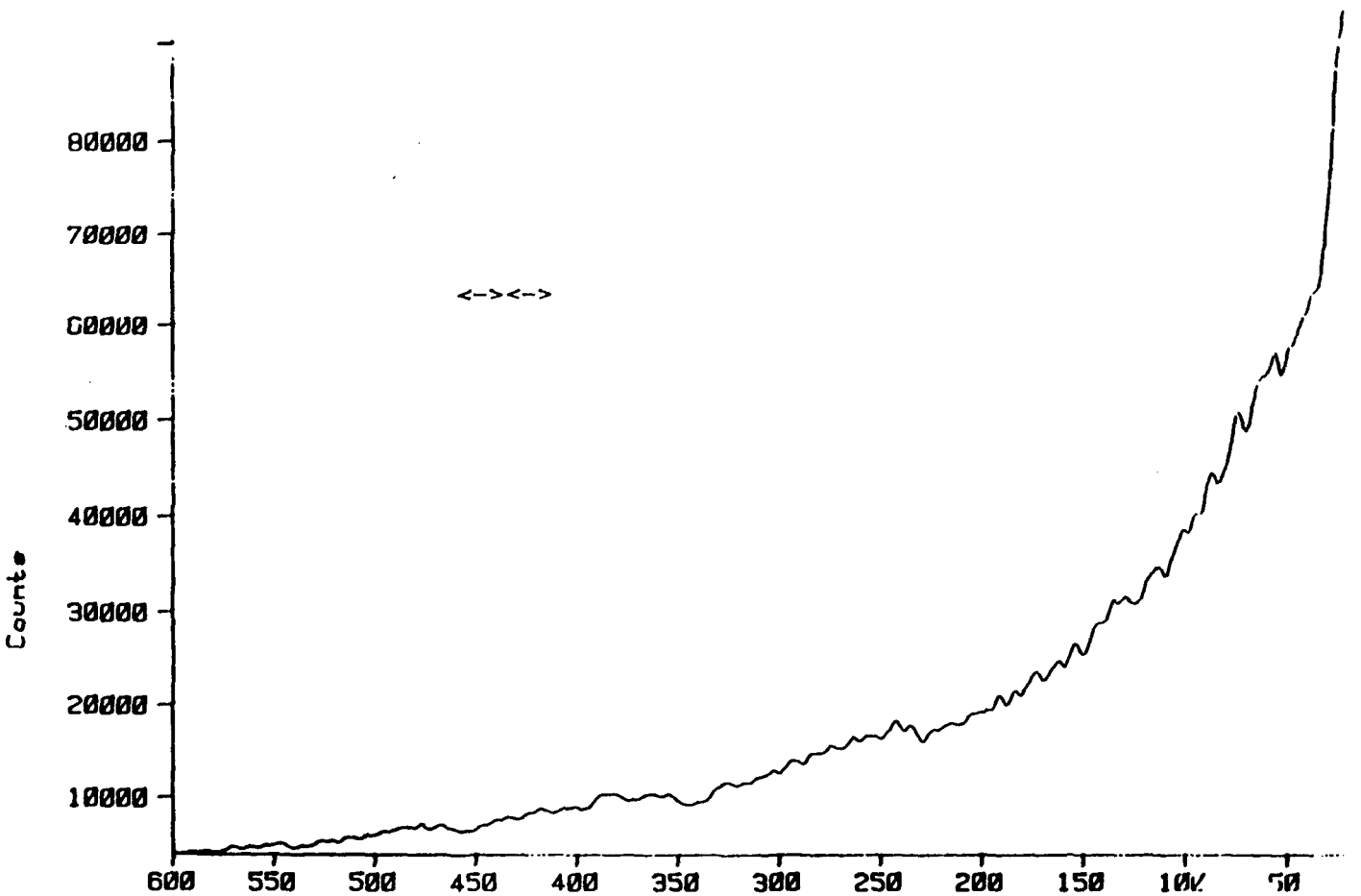
8/27/91 GaAs(110)/W(110)/Si 23mW 2e-6 torr
Counts
80000
70000
60000
50000
40000
30000
20000
10000
600
550
500
450
400
350
300
250
200
150
100
50

Figure 34.

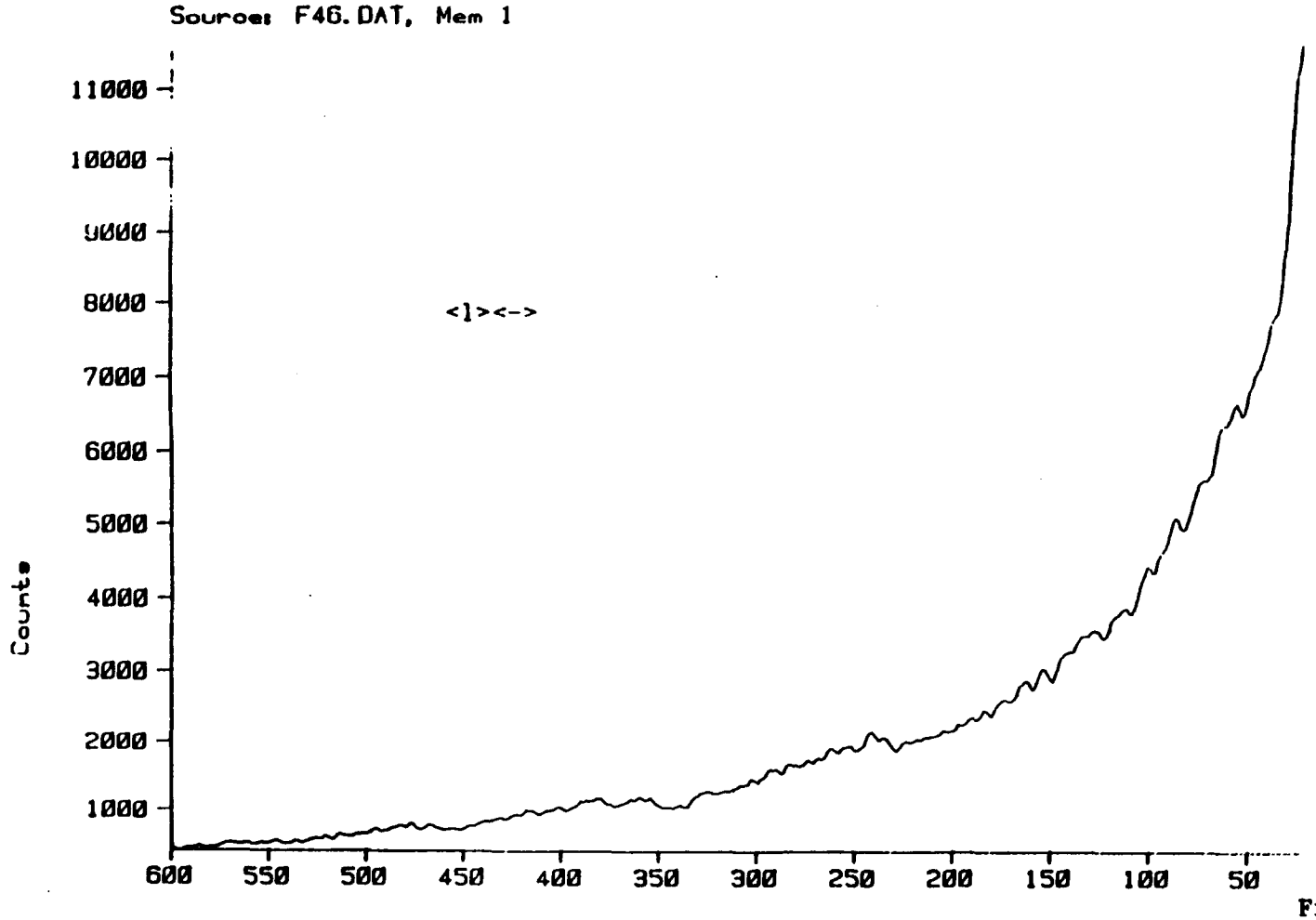
8/27/91 GaAs(110)/W(110)/Si 23mW 2e-6 torr
Source: F46.DAT, Mem 1
11000
10000
9000
8000
7000
6000
5000
4000
3000
2000
1000
Counts
<1><->
600
550
500
450
400
350
300
250
200
150
100
50

Figure 35.

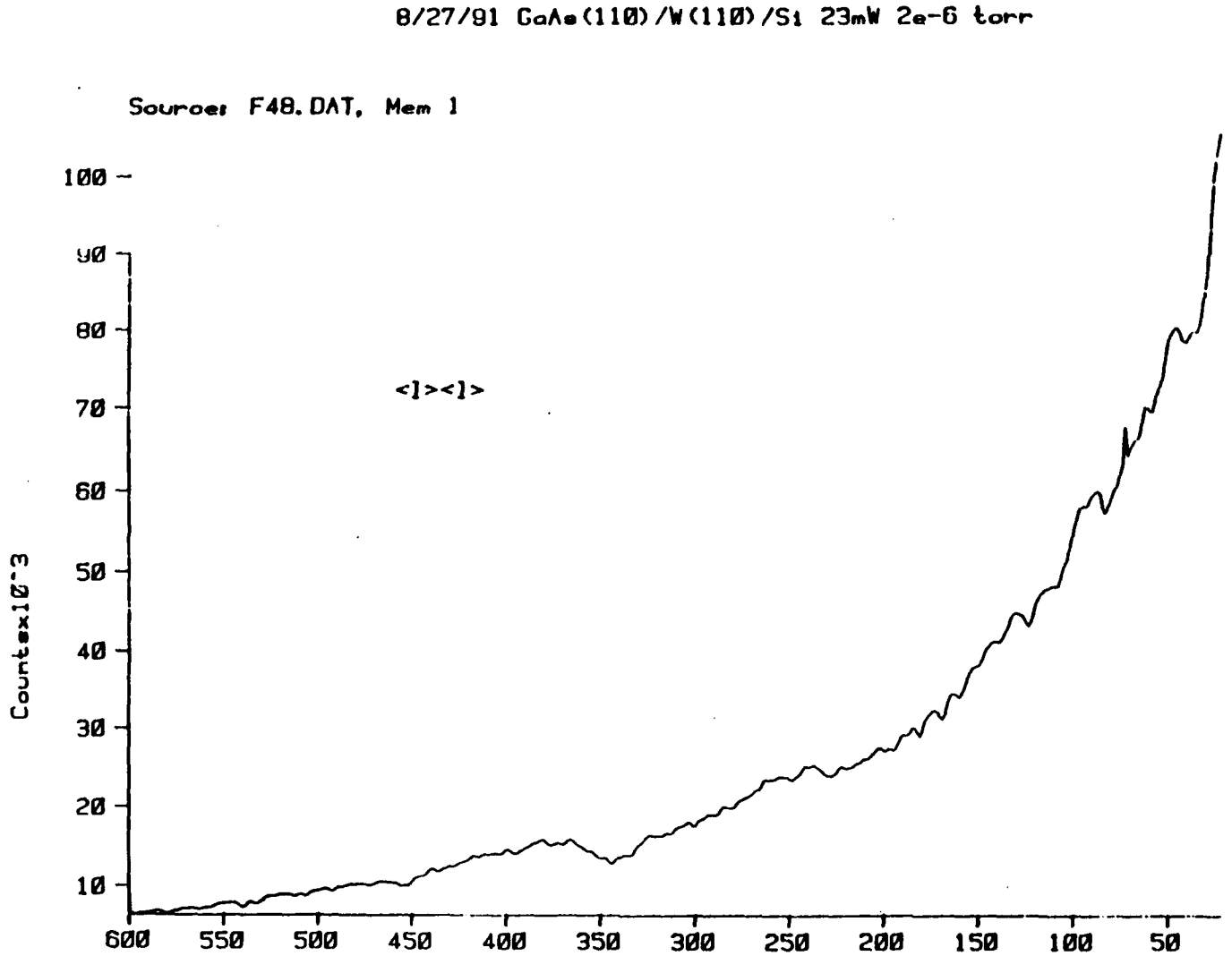
8/27/91 GaAs(110)/W(110)/Si 23mW 2e-6 torr
Source: F48.DAT, Mem 1
<1><1>
Counts x10^3
100
90
80
70
60
50
40
30
20
10
600
550
500
450
400
350
300
250
200
150
100
50

Figure 36.

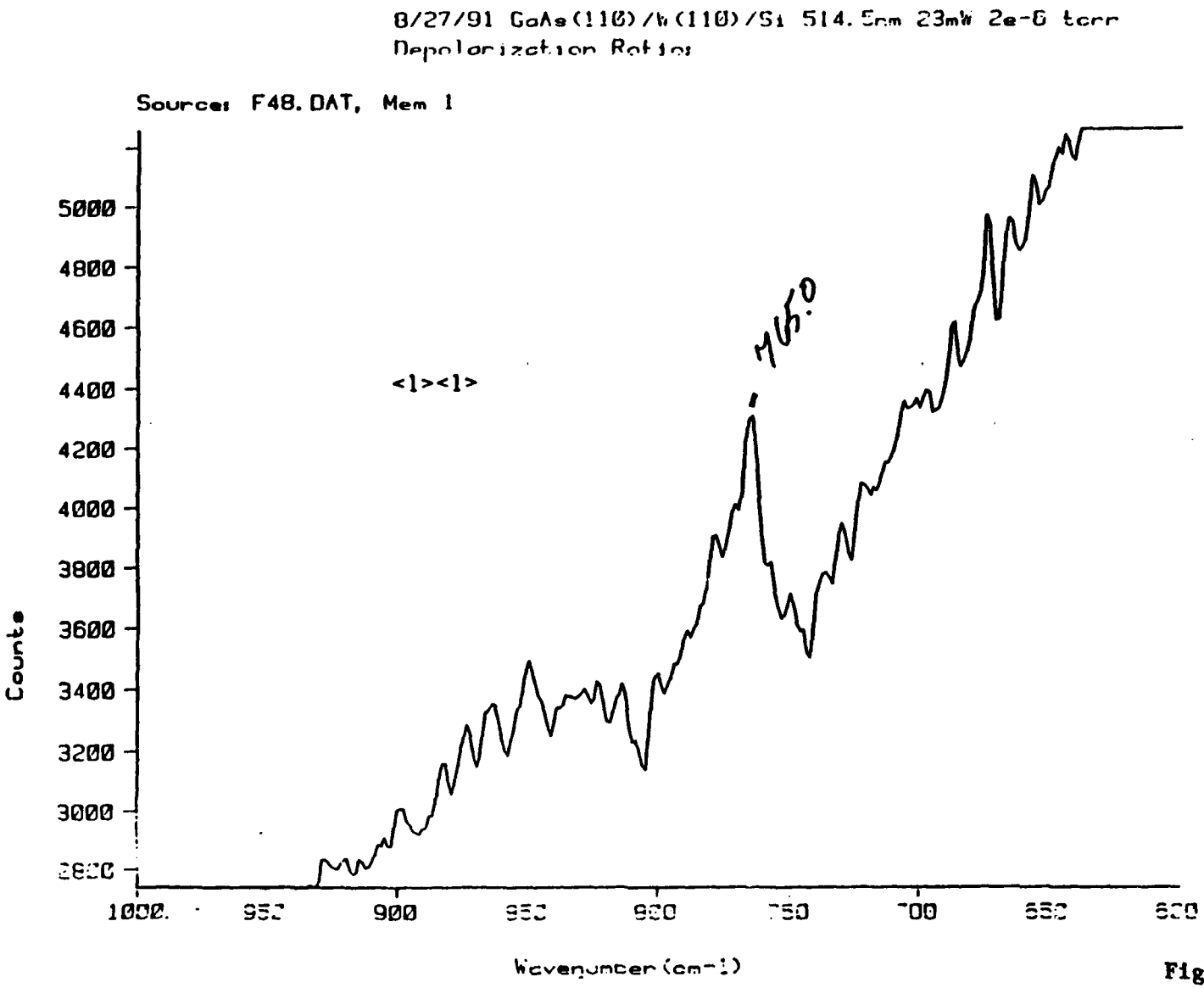
8/27/91 GaAs(110)/W(110)/Si 514.5nm 23mW 2e-6 torr
Depolarization Ratio
Source: F48.DAT, Mem 1
<1><1>
465.0
Counts
5000
4800
4600
4400
4200
4000
3800
3600
3400
3200
3000
2800
1000.
950
900
850
800
750
700
650
600
Wavenumber(cm-1)

Figure 37.

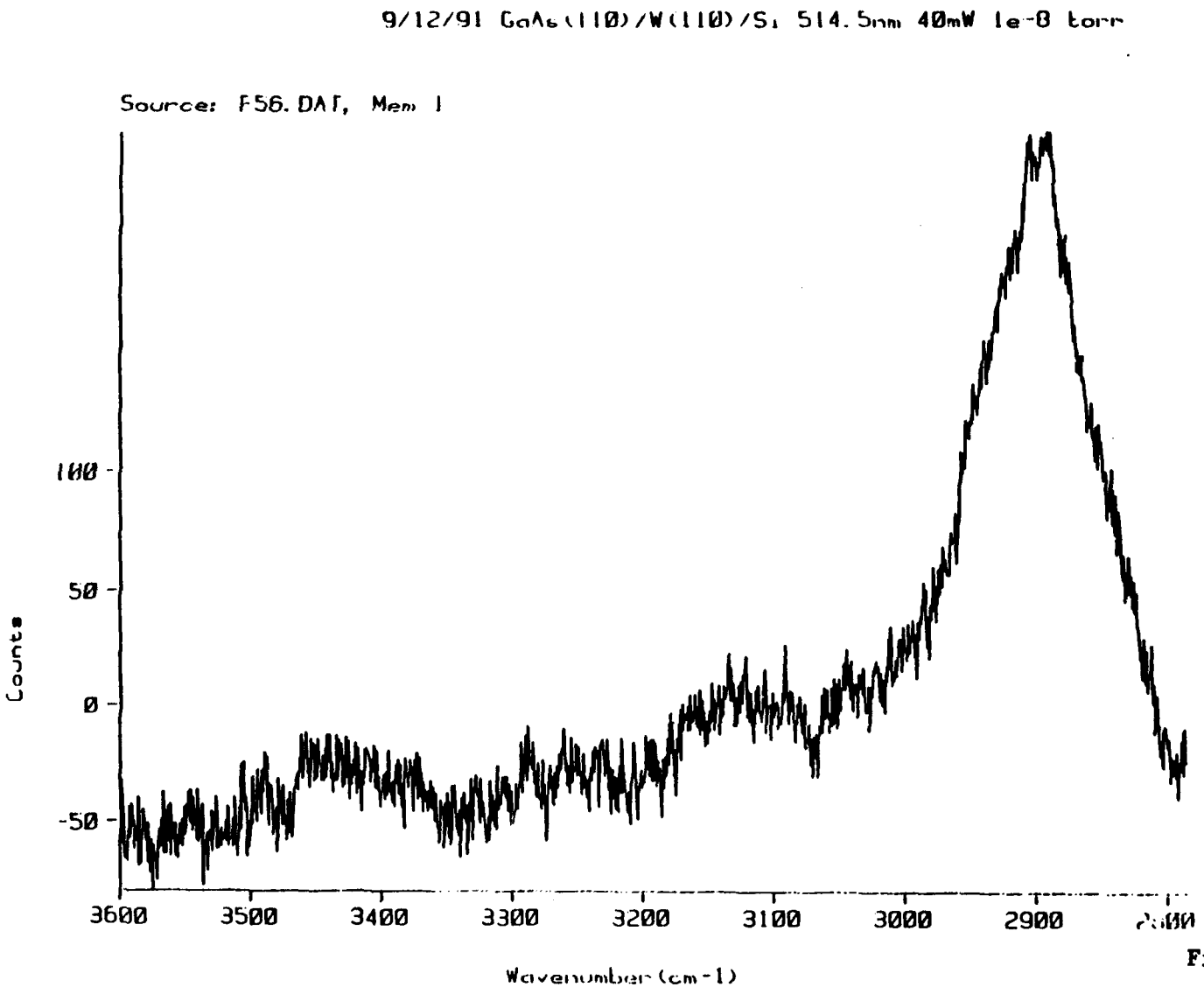
9/12/91 GaAs(110)/W(110)/Si 514.5nm 40mW 1e-8 torr
Source: F56.DAT, Mem 1
100
50
0
-50
Counts
3600
3500
3400
3300
3200
3100
3000
2900
Wavenumber (cm-1)

Figure 38.

the laser was not rastered. It was placed in one position and successive Raman spectra were taken with incident light of successively greater intensity. Some effects were clearly seen, as suggested in Figure 39. Spectra taken before and after such an annealing experiment are also shown. The strength of the low- frequency activity is reduced relative to the WO_3 signal, suggesting that the laser can be used to induce morphological changes.

Raman spectra of the same sample(110) after a manual rastering of the laser beam across a 3mm x 3mm region over a ten minute period show similar effects. The sample was at room temperature and, with the plasma line filter removed, the laser was delivering ≥80 mW to the sample focussed into a ≈100μm spot. This sample trilayer was not particularly optimal, due to ambiguity with regard to the continuity of the GaAs layer, but Raman spectra obtained at various times and in various places in the "raster zone" showed definite variation.

A similar graphoepitaxy study was conducted using the GaAs-on-glass sample which had a (111) fiber axis. It was hoped that this material would be sufficiently amorphous at the outset, due to the glass substrate, so that laser- induced changes would be even more evident than in the first example. What happened was that very few if any changes were seen to occur. This sample of GaAs on glass showed the fiber structure because it was deposited at high temperature (Table I), and the other GaAs-on-glass sample was amorphous because it was deposited at room temperature. Optical microscopy shows that the glass has striations which could have served as nucleation sites, but this does not explain the variation in morphology of samples on glass substrates.

4. Discussion

The results presented can be summarized as follows. First, Raman spectroscopy is capable of obtaining orientational and morphological information about GaAs films non-invasively. Second, Raman spectroscopy is sensitive to changes induced by intentional laser heating of GaAs samples. We now discuss the relevance of these facts to the MMIC program.

As suggested in the Introduction , our goal was to show the feasibility of using graphoepitaxy to fabricate specific orientations of GaAs directly on backplane materials, which themselves have been directly deposited on an insulating substrate. The goal is to produce GaAs

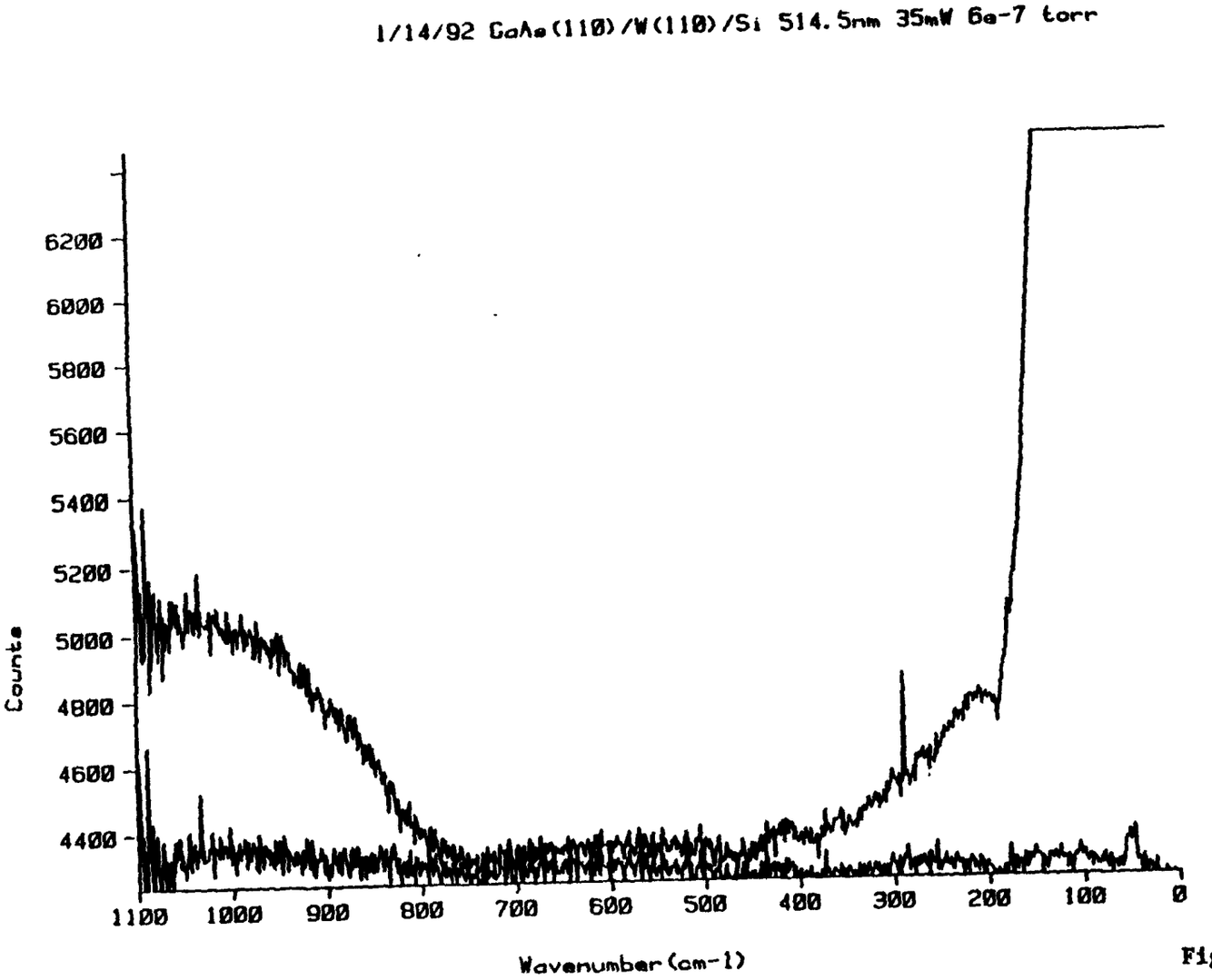
1/14/92 GaAs(110)/W(110)/Si 514.5nm 35mW 6e-7 torr
Counts
6200
6000
5800
5600
5400
5200
5000
4800
4600
4400
1100
1000
900
800
700
600
500
400
300
200
100
0
Wavenumber (cm-1)

Figure 39.

adequate to serve as a substrate for a device- quality epilayer. We have guardedly assumed that the (100) GaAs we obtained from GE was adequate for this purpose, and that any sample we might prepare should have equal directionality and crystallinity if it is good enough to serve as a substrate for a device-quality epilayer. We bear in mind that in production a given substrate might require etching before deposition of the epilayer, but this is a constraint on thickness. The question of thickness is an important one because strains could develop as a GaAs film gets thicker, and ultimately cause cracking.

Still, on the basis of the spectra we have obtained, it seems likely that, given adequate thickness to allow for back-etching if required, at least some of the samples produced during this program would be adequate to serve as a substrate for a device- quality epilayer. Vook produced samples with substantial directionality which displayed good agreement with selection rules. The degree of directionality observed for either of the (111) samples was equal to or greater than that observed for the (100) sample.

The behavior of the tungsten in the (110) sample was unfortunate and suggests that its strong tendency towards passivation renders it unsuitable for graphoepitaxy. We had hoped that perhaps a silicide layer would form between the tungsten layer and the silicon substrate which would aid in adhesion of those two layers. We have no evidence that such a silicide formed, and reasonable evidence to suggest that the GaAs simply did not form a contiguous film. Given the success of Vook in growing good GaAs on CaF_2, this study has distilled the entire MMIC problem down to choosing the correct metallization, which would transmit the natural (111) CaF_2 surface to the growing GaAs while still serving as an electrical backplane. Given the myriad factors which must be considered to execute graphoepitaxy, having now focussed discussion on only one factor should be viewed as a major accomplishment.

The graphoepitaxy experiment which utilized the (110) sample suggested that very modest laser power is adequate to effect changes in some kinds of samples which can be seen using Raman. The nature of the changes was not at all clear, but continued study would no doubt identify the effects. The fact that we were not able to effect any comparable changes in the (111)fiber axis GaAs- on- glass material at any laser power, but were able to see changes in the nominal (110) material, suggests that the substrate had no major interaction with the (110) case but was more strongly involved in the glass sample. It would be advantageous to repeat these experiments with a

much more intense laser, i.e. >2 watts CW. As mentioned in the Introduction, Raman experiments on GaAs have previously been executed using as much as 1-2 watts of CW laser power without reporting damage. An extension of our work would be to use an infrared laser of the correct power range to execute the rastering/annealing process.

Impurity modes are- well known for materials like GaAsP and GaAlAs of various stoichiometries, and so, if during the course of our work we had induced substitutional disorder due to loss of arsenic, there is a good chance we would have seen it. Raman spectroscopy can be used to monitor graphoepitaxy without itself inducing changes. Similar experiments on the undoped materials showed that after hours of exposure, only very slight changes could be observed in the Raman spectrum.

5. Conclusions

Raman spectroscopy is an excellent technique for the noninvasive characterization of GaAs films. The progress of graphoepitaxy can be monitored using Raman spectroscopy in situ in a production environment. It is possible to grow GaAs films on dielectric surfaces with good crystallinity, adhesion and stoichiometry.

References to Section C

1. See Ushioda, S. *Solid State Commun.* **1974**, 15 149, or Skuker, R.; Gammon, R.W.; *Phys. Rev. Lett.* **1970**, 25, 222.
2. Glembocki, O.J.; Dobisz, E.A. *J. Vac. Sci. Technol.* **1991**, B9,1403.
3. Evans, D.J. Ushioda, S. *Solid State Commun.* **1972**,11,1043.
4. Kawamura, H.; Tsu, R.; Esaki, L.*Appl. Phys. Lett.* **1972**,29,1397.
5. Loudon, R. *Advances in Phys.* **1964**,13, 423 see also Loudon, R. *Proc. Roy. Soc.* **1964**, 84, 370.
6. Evans, D.J.; Ushioda, S.; McMullen, J.D. *Solid State Commun.* **1973**, 31,369.
7. See Geis, M.W.; Antonaidis, D.; Silverstein, D.J.; Mountain, R.W.; Smith, H.I. *Appl. Phys. Lett.* **1980**, 37,454 and other references in original proposal.

8. Waugh, J.L.T.; Dolling, G. *Phys. Rev.* **1963**, 132, 2410.

9. Cochran, W.; Fray; S.J.; Johnson, F.A.; Quarrington, J.E.; Williams, N. *J. Appl. Phys.* **1961**, 32, 2102.

10. Tsen, K.T.; Smith, D.J.; Tsen, S.S.-C; Kumar, N.S.; Morkoc, H. *J. Appl. Phys.* **1991**, 70, 418.

11. For an example of an alternative approach see the Experimental Section of Sela, I.; Beserman, R.; Morkoc, H. *Phys. Rev.* **1989**, B39, 3254.

12. For a description of a very similar apparatus see Exarhos, G. *J. Vac. Sci. Technol.* **1986**, A4, 2962; see also Figure 4 of RADC-TR-90-94 for a schematic diagram of the apparatus. Changes made since that figure was prepared are described in the text of this report.

13. Nye, J.F., "Physical Properties of Crystals", Oxford Press: Clarendon (1985).

14. Desbat, M.F.; Daniel, M.F.; Lassagues; J.C.; Gaire, R. *J. Solid State Chem.* **1988**, 73, 127.

D. Metal-Ceramic Bonding and Interface Stabilization. J.A. Schwarz

The initial investigation of Professor Schwarz's group centered around the molecular bonding of copper, as a prototype, to a ceramic base, specifically aluminum oxide, to provide insight into solving the processing problems inherent in GaAs technology. Stabilization of a reducible second phase ceramic on a primary ceramic was an attractive approach for mounting a bulk metal. This is extremely important, because of the two- fold role of a metal buffer layer as a site for GaAs crystal growth and as a heat sink. Once a suitable bonding layer has been established on the secondary phase, the growth of single crystal GaAs by graphoepitaxy may be possible.

Initially the second phase oxide was chosen as TiO_2, but the thermal properties were undesirable, and WO_3 was chosen as a more suitable oxide. Another factor which arose during the initial study was the intrusion of the doped metal species into the Al_2O_3 support to form a spinel-like compound. The introduction of WO_3 as the second-phase oxide served as a barrier to this spinel-like formation.

The characterization of these effects was accomplished using the techniques of

Temperature- Programmed Reduction(TPRd) and Temperature- Programmed Oxidation(TPO). Spectra obtained from the TPRd and TPO techniques can be used as fingerprints for the reduction and oxidation characteristics of stabilized compounds, and allow the stoichiometry of those compounds to be found. Repeating the reduction-oxidation cycle at elevated temperatures (~1300 K), allows for quick stabilization of these compounds.

The investigation centered on the stability of the WO_3 supported on γ-Al_2O_3. A series of samples with increasing weight loadings of WO_3 (2,7,12,20 and 30%) showed increasing characteristics of bulk unsupported WO_3. Those results indicated that the supported WO_3 was stable on the γ-Al_2O_3 surface up to 1300 K. The O/M and H/M ratios, which represent the stoichiometry of the compounds, supported the analysis of the spectra.

Building on the results of the investigation, cobalt was used as the next metal. Cobalt, as does nickel, forms a spinel-like structure with Al_2O_3. The results obtained using cobalt indicated that the spinel-like compound was not reduced to a large enough extent to study. Multiple overlapping reduction and oxidation states were present. Therefore, nickel was substituted for cobalt in the remainder of the study. The spectra obtained for the Ni/Al_2O_3 samples indicated that the supported nickel oxide formed a complex with the Al_2O_3. This was apparent in the disappearance of the reduction profile for nickel, around 670K, and the appearance of a stable reducible species, around 1150K. The $Ni/x\%WO_3/Al_2O_3$ samples showed features indicating partial reduction of supported WO_3, as well as complexing of both Ni & WO_3 and Ni & Al_2O_3 to form $NiWO_4$ and $NiAl_2O_4$, respectively. The spectra obtained for unsupported and supported $NiWO_4$ indicate that this species is more readily reduced and is more stable to oxidizing conditions then $NiAl_2O_4$.

Expanding on these phenomena by exploiting the surface charge characteristics of the support (pH_{PZC}) as a function of impregnation pH, the nickel cation can possibly be preferentially directed to the WO_3 sites. Experimentally, impregnation solutions were held at constant pH's of 4, 5, and 6 for supports composed of Al_2O_3, $12\%WO_3/Al_2O_3$, $20\%WO_3/Al_2O_3$, and $30\%WO_3/Al_2O_3$. The weight loadings of Ni, for a 1 hr. contact time, on these supports are found in Table II:

Table II: Ni weight loadings as functions of support and impregnation pH.

Support	Nickel wt. loading (%) Impregnation pH		
	4	5	6
Al_2O_3	1.09	1.67	2.31
$12\%WO_3/Al_2O_3$	0.99	1.11	2.01
$20\%WO_3/Al_2O_3$	0.94	1.03	1.92
$30\%WO_3/Al_2O_3$	0.81	0.85	1.62

The results obtained so far permit the following conclusions:

1) WO_3 is stable on Al_2O_3 up to 1300K,
2) Ni is stabilized by complexation with WO_3, and
3) Ni can be preferentially placed onto WO_3 sites.

This study into the stabilization effects of supported oxides is an ongoing investigation, and will be extended from dispersed Ni to Ni foil.

III. FUTURE RESEARCH

Future research must focus on the most productive research pathways, which also have the most technological potential. Several have already registered successes, and others are on the verge of reaching their goals.

The MBE work, which has produced promising $CaF_2/Pd/CaF_2/GaAs$ multilayer structures, is one of the major proposed avenues of continuing activity. At the present time we have formed a multilayer thin- film structure consisting of a bulk $CaF_2(111)$ single-crystal substrate on which epitaxial films of first Pd(111) and then $CaF_2(111)$ have been grown. On top of this multilayer we have grown polycrystalline GaAs with a strong (111) fiber axis. Further work is needed to find the epitaxial conditions required for final GaAs epitaxy.

During the past month we have been attempting to grow the epitaxial $CaF_2(111)$/Pd(111)/bulk $CaF_2(111)$ multilayer in a separate UHV system that has not been contaminated with Ga or As and has a lower base pressure ($6x10^{-10}$ torr). We believe we may be able to improve the microstructure of this multilayer, and thus provide a more ordered substrate for depositing the final GaAs film, which will be done in the MBE system previously constructed for this project. The air exposure should not seriously affect the $CaF_2/Pd/CaF_2$ multilayer, since all these materials are stable in air. Gaseous adsorbates, on the other hand, will be desorbed during system bakeout and subsequent heating to the GaAs deposition temperature (approximately 550°C).

Our proposal is to continue this research in order to determine the epitaxial conditions for the final GaAs film. These conditions include the substrate temperature, deposition rate, and possibly the vacuum in the system. It might be mentioned here that a colleague of Professor Vook in Japan has been able to deposit epitaxial metal films on alkali halide surfaces at room temperature (instead of at several hundred degrees Celsius) by introducing Ar gas into the system at relatively high pressures. The Ar apparently bombards the substrate and growing film surfaces, thereby enhancing the surface mobility of the incident metal atoms (which is what is also accomplished in normal high temperature epitaxy). It's a trick that just might also work with GaAs on CaF_2, and we will try it along with the standard approaches.

Prof. Spencer has developed CVD techniques for depositing conducting borides of Ni, W,

Ga and La. Such films may thus be used as conducting ground planes. If they could be grown epitaxially on, for example, CaF_2, then possibly GaAs could be grown epitaxially on the boride. At the present time it is not known whether these borides are stable at high temperatures in the presence of GaAs. But this method, if it works, may be a simpler way of forming an epitaxial GaAs/boride/insulator(CaF_2) multilayer for MMIC devices.

As in the past, the samples would be evaluated by x-ray diffraction(XRD) and reflection high -energy electron diffraction(RHEED). The former gives the bulk structure, while RHEED gives the surface structure. Scanning electron microscopy (SEM) and x-ray energy spectroscopy (XES) are also used to investigate topography and sample composition. Characterization of each sample is essential in order to plan subsequent experiments. Additionally, Prof. Chaiken will use Raman spectroscopy to characterize our films. We propose to supply him with GaAs films that are 1) randomly oriented, 2) have a (111) fiber texture, 3) an epitaxial GaAs(111) film grown on a bulk CaF_2(111) cleavage face, and, if we're successful, 4) an epitaxial GaAs(111) film grown on an epitaxial CaF_2(111)/Pd(111) bilayer grown on bulk CaF_2(111). Some of these films have already been characterized by Prof. Chaiken; but doing work on all four should be very helpful in interpreting the Raman spectra and their dependence on microstructure.

While this series of experiments continues, lithographed substrates, properly ruled for the <111> columnar growth pattern of GaAs presently achieved by Professor Vook, will be prepared at the Center of X-ray Lithography in Wisconsin (CXRL) or at Cornell University.*

To intensify the graphoepitaxy effort, and test this methodology, we propose to

1. Complete the laser rastering system. This will require completion of the computer control programming, assembly of the optical system and mounting on a vibration-free optical bench, as well as vibration isolation of the chamber.
2. Integrate a Quadrupole Mass Spectrometer with the rastering system (if organometallic materials are to be used via OMVPE deposition) to monitor sample

---

*We envision four 1 cm^2 samples for the final testing of graphoepitaxy; it would in all likelihood be most rapid, efficient and cost-effective to subcontract their preparation . This would permit Prof. Dowben to devote his time to the completion of the laser rastering system and associated components.

purity.

3. Provide in situ capability for monitoring surface roughness, after graphoepitaxy and annealing, to determine whether a sufficiently flat GaAs surface was achieved for device-grade use.

The final system, if design specifications are achieved, would be an ion-pumped, vibration-free, laser-rastered system with 1/2-μ spatial resolution. A CO_2 laser would be used for annealing, and a He-Ne laser to determine surface roughness by measuring surface scattering. A diode detection system integrated with the laser-rastering system would provide computer-aided images of the growth and annealing process with both lasers running simultaneously.

Thermal desorption spectroscopy (TDS) into the QMS, or laser-induced SIMS, (commonly known as LAMMA, laser microprobe mass analysis) will also provide some in situ characterization. Ar^+-ion sputtering will provide some modicum of substrate preparation.

We would expect to install this entire system at the MBE UHV system when the CaF_2 experiments have reached an appropriate point. Much of the development can be done in parallel.

The third major track - the synthetic effort - will be continued by Professor Spencer along already successful paths, and focus on two primary goals: (1) the continuation of our synthetic studies of novel source compounds for GaAs and AlGaAs, and epitaxial studies of these compounds (especially the deposition of pure aluminum films for AlGaAs formation and aluminum oxide and aluminum boride films for the formation of "upside down" heterostructures) and (2) the formation and study of metal boride films for use as ground plane and interconnect materials in these heterostructural systems-- a new and promising application. Each of these goals is briefly outlined below.

Our synthetic studies will be directed primarily toward the synthesis of new chemical vapor deposition (CVD) precursors for aluminum-containing materials. We will continue our modelling studies using *semiempirical* and *ab initio* calculational methods in an effort to identify new source materials with favorable fragmentation pathways for clean depositions.[1]

We propose to continue our synthetic and epitaxial studies of aluminum-containing materials by the synthesis and application of the source compounds modelled in the theoretical calculations. We have recently reported the results of our studies involving the formation of pure, polycrystalline aluminum thin films and aluminum oxide thin films (for "upside down"

heterostructures) from a novel aluminaborane precursor complex.[2-5] The aluminaborane source compounds were, in general, relatively thermally stable, volatile, air-sensitive liquids, thus providing nearly ideal precursor properties for chemical vapor deposition experiments. "Upside-down" GaAs heterostructures use a variety of materials as buffer layers between GaAs and ceramic layers. Necessary properties of the buffer layer are that it should have good adhesion properties, sufficient thermal conductivity, and a reasonable thermal expansion match. Aluminum oxide is a excellent material for such buffer layers. In this structural approach, the metallic buffer layer is deposited in correct stoichiometric ratio upon crystalline GaAs. We will continue these synthetic studies and also initiate new investigations into the deposition mechanisms of new thin film materials using these and other members of the boron-containing class of CVD source compounds. These studies are designed to provide further insights into the deposition chemistry of these source compounds and to elucidate the important factors for determining the suitability of a source compound for the formation of pure, polycrystalline aluminum thin films (for AlGaAs applications) and aluminum oxide thin films (for "upside down" structures) from a novel aluminaborane precursor complex.

As a second primary focus of the work, we will continue a very intriguing spinoff of our boron chemistry investigations: our exploration of the use of new metallaborane complexes in the formation of technologically very important metal boride thin films. Metal borides are typically extremely refractory materials with melting points frequently far in excess of the pure metal or other metal binary systems. These metal borides are also exceptionally hard materials which are not significantly affected even by the most rigorous of chemical environments. The metal borides are typically rather good electrical conductors with some displaying superconducting properties at low temperatures. Thus, metal borides have found increased use not only in traditional applications such as hard coatings for cutting tools, but also in thermally and chemically taxed aerospace components, in high-energy optical systems, in highly conducting materials and in new magnetic materials. These metal borides should make very good ground plane materials in heterostructural devices. The application of a metal boride ground plane is shown in Figure 40. This architecture would effectively replace both the Pd(111) ground plane and the CaF_2 with a single, refractive metal boride ground plane.

Figure 40. Heterostructure Stratigraphy.

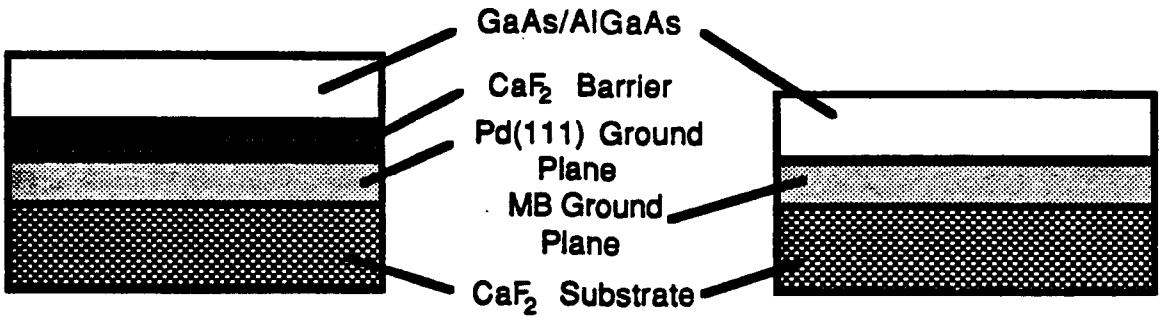

We initially investigated the formation of nickel boride films and have found that high purity conformal nickel boride thin films can be readily prepared with stoichiometric control from the pyrolytic reaction of $NiCl_2$ with boron clusters.[6-9] Films with nickel contents as high as 99.9 % and as low as 56.6 % have been prepared using this technique. The thin films were characterized by XES, AES, SEM, XRD, FT-IR, TEM and electron diffraction experiments. The films were shown by AES to be compositionally uniform in the bulk sample, Figure 41. The films were found by SEM, TEM and XRD to be highly crystalline materials. We have continued our investigation of this deposition and CVD chemistry, including the applicability of the process to other metal systems. Recent results have shown that films of titanium, iron and lanthanum boride are formed in analogous deposition chemistry. In addition, pure copper films were prepared from the CVD of Cu_2Cl_2 and B_5H_9 in a similar process. The mechanism of the deposition and the electronic properties of the thin films need to be further investigated. In this work, we propose to continue these metal boride synthetic and deposition studies, and to explore the possible application of metal boride crystalline films are ground planes for heterostructural systems. After we deposit the metal boride layer on the CaF_2 substrate, the final GaAs layer will be deposited using conventional techniques (Prof. Vook's lab) for further graphoepitaxial studies.

Figure 41. Representative Auger electron spectrum of a nickel boride thin film deposited using a *nido*-pentaborane(9), B_5H_9, borane source kept at -78° C during the deposition. The depth profile was constructed from Auger electron spectra as the film was sputtered using Ar+ ion milling. Sputter times are given in minutes and the atomic compositions are given in percent.

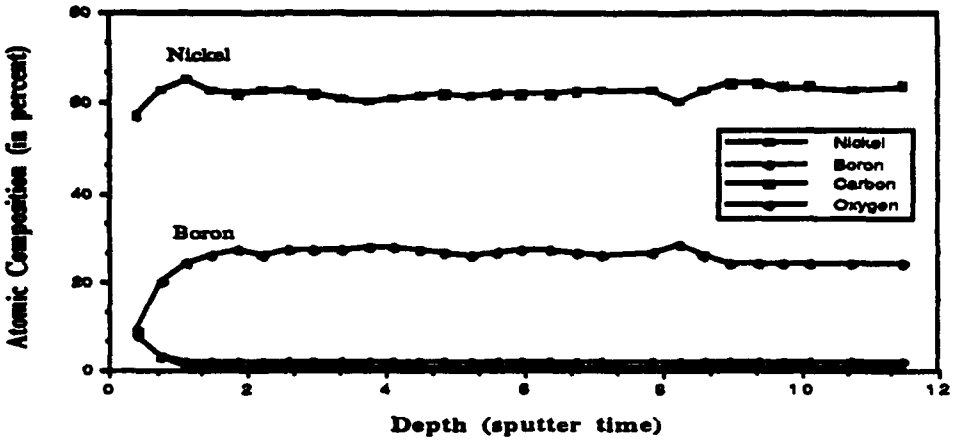

References to Section III:

1. Glass, J. A., Jr.; Whelan, T. A.; Spencer, J. T. *Organometallics* **1991**, 10, 1148.
2. Glass, J. A., Jr.; Kher, S.; Hersee, S. D.; Ramseyer, G. O.; Spencer, J.T. *Mat. Res. Soc. Symp. Proc.* **1991**, 204, 397.
3. Glass, J. A., Jr.; Kher, S.; Spencer, J. T. *Thin Solid Films* **1992**, 207, 15.
4. Glass, J. A., Jr.; Kher, S.; Spencer, J. T. *Chem. Mater.* **1992.**
5. Datta, S.; Glass, J. A., Jr.; Kher, S.; Kim, Y. -G.; Dowben, P. A.; Spencer, J. T. *Electrochem. Soc. Symp. Proc.* **1992.**
6. Glass, J. A., Jr.; Kher, S.; Kim, Y. -G; Dowben, P. A.; Spencer, J. T. *Mat. Res. Soc. Symp. Proc.* **1991**, 204, 439.
7. Kher, S.; Spencer, J. T. *Chem. Mater.* **1992.**
8. Kher, S.; Spencer, J. T. "Chemical Vapor Deposition of Pure Nickel and Nickel Boride Refractory Thin Films From Borane Cluster Compounds" *Mat. Res. Soc. Symp. Proc.* **1992** in press.
9. Kher, S.; Spencer, J. T. in preparation for submission to *Chem. Mater.*

IV. PUBLICATIONS RESULTING FROM THIS PROJECT

1. Brady, R.L.; Southmayd, D.; Contescu, C.; Zhang, R.; Schwarz, J.A. "Surface Area Determination of Supported Oxides: WO_3/Al_2O_3", *J. Catalysis* **1991**,129,195.
2. Chang, S.; Brillson, L.J.; Kime, Y.J.; Rioux, D.S.; Woodall, J.M. "Orientation-Dependent Chemistry and Schottky Barrier Formation at Metal-GaAs Interfaces", *Phys. Rev. Lett.* **1990**,69, 2851; and *J. Vac. Sci. Technol.* **1990**,B8,1008.
3. Glass, J.A., Jr.; Whelan, T.A.; Spencer, J.T. "Small Heteroborane Cluster Systems. 1. Theoretical Study of Fridged and Cage-Inserted Phosphaborane Cluster Compounds Using Semiempirical Molecular Orbital Calculations", *Organometallics* **1991**,10,1148.
4. Glass, J.A., Jr.; Kher, S.; Hersee, S.D.; Ramseyer, G.O.; Spencer, J.T. "The Deposition of Aluminum and Aluminum Boride Thin Films by Aluminaborane Cluster Compounds", *Mat. Res. Soc. Symp. Proc.* **1991**, 204, 397.
5. Glass, J.A., Jr.; Kher, S.; Kim, Y.-G.; Dowben, P.A.; Spencer, J.T. "The Deposition of Nickel Boride Thin Films by Borane and Metallaborane Cluster Compounds", *Mat. Res. Soc. Symp. Proc.* **1991**,204,439.
6. Goodreau, B.H.; Ostrander, R.L. ; Spencer, J.T. "Small Heteroborane Cluster Systems. 3. Characterization, Deprotonation and Transition Metal Chemistry of the Small Phosphorus-Bridged Pentaborane(9) System, μ-Diphenylphosphinopentaborane", *Inorg. Chem.* **1991**,30, 2066.
7. Mancini, D.C.; Varma, S.; Simons, J.K.; Rosenberg, R.A.; Dowben, P.A. "Synchrotron Radiation Induced Chemical Vapor Deposition of Thin Films from Metal Hexacarbonyls", *J. Vac. Sci. Technol.* **1990**,B8,1804.
8. Mazurowski, J.; Baral-Tosh, S.; Ramseyer, G.O.; Spencer, J.T.; Kim, Y.-G.; Dowben, P.A. "Novel Methods for Deposition of Boride Carbide Films", *Mat. Res. Soc. Symp. Proc.* **1991**,190, 101.
9. Miller, R.W.; Donaghy, K.J.; Spencer, J.T. "The Preparation, Characterization and Reaction Chemistry of Small Bridging Phosphaborane Systems Prepared from the Reaction of [(2,2-Dimethyl-1-(trimethylsiloxy)propylidene)-trimethysilphosphine] with

Pentaborane(9)", *Phosphorus, Sulfur and Silicon* **1991**,57, 287.

10. Miller, R.W.; Donaghy, K.J.; Spencer, J. T. "Small Heteroborane Cluster Systems. 2. Preparation of Phosphaborane Systems From the Reaction of Small Boron Cages with Low Coordinate Phosphorus Compounds: The Reaction Chemistry of Phosphaalkenes with Pentaborane(9)," *Organometallics* **1991**,10,1161.
11. Perkins, F.K.; Rosenberg; R.A.; Lee, S.; Dowben, P.A. "Synchrotron-Radiation-Induced Deposition of Boron and Boron Carbide Films from Boranes and Carboranes: Decaborane", *J. Appl. Phys.* **1991**,69,4103.
12. Rosenberg, R.A; Perkins, F.K.; Mancini, D.C.; Harp, G.R.; Tonner, B.P.; Lee, S.; Dowben, P.A. "Selective Area Deposition of Boron on Si(111) Induced by Synchrotron Radiation", *Appl. Phys.Letters* **1991**,58,607
13. Varma, S.; Kim, Y.-G.; Psenicnik, Z.; Dowben, P.A.; Birge, R.R. "The Deposition of Mo and $Mo(CO)_6$", *T.M.S. Proc.* **1990**,101.

In preparation:

14. Miller,R.W.; Spencer, J.T. "The Reaction of a Phosphaalkyne with Bis(acetonitrile)Decaborane(14). A New Synthetic Route to Phosphaborane Cluster Compounds"; approved by RADC.

MISSION

OF

ROME LABORATORY

Rome Laboratory plans and executes an interdisciplinary program in research, development, test, and technology transition in support of Air Force Command, Control, Communications and Intelligence (C^3I) activities for all Air Force platforms. It also executes selected acquisition programs in several areas of expertise. Technical and engineering support within areas of competence is provided to ESD Program Offices (POs) and other ESD elements to perform effective acquisition of C^3I systems. In addition, Rome Laboratory's technology supports other AFSC Product Divisions, the Air Force user community, and other DOD and non-DOD agencies. Rome Laboratory maintains technical competence and research programs in areas including, but not limited to, communications, command and control, battle management, intelligence information processing, computational sciences and software producibility, wide area surveillance/sensors, signal processing, solid state sciences, photonics, electromagnetic technology, superconductivity, and electronic reliability/maintainability and testability.